SCUOLA DI DOTTORATO
UNIVERSITÀ DEGLI STUDI DI MILANO-BICOCCA

Department of Earth and Environmental Sciences

PhD program CHEMICAL, GEOLOGICAL AND ENVIRONMENTAL SCIENCES
Cycle XXXIII

Curriculum in Environmental Sciences

NANOPARTICLES FOR THE REMOVAL OF CONTAMINANTS FROM WASTEWATER

Surname Mantovani Name Marco

Registration number 750959

Tutor EMILIO PADOA-SCHIOPPA

Supervisor: ELENA COLLINA

Coordinator: MARIA LUCE FREZZOTTI

ACADEMIC YEAR 2019-2020

TO MY PARENTS

The imagination of nature is far, far greater than the imagination of man.
There is plenty of room at the bottom.

Richard Feynman

Table of contents:

1. Introduction

1.1 The importance of water

The concept of Water as an essential good is a keystone of the common knowledge: life cannot be possible without water as it is indispensable in every ecosystem to sustain the flora and fauna. Humankind needs water not only for mare survival. Since most of the human activities are water-based (i.e. food production, transport, energy generation), water can be considered in effect as a crucial factor for the economic development. It provides human with ecosystem services like freshwater, fishes, fruits, vegetables and woods supply, climate regulation, flood prevention as well as aesthetic, recreational and educational values (Capot et al., 2013).

The contemporary western world still takes water viability for granted. Nowadays, water global consumption is estimated at 4×10^{12} $m^3 year^{-1}$. Most of it (69%) is used in agriculture, while the 19% is destined to industrial activities and the remaining 12% is used for domestic necessity. (FAO, 2018). However, over the last decades the increasing anthropogenic pressure towards water compartment has become more evident as the human use of water grow alongside with world population, leading to pollution and water quality degradation. This is a very important issue that cannot be underestimated as it can trigger other problems including loss of biodiversity and scarcity of drinking water supplies, especially in the poorest countries (Jury and Vaux, 2007).

Therefore, wastewater treatment plant (WWTP) must be considered a crucial asset, something to invest in attention and money on in order to improve not only the quality of the treated effluents, but also their carbon footprint and sustainability. WWTP must be effective to convert pollution sources in valuable resources, recovering nutrients and water, possibly coupling their treatment with energy production in accordance with the circular economy perspective (Geissdoerfer et al., 2017).

Current water quality guidelines for wastewater treatment focuses on specific chemical parameters, like Biological Oxygen Demand (BOD) and Chemical Oxygen Demand (COD). The risk associated with microorganisms, in particular *E. coli* and other pathogenic bacteria is also held in high regard. Quite satisfactory results have already been achieved in terms of nutrients and organic matter removal from wastewater using conventional treatment technologies. A conventional wastewater treatment facility does include a water line and a sludge line. The first one aims at obtaining a treated effluent having physio-chemical properties compatible for discharge to natural water bodies. In the process, a sludge rich of organic matter and nutrients is

formed, which can undergo different destinies depending on the type of WWTP. Some of them can use the sludge, prior dewatering, to produce biogas through anaerobic digestion. Municipal digestate is often centrifuged to separate the solid content from the supernatant. So, a liquid fraction called centrate is formed which is particularly rich in nitrogen. This wastewater is usually redirected back to the beginning of the water line to be treated. However, as the removal of nitrogen involves high energy demand (Rosso et al., 2008), the research of alternatives allowing high efficiencies while reducing the WWTP management costs is still an important issue.

The most recent challenges now concern the removal of micropollutants, including heavy metals and the so-called emerging organic pollutants. The definition of emerging pollutants refers to a heterogeneous class of synthetic or naturally-occurring chemical substances, often found in the aquatic environment at very low concentrations (between 10^{-8} and 10^{-5} gL^{-1}) (Sauvé and Desrosiers, 2014). It is also important to highlight that those substances have been released to the environment for decades, but most of them could only be assessed recently thanks to the development of more sophisticated analytical and detection methods (Geissen et al., 2015). Furthermore, due to the lack of monitoring campaigns and regulation they are also called "contaminants of emerging concern" (CECs). Pharmaceutical compounds, personal care products, pesticides, steroids, hormones, industrial additives and surfactants deserve mention as common substances included in this category (Houtman, 2010). Many of those compounds (of course not all of them) can be persistent in the environment, posing a potential or real risk associated with humans and environmental exposure (Gasperi et al. 2008; Lindberg et al 2014). In fact, although the concentrations of some emerging pollutants (EPs) are not always high enough to represent a real risk to human health, this is not always guaranteed for other trophic levels (Nurizzo et al. 1994).

Many organic pollutants, like pharmaceutical compounds, can bioaccumulate in the organisms and that is why wastewater reuse for irrigation purposes is discouraged. The emerging pollutants heterogeneity is also an important issue. This makes the assessment of the environmental risk they pose extremely difficult, which does not depend exclusively on the starting compound but also on its metabolites and degradation products (Escher and Fenner, 2011). The pollution caused by the presence of pharmaceutical compounds in water is a recognized problem in several countries. It is also known that a poor management of wastewater leads to the contamination of surface water, groundwater and drinking water. Therefore, in recent years several advanced processes have been tested including ozonation, photocatalysis and adsorption on activated carbon to deal with the

issue. Ozonation is a chemical treatment exploiting the high reactivity of ozone (O_3), which is a very strong oxidant agent. This technique is based on the in-situ production of O_3 which can react with a wide range of substances in a water solution (Ikehata et al., 2006). Not only it can be very effective on the degradation of organic compounds, but ozone can have a strong disinfectant potential, attacking different microorganisms. Ozonation is considered a very interesting technique among the advanced oxidation processes due to its effectiveness over a wide range of pH, both on organics degradation and inorganics removal, also allowing color, taste and odor removal (Wei et al., 2017). However, the production of O_3 does involve relatively high equipment costs and high energy demands (as O_2 is subjected to high electric voltage or to UV radiation to form ozone). Furthermore, the possible formation of hazardous by-product after the treatment must be considered. Photocatalysis is a chemical process occurring when light interacts with a catalyst, a semiconductor material leading to the formation of strong oxidation agents able to breakdown the organic matter in water. Nano-catalysis is an interesting technique for wastewater remediation working both with sunlight and artificial ultraviolet (UV)-light (Bernabeu et al., 2011; Sharma et al., 2012). In particular, TiO_2 is suitable for photocatalysis due to its common availability, relatively low cost, and high chemical stability. At present, the main technical issues preventing its use at real scale are associated to the costs to maintain the UV source, the post-recovery of the catalysts after water treatment, and the variable efficiency of the photocatalytic treatment (Horikoshi and Serpone, 2020).

Therefore, the results obtained with those techniques have not been completely exhaustive, and the cost of such processes is still very high. So, there is the need to develop and assess new proposals (Klavarioti et al. 2009).

Heavy metals are another important class of contaminants affecting soil and groundwater. Their final concentrations are often too high to prevent damages to the receiving waterbodies but at the same time, too low to be effectively removed by traditional processes. Although the environmental risk associated to some of them is already known and studied, there is not yet an applicable large-scale method for their removal (Fatta-Kassinos et al. 2011).

Nowadays, the most used technology for the removal of heavy metals from wastewater consists in chemical treatments to favor precipitation processes. By adding alkaline reagents, the wastewater pH is increased to promote the formation of insoluble hydroxides which can be removed by flocculation or sedimentation. However, this technique involves some severe limitations at large-scale: the use of chemicals determine high costs; the hydroxides solubility can

be lowered by the complexity of the wastewater due to the interaction between metals and chelates; when effective, the process does generate a large amount of sludge. Of course, alternatives have been proposed such as reverse osmosis, adsorption through activated carbons, ion exchange, membrane filtration and ultrafiltration. However, for various reasons, they are still not sustainable at real scale (Fu and Wang, 2011).

Nanotechnology could play an important role in this research topic. In fact, nanomaterials often show very different physical, chemical, and biological properties compared to their macroscopic counterpart. This results from their larger surface area per unit of volume and from the quantum effects (Li et al., 2016). Promising nanoscale solutions, which can be applied to water treatment, already exist. However, the current cost of these materials commonly prevents their large-scale applications. Thus, developing a low-cost nanotechnology to remove pollutants from water is still an important goal.

In the last years, Zero-Valent Iron (ZVI) has been tested for this purpose. This chemical element is quite abundant, not toxic, cheap and easy to produce. ZVI is a reactive metal that acts as a reducing agent, transforming pollutants in not toxic or less toxic compounds by a reductive process, opposite to the most common oxidative processes used in wastewater treatment. ZVI has proven effective in removing a wide range of chemical contaminants in aqueous solutions such as chlorinated organic compounds, metals and pharmaceutical compounds (Fan et al., 2009; Tosco et al., 2014).

Recent studies have shown an increased attention in the use of nanoparticles of Zero-Valent iron (nZVI) to remove different pollutants, thanks to their large specific surface area and their enhanced reactivity. nZVI acts both as an adsorbent and as a reducing agent, causing organic pollutants to break down (Kharisov et al. 2014).

However, nZVI used in wastewater treatment involve some not entirely negligible problems. In fact, their application is limited due to the rapid oxidation, their aggregation in water solution and the problem of ageing effect (Calderon and Fullana 2015). Moreover, the conventional synthesis process of the nanoparticles is quite expensive, and it is very difficult to separate nZVI from the treated media. To solve the mentioned complications, the most recent studies have focused on finding cheaper synthesis methods to make solid porous materials, which act as physical support for the iron nanoparticles (Zhu et al. 2014).

A promising approach is the combination of nZVI with carbon materials through the encapsulation of the iron particles inside micro or nanocarbon spheres (6-8 μm). This process can be made via an in-situ formation through Hydrothermal Carbonization (HTC) from an iron salt and an organic compound with reducing properties. The synthesis process uses an aqueous solution of iron (III) nitrate mixed to the chosen biomass according to appropriate ratio. The combination of these substances is treated in a reactor in inert reaction atmosphere and heated at different temperatures between 200 and 300 °C. This leads to the reduction of the carbonaceous biomass and the formation of microspheres, in which the iron salts are incorporated. Furthermore, the absence of oxygen in the HTC process causes the reduction of Fe (III) to Fe (0). The result is represented by iron nanoparticles trapped in carbon microcapsules, Carbon-Encapsulated nZVI or CE-nZVI (Sunkara et al., 2010).

The advantages of this solution seem very encouraging: the nZVI component implies a high chemical reducing capability, whereas the carbon fraction has a high sorption capacity; moreover, including nZVI in an organic compound makes the separation of nZVI from the treated systems easier (Hoch et la., 2014). The carbon substrate can be obtained from different sources like biomass waste, organic fraction of municipal waste, sewage sludge and residues from food farming industry. The use of algal biomass as a substrate to be submitted to the HTC process is also mentioned in literature. This solution could be ideal for exploiting the algal biomass grown on urban wastewater (Mäkelä et al., 2015; He et al. 2013; Berge et al. 2011; Lu et al., 2015).

1.2 Microalgae

Microalgae are photosynthetic microorganism with variable cytological characteristics; usually they are characterized by a single eukaryotic cell featuring a cell-wall, vacuole, plastids and auxiliary structures such as flagella. Those microorganisms have simple growing requirements and that is the secret of their evolutionary success as they can survive in different environments: actually they can be found not only in freshwater bodies and oceans but also in peculiar habitats such as glaciers and geothermal springs (Hopes and Mock, 2015).

In recent years, microalgae have been used directly in the wastewater treatment sequence with the double aim of removing nutrients and harvesting biomass, which could be used for anaerobic

digestion or for other purposes. In fact, microalgae directly assimilate dissolved nitrogen and phosphorus from their growth media and can improve the energy balance in biological oxidation by providing oxygen to heterotrophic aerobic bacteria (Abdel-Raouf et al., 2012). Furthermore, the interaction between microalgae and nitrifying bacteria seems very interesting as the photosynthesis can sustain the oxygen demand of Ammonia Oxidizing Bacteria (AOB) and Nitrite Oxidizing Bacteria (NOB).

Microalgae have historically attracted the interest of the scientific community. This is clear by checking through literature as they still pose a trending topic. Microalgae possess a lot of qualities that can be suitable for different applications. They can be significant sources of bio-compounds such as carotenoids, lipids, proteins, polysaccharides, pigments, vitamins etc. or they can be used in energy production (biofuels), pharmaceutical, cosmetic and food industries (de Souza et al., 2019; Gaignard et al., 2019) . However, it is not that simple, and the properties of the microalgae does not only depend on the species but also on the environmental conditions, the type of cultivation strategy (in-door or outdoor) and of course on the type of growth media. Many potential valorization strategies must be ruled out when microalgae are grown on wastewaters due to local regulation, health insurance issues and public opinion. Those are important limitations that could turn off the interest in using microalgae for wastewater treatment. Therefore, finding good solutions for the valorization of microalgae is still important to lower the high costs associated with their cultivation.

1.3 Thesis objectives

This thesis work is part of PerFORM WATER 2030 (Platform for Integrated Operation Research and Management of Public Water towards 2030), a project financed by the Lombardy region and the European Regional Development Fund. The objective is to integrate microalgae within a conventional wastewater treatment plant (WWTP) as an unconventional biological treatment, for the remediation of the liquid fraction of municipal digestate (centrate) also providing a further valorization for the obtained biomass. The goal, in fact is to produce laboratory-scale zero valent iron nanoparticles encapsulated in a carbonaceous matrix (ME-nFe), a material with reducing properties and high adsorption capacity that can be used in wastewater treatment. The synthesis

of the nanoparticles is achieved through hydrothermal carbonization (HTC) starting from microalgal biomass grown in the pilot plant located at the Bresso-Niguarda (Milan) wastewater treatment plant (WWTP).

Beside the introduction chapter, the thesis is made of five main chapters. Chapter 2 shows the result achieved during an outdoor cultivation of microalgae directly within the conventional WWTP of Bresso-Niguarda, where an high rate algal pond (HRAP) was installed to evaluate the feasibility to use microalgae to treat municipal centrate, removing nitrogen and phosphorus.

Chapter 3 is a critical review on the hydrothermal carbonization (HTC) applied to microalgal biomass grown on wastewaters. The fate of the microalgal biomass is crucial to make microalgal-based process more sustainable and more appealing from an economic point of view. In this section of the thesis the use of microalgal biomass as such to produce fuels, soil amending and adsorbents for wastewater remediation are compared with the use of microalgal hydrochar (the main product of HTC).

Chapter 4 shows the result obtained during the laboratory-scale production of microalgal-based iron nanoparticles (ME-nFe) starting from the microalgae grown in Bresso in combination with an iron salt through HTC. The production of different samples, changing the operative parameters (temperature, iron sources and the proportion between the biomass and the iron salt) are described. The obtained adsorbents have been characterized in terms of iron content, morphology and BET surface area to highlights the best ones end to define a proper protocol for the synthesis. The best prototypes were selected for the application step, involving Jar tests to remove Zinc, Cadmium, Copper, Chromium and Nickel from water solutions and treated effluents.

Chapter 5 deals with the liquid byproduct obtained during the HTC of microalgae, which was named Hydrothermal carbonization liquid fraction (HTC-LF). That wastewater was studied, assessing its toxicity for water compartment through Microtox and Phyto-PAM tests. Due to its high nutrient concentrations, the use of diluted fraction of the wastewater was proposed for laboratory-scale cultivation of microalgae. Pure and mixed microalgal cultures were able to grow on a 20% dilution of the HTC-LF both in batch and in continuous feeding, suggesting the possibility to redirect the HTC-LF produced during the synthesis of the ME-nFe to obtain new biomass for subsequent synthesis, making the entire process more sustainable. Finally, chapter 6 summarize the general aspects of the entire study, giving some future perspective

1.4 References

Abdel-Raouf, N., Al-Homaidan, A. A. and Ibraheem, I.B.M. (2012). Microalgae and Wastewater Treatment. Saudi Journal of Biological Sciences 19, 257–275

Bernabeu, A., Vercher, R.F., Santos-Juanes, L., Simón, P.J., Lardín, C., Martínez, M.A., Vicente, J.A., González, R., Llosá, C., Arques, A., Amat, A.M., 2011. Solar photocatalysis as a tertiary treatment to remove emerging pollutants from wastewater treatment plant effluents. Catal. Today. https://doi.org/10.1016/j.cattod.2010.09.025

de Souza, M.P., Hoeltz, M., Gressler, P.D., Benitez, L.B., Schneider, R.C.S., 2019. Potential of Microalgal Bioproducts: General Perspectives and Main Challenges. Waste and Biomass Valorization. https://doi.org/10.1007/s12649-018-0253-6

Escher, B.I., Fenner, K., 2011. Recent advances in environmental risk assessment of transformation products. Environ. Sci. Technol. https://doi.org/10.1021/es1030799

Fan, J., Guo, Y., Wang, J., Fan, M., 2009. Rapid decolorization of azo dye methyl orange in aqueous solution by nanoscale zerovalent iron particles. J. Hazard. Mater. https://doi.org/10.1016/j.jhazmat.2008.11.091

Fu, F., Wang, Q., 2011. Removal of heavy metal ions from wastewaters: A review. J. Environ. Manage. https://doi.org/10.1016/j.jenvman.2010.11.011

Gasperi, J., Garnaud, S., Rocher, V., Moilleron, R. (2008). Priority pollutants in wastewater and combined sewer overflow. Sci. Total Environ. 407, 263−27

Gaignard, C., Gargouch, N., Dubessay, P., Delattre, C., Pierre, G., Laroche, C., Fendri, I., Abdelkafi, S., Michaud, P., 2019. New horizons in culture and valorization of red microalgae. Biotechnol. Adv. https://doi.org/10.1016/j.biotechadv.2018.11.014

Horikoshi, S., Serpone, N., 2020. Can the photocatalyst TiO2 be incorporated into a wastewater treatment method? Background and prospects. Catal. Today. https://doi.org/10.1016/j.cattod.2018.10.020

Houtman, C.J., 2010. Emerging contaminants in surface waters and their relevance for the production of drinking water in Europe. J. Integr. Environ. Sci. https://doi.org/10.1080/1943815X.2010.511648

Geissen, V., Mol, H., Klumpp, E., Umlauf, G., Nadal, M., van der Ploeg, M., van de Zee, S.E.A.T.M., Ritsema, C.J., 2015. Emerging pollutants in the environment: A challenge for water resource management. Int. Soil Water Conserv. Res. https://doi.org/10.1016/j.iswcr.2015.03.002

Ikehata, K., Jodeiri Naghashkar, N., Gamal El-Din, M., 2006. Degradation of aqueous pharmaceuticals by ozonation and advanced oxidation processes: A review. Ozone Sci. Eng. https://doi.org/10.1080/01919510600985937

Li, L., Hu, J., Shi, X., Fan, M., Luo, J., Wei, X., 2016. Nanoscale zero-valent metals: a review of synthesis, characterization, and applications to environmental remediation. Environ. Sci. Pollut. Res. https://doi.org/10.1007/s11356-016-6626-0

Lindberg, R., Östman, M., Olofsson, U., Grabic, R., Fick, J. (2014). Occurrence and behaviour of 105 active pharmaceutical ingredients in sewage waters of a municipal sewer collection system. Water Res. 58, 221-229

Nurizzo, C., Mezzanotte, V. (1994). Legislative, economical and technical aspects of irrigation with reclaimed wastewater in Italy. Resour. Conserv. Recycl. 10, 301-316

Fatta-Kassinos, D., Meric, S., Nikolaou, A. (2011). Pharmaceutical residues in environmental waters and wastewater: Current state of knowledge and future research. Anal. Bioanal. Chem. 399, 251-275

Klavarioti, M., Mantzavinos, D., Kassinos, D. (2009). Removal of residual pharmaceuticals from aqueous systems by advanced oxidation processes. Environ. Int. 35, 402-417

Kharisov, B.I., Rasika Dias, H.V., Kharissova, O.V., Jiménez-Pérez, V.M., Olvera Pérez, B., Muñoz Flores, B. (2012). Iron-containing nanomaterials: Synthesis, properties, and environmental applications. RSC Adv. 2, 9325-9358

Calderon, B., Fullana, A. (2015). Heavy metal release due to aging effect during zero valent iron nanoparticles remediation. Water Res. 83, 1-9

Zhu, X., Liu, Y., Qian, F., Zhou, C., Zhang, S., Chen, J. (2014). Preparation of magnetic porous carbon from waste hydrochar by simultaneous activation and magnetization for tetracycline removal, Bioresour. Technol. 154, 209-214

Hoch, L.B., Mack, E.J., Hydutsky, B.W., Hershman, J.M., Skluzacek, J.M., Mallouk, T.E. (2008). Carbothermal synthesis of carbon-supported nanoscale zero-valent iron particles for the remediation of hexavalent chromium. Environ. Sci. Technol. 42, 2600-2605

Mäkelä, M., Benavente, V., Fullana, A. (2015). Hydrothermal carbonization of lignocellulosic biomass: effect of process conditions on hydrochar properties. Appl. Energy 155, 576-584

He, C., Apostolos, G., Jing-Yuan, W. (2013). Conversion of sewage sludge to clean solid fuel using hydrothermal carbonization: hydrochar fuel characteristics and combustion behavior. Appl. Energy 111, 257-266

Berge, N.D., Ro, K.S., Mao, J., Flora, J.R.V., Chappell, M.A., Bae, S. (2011). Hydrothermal carbonization of municipal waste streams. Environ. Sci. Technol. 45, 5696-5703

Lu, Y., Levine, R. B., Savage, P.E. (2015). Fatty Acids for Nutraceuticals and Biofuels from Hydrothermal Carbonization of Microalgae. Industrial & Engineering Chemistry Research 54. 4066-4071.

Rosso, D., Larson, L.E., Stenstrom, M.K., 2008. Aeration of large-scale municipal wastewater treatment plants: State of the art. Water Sci. Technol. https://doi.org/10.2166/wst.2008.218

Sauvé, S., Desrosiers, M., 2014. A review of what is an emerging contaminant. Chem. Cent. J. https://doi.org/10.1186/1752-153X-8-15

Sharma, M., Jain, T., Singh, S., Pandey, O.P., 2012. Photocatalytic degradation of organic dyes under UV-Visible light using capped ZnS nanoparticles. Sol. Energy. https://doi.org/10.1016/j.solener.2011.11.006

Sunkara, B., Zhan, J., He, J., McPherson, G.L., Piringer, G., John, V.T. (2010). Nanoscale zerovalent iron supported on uniform carbon microspheres for the in situ remediation of chlorinated hydrocarbons. ACS Appl. Mater. Interfaces 2, 2854-2862

Tosco, T., Petrangeli Papini, M., Cruz Viggi, C., Sethi, R., 2014. Nanoscale zerovalent iron particles for groundwater remediation: A review. J. Clean. Prod. https://doi.org/10.1016/j.jclepro.2013.12.026

Wei, C., Zhang, F., Hu, Y., Feng, C., Wu, H., 2017. Ozonation in water treatment: The generation, basic properties of ozone and its practical application. Rev. Chem. Eng. https://doi.org/10.1515/revce-2016-0008

Chapter 2

2. Integration of microalgae in a conventional wastewater treatment plant

This chapter is based on the following publication:

Mantovani, M., Marazzi, F., Fornaroli, R., Bellucci, M., Ficara, E., Mezzanotte, V., 2020. Outdoor pilot-scale raceway as a microalgae-bacteria sidestream treatment in a WWTP. Sci. Total Environ. 710, 135583. https://doi.org/10.1016/j.scitotenv.2019.135583

2.1 Introduction

According to ISTAT data (2015) in Lombardy (the most populated region of Northern Italy) there are 1,498 wastewater treatment plants (WWTPs), 700 of which based on primary treatment, 400 on secondary treatment and 373 on tertiary treatment. Many of these are subject to particular restrictive limits for nutrients due to the sensitiveness of the area in terms of pollution or to the limited dilution potential of the receiving water body.

Wastewaters are not only rich in nutrients like nitrogen and phosphorus, but they also include inorganic components like sodium, potassium, magnesium, calcium, sulfur, chlorine, phosphates, bicarbonates and heavy metals. Urban wastewaters have historically been used as growth medium for microalgal cultivation and several studies have focused on specific microalgae strains and their ability to uptake nitrogen (NH_4-N, NO_3-N) and phosphorus. Usually, major treatment performances involve higher total operating expenses. Energy consumption contributes substantially to the operating costs of conventional WWTPs. It is estimated that the aeration needed for nitrification accounts for 45-75% of the global costs of the treatment (Rosso et al., 2008).

Microalgae are very versatile photosynthetic microorganisms that can grow in different kinds of environments, especially aquatic ones. They can adapt to wide ranges of pH, temperature, turbidity, concentration of carbon dioxide and nutrients (Jones et al., 2012). Currently, there is a worldwide gradual increase in microalgal cultivation aimed at using microalgal biomass as a source of valuable metabolites. Although water, nutrients and energy consumption limit the use of microalgae for commercial applications, the possibility to grow them using poor quality growth media like wastewaters is a promising strategy to make the microalgae production more cost-effective (Abdel-Raouf et al., 2012; Franchino et al., 2016; Pittman et al., 2011).

Processes based on microalgae/bacteria consortia could be very interesting for wastewater treatment since the two components may interact synergistically in different ways (Ramanan et al., 2016). Microalgae could be able to improve the removal efficiency of Biochemical oxygen demand (BOD) from wastewater by providing O_2 through photosynthesis. In fact, heterotrophic aerobic bacteria can use this low cost source of oxygen to degrade several pollutants (Muñoz et al., 2006). The concentration and availability of nutrients are surely crucial factors in the interaction between microalgae and bacteria; however, pH, global radiation and temperature are also very important (Delgadillo-Mirquez et al., 2016). Further, the oxidation of ammoniacal nitrogen by the ammonia oxidizing bacteria (AOB) exploiting the oxygen produced by

photosynthetic organisms could be a promising way to reduce the aeration request (Karya et al., 2013).

Centrate from biosolid dewatering seems particularly interesting as microalgal feed since it can provide an adequate source of macronutrients and allows light penetration (Wang et al., 2010).

The pilot-scale research presented in this paper aims at evaluating the feasibility of exploiting the microalgae-bacteria consortia as an additional process to be included into existing WWTP. The proposed idea is to use microalgae-bacteria consortia to treat the sidestream flow of centrate (Mezzanotte and Ficara, 2014). Because of its high nitrogen concentration, centrate cannot be discharged as it is, so it is normally sent back to the water line of the wastewater treatment plant. The retrofitting of existing WWPTs by integrating the treatment of centrate by microalgae/bacteria consortia before sending it back to the water line would allow to decrease the inflowing load of ammoniacal nitrogen. In fact, the contribution of recycled centrate normally makes about 20-30% of the nitrogen load entering a conventional WWTP (Van Kempen et al., 2001).

Such kind of upgrading would not require a complete redesign of the overall treatment sequence. The produced algal biomass could be sent to the anaerobic digester of the plant, to increase biogas production, thus further improving the energy balance and the carbon footprint of the entire process.

2.2 Materials and Methods

2.2.1. WWTP

This experimentation was carried out at the Bresso-Niguarda wastewater treatment plant, in the outskirts of Milan (I). The WWTP serves a population of 200,000 inhabitant equivalents (I.E). It includes a water line consisting in mechanical treatments, primary settling, secondary treatment with activated sludge process, tertiary treatment by filtration and disinfection by UV irradiation. The sludge line includes two mesophilic anaerobic digesters (operating at 35°C temperature), post-thickening and dewatering by centrifuging.

2.2.2 Microalgae inoculum

Based on previous experiences, *Chlorella* spp., *Scenedesmus* spp. and *Chlamydomonas* spp. were chosen for the outdoor cultivation on Bresso centrate. The strains were provided by Istituto Spallanzani (Rivolta d'Adda, CR, Italy) and grown in laboratory on Bresso centrate to prepare a 4.5 L inoculum. The counts of *Chlorella* spp., *Scenedesmus* spp. and *Chlamydomonas* spp. in the inoculum were 1.34x 10^5 cells mL^{-1}, 1.21x 10^5 cells mL^{-1} and 1.11x 10^5 cells mL^{-1}, respectively). The obtained suspension was first inoculated in 55 L of centrate in an outdoor PolyEthylene Terephthalate (PET) column to achieve the amount needed to inoculate a 1,200 L raceway pond. An air compressor connected to a fine bubble diffuser was used to ensure a continuous mixing of the algal suspension in the column while a heater was used to mitigate the temperature daily variations. The bubble column was operated in batch for 41 days (from the end of March to May 2017).

2.2.3 Raceway pond

The pilot raceway pond was located on a flat concrete platform. The raceway basin is made of two channels (each one 5 m long and 0.5 m wide) connected by 180° bends corresponding to an overall elliptical surface of 5.78 m^2. An overflow drain ensured a water height of 0.2 m for an average final volume of 1,200 L. The centrate was stored in 1,000 L tanks and fed continuously by a pump with a maximum flow rate (Qmax) of 15 L h^{-1} that could be regulated to obtain the desired hydraulic retention time (HRT).

A 70 L PET column was dedicated to gas transfer: there the microalgae culture was recirculated from and back to the raceway by a peristaltic pump. Air was bubbled to the bottom of the column through fine bubbles diffusers. The raceway was equipped with a cooling system consisting in a coil cooler exchanger where tap water ran during the hot summer months. The discharged microalgae suspension was stored in a 1,000 L tank.

The pilot reactor was also provided with probes for the monitoring of dissolved oxygen (Hack Lange, LDO sensor), pH and temperature (Hach Lange, pHD sc Digital Differential pH/ORP Sensors), and turbidity (Hack Lange, Solitax sc Sensors), which were installed upstream to the paddlewheel.

All the devices were connected to a Programmable Logic Controller (PLC) that allowed the real time monitoring and setting of all the operative parameters.

2.2.4 Experimental protocol

The raceway was initially filled with the content of the above described PET column (60 L) with a mix of centrate and tap water (50/50% v/v). After a short batch phase, the raceway was continuously fed with undiluted centrate. The average HRT was 10 days, chosen according to a previous work using Bresso centrate as influent (Francesca Marazzi et al., 2017). Samples from the inlet and outlet of the raceway were collected routinely for chemico-physical and microbiological analyses. Daily average values of temperature, irradiance and rainfall were taken from the meteorological station of Bresso WWTP.

2.2.5 Feed

The supernatant from sludge dewatering was collected from Bresso WWTP. Since it is obtained by centrifugation of the digested sludge, it is also called centrate. As shown by previous experiences (Ficara et al., 2014; F. Marazzi et al., 2019; Francesca Marazzi et al., 2017), the relatively low concentration of NH_4-N in Bresso centrate (Table 1) allowed its use as such, without any dilution. Even if N/P value did not respect the Redfield molar ratio, such centrate had been proven to be suitable as a microalgae growth medium. TSS concentration and the resulting turbidity in the centrate were quite variable due to the variable performances of the anaerobic digestion and, especially, of the centrifugation of sludge. The lowest ammonium and TSS concentrations were observed in summer when the city was less populated.

Table 1. Chemico-physical characteristics of the feed. All data are expressed as mean ± standard deviation (n=35)

NH_4-N ($mg\ L^{-1}$)	**NO_3-N** ($mg\ L^{-1}$)	**NO_2-N** ($mg\ L^{-1}$)	**PO_4-P** ($mg\ L^{-1}$)	**TSS** ($mg\ L^{-1}$)	**Optical density** $_{680nm}$	**COD** ($mg\ L^{-1}$)	**Conductivity** ($\mu S\ cm^{-1}$)	**pH**
244 ± 78	0.2 ± 0.2	0.4 ± 03	5.7 ± 0.8	83 ± 40	0.1 ± 0.1	112 ± 34	1492 ± 270	8.2 ± 0.3

2.2.6 Sampling and analyses

Samples were collected upstream to the paddlewheel, twice a week (on Monday and Friday) to perform the chemical analyses that were carried out on filtered samples using Hach-Lange kits for spectrophotometric quantitative measurements. Fresh samples (2 mL) were also collected from the raceway pond and stored at -20°C in ethanol 96% (sample-ethanol ratio 50%-50% v/v). Chemical analyses were carried out on filtered samples using Hach-Lange kits for spectrophotometric quantitative measurements. In detail, LCK 339, LCK 342, LCK 303, LCK 348, and LCK 314 kits have been used to assess the concentration of nitrate, nitrite and ammonium, phosphate-phosphorus and soluble COD respectively. Gravimetric analysis was performed to determine total suspended solids (TSS) and volatile suspended solids (VSS) according to Standard methods (APHA/AWWA/WEF, 2012). Optical density (OD) and turbidity were measured at 680 nm and 780 nm wavelength, respectively, by a spectrophotometer (DR 3900, Hach Lange, Germany). Microalgae were also counted using an optical microscope 40X (B 350, Optika, Italy) and a hemocytometer (Marienfeld, Germany). The different strains were distinguished on the basis of their morphology and size. Their number was estimated by the mean of 72 square observation. (0.04 mm^2) and expressed as cell mL^{-1}.

The elemental analysis on dried samples was performed by a Perkin Elmer CHNS/O analyzer 2400 series II. Phosphorus was determined after acid digestion (with H_2NO_3 and H_2O_2) of the dry biomass in a microwave digester (ETHOS 1600, Milestone) according to Green algae procedure (DG-EN-25).

2.2.7 Fluorescent in-Situ Hybridization (FISH)

Detection and semi-quantitative analyses of the nitrifying bacteria, AOB and NOB, in the microalgal suspension were performed using FISH assays. Fresh samples (2 mL) were collected from the raceway pond and stored at -20°C in ethanol 96% (sample-ethanol ratio 50%-50% v/v) prior to be fixed. Fixation was carried out using in 4% paraformaldehyde according to (Rudolf I. Amann, 2011; Micol Bellucci & Curtis, 2011). For the hybridization step, the microalgal suspension (20 µL) of each sample was placed in a well of the slide and CY3-fluorescently labelled probes (50 ng μL^{-1}) targeting the all phylogenetic group of the AOB, NOB and the entire bacterial community were added according to the protocol described in Bellucci et al. (2013). In particular, the probes Nso1225, NEU, and 6a192 were used to detect the AOB as recommended

in (Micol Bellucci & Curtis, 2011). Probes NIT3 and Ntspa662, plus the corresponding competitor probes, were applied for the identification of the nitrite oxidizing bacteria (NOB) (Holger Daims et al., 2001; Wagner et al., 1996) while EUB mix was applied to target the total bacterial community (R I Amann et al., 1990; H Daims et al., 1999). A few drops of a Fluoroshield mounting medium with DAPI (WVR, Italy) were added before covering the slide with the cover glass. Then, the hybridized biomass was observed by a Zeiss fluorescence microscope Axio Scope HBO 50. The low aggregation of the suspension, as well as the adequate dilution of the biomass in the well, allowed to visualize a mono layer of cells/colonies avoiding the need of using the Confocal Laser Scanning Microscope, highly recommended for FISH quantification. Images of each well (ca. 20) were captured randomly at 40x magnification and processed with Image J (Rasband, 2016) in order to determine the percentages of the targeted hybridized group within the total biomass. By considering the total biomass concentration expressed as VSS (mg L^{-1}), the AOB percentages were transformed into VSS_{AOB} mg L^{-1} and then into number of cells considering the diameter and total density of an AOB cell to be equal to 1 µm and 0.636 g cm^{-3}, respectively (Coskuner et al., 2005). By knowing the total number of AOB cells, it was possible to calculate the cell-specific ammonia oxidation as specified by Daims et al. (2001). The obtained data were then compared with the expected percentages of AOB biomass as a function of the ammoniacal oxidation rate of the RW using the following equation (Rittmann et al., 2001):

$$X_{AOB} = \left[Y_{AOB} * \frac{1 + (1 - f_d) * b_{AOB} * \theta}{1 + b_{AOB} * \theta} \right] * \Delta NH_4^+{}_{ox} - N$$

Where X_{AOB} is expressed as mg L^{-1}, θ is the solid retention time that is here equal to the HRT, *b* is the endogenous respiration rate (0.15 d^{-1}), *fd* is the biodegradable fraction of the active biomass (0.8), and Y_{AOB} is the AOB yield (0.34 kg VSS kg NH_4-N^{-1}). $\Delta NH_4{}^+{}_{ox}$ is the ammonium oxidized by AOB.

X_{AOB} was then converted into AOB %, by considering the total VSS concentration of the suspension.

2.2.8 Data processing

Assuming a constant volume for the raceway at the overflow level, the water balance was set across a time interval as:

$$Q_{out} = Q_{in} + P - Ev$$

Where: Ev is the average daily evaporation (L d^{-1}) and P is the average value of the daily cumulated precipitation (L d^{-1}), Q_{in} and Q_{out} were the inlet and outlet flow, respectively. Q_{in} was known and defined by the feeding pump, while Q_{out} was computed by using the water balance. Evaporation is a very important factor in the water balance of the raceway. In absence of daily measurements, it was calculated using the Penman equation (Penman, 2013), rewritten according to the SI by Shuttleworth (Shuttleworth, 2007).

Flows and concentrations were taken as mean values within a time interval $[t_i;t_{i+1}]$. Rates of relevant processes were calculated as follows:

$$r_x = \left[V * \left(\frac{Xout_{i+1} - Xout_i}{t_{i+1} - t_i}\right) - Q_{in} * \left(\frac{Xin_{i+1} + Xin_i}{2}\right) + Q_{out} * \left(\frac{Xout_{i+1} + Xout_i}{2}\right)\right] * \frac{1}{S}$$

Where $Xout_i$, $Xout_{i+1}$ are the concentration (on a mass basis) of a chemical/component X in the reactor at time t_i and t_{i+1}, respectively; Xin_i, Xin_{i+1} are the inlet concentration of X at time t_i and t_{i+1}, respectively; S is the area of the raceway and V is the volume.

The oxygen produced by microalgae (OPR) was evaluated as 1.55 g O_2 g^{-1} TSS, following the stoichiometry proposed by Vargas et al. (2016). The activity of AOB and NOB was also indirectly evaluated: AOB activity (rAOB) and NOB activity (rNOB) were assessed as nitrite and nitrate production rates, respectively (Pizzera et al., 2019). Finally, the oxygen request for nitrification (OR) was estimated as OR = 3.4 x rAOB + 1.1 x rNOB considering the stoichiometry of both nitrification reactions (Van Loosdrecht et al. 2016).

The nutrients removal efficiency (ηrim) was computed on a mass flow basis, according to the following formula:

$$\eta\text{rim} = \frac{(Q_{in} * X_{in}) - (Q_{out} * X_{out})}{(Q_{in} * X_{in})}$$

The daily partitioning of nitrogen in the effluent was obtained from the daily residual output loads of NH_4-N, of NO_2-N and NO_3-N (NO_2-N + NO_3-N was also considered as total oxidized nitrogen), of N in the algal biomass and of stripped N with respect to the total N load in the influent (N_{in},tot). The amount of nitrogen in algal biomass was computed by multiplying the outflowing TSS load

by 0.08 g N g TSS^{-1}, which is the average nitrogen concentration in the algal biomass according to the results of elemental analysis. The nitrogen removed by stripping was calculated as the complement to 100% with respect to the sum of the other fractions.

The estimate of the maximum algal productivity was finally computed as follows by assessing the maximum daily production per surface unit evaluated according to Park et al. (2011), considering light availability and photosynthetic efficiency as the drivers:

$$rTSS\_opt\left[\frac{gTSS}{m^2}\right] = \frac{Io\left[\frac{MJ}{m^2 d}\right] * H[\%]}{Ec\left[\frac{MJ}{gTSS}\right]}$$

where: rTSS_opt is the maximum algal productivity; I_0 is the average solar radiation in the considered time window; Ec is the energy content of algal biomass in terms of heat power (0.021 MJg^{-1} TSS); H is the maximum efficiency of photosynthetic solar energy conversion, which was assumed equal to 1.3 % of total solar radiation due to reflection loss and light saturation of algal photosystem (Park et al., 2011; Walker, 2009).

2.2.9 Statistical analyses

Statistical analyses were carried out using R project software (R Core Team, 2018) to study the relationship between microalgal and bacterial growth with environmental conditions. Generalized linear models (GLMs) were used to analyze the effects of both continuous ad categorical variables at the same time. The independent variables used in the GLMs were the NH_4-N, TSS, COD and PO_4-P concentration in the centrate, cumulative irradiance, cumulative air temperature and rain (n=4 days) (Marazzi et al., 2017). The continuous variable rain was transformed into a categorical one, dividing the trial in “rainy days” and “sunny days”. All these independent variables were chosen among the full starting group using the VIF value (Variance Inflation Factor, threshold <10) to minimize multicollinearity. Restricted models were generated by removing variables in a backward-stepwise procedure and compared with the full GLM model by ANOVA. The computed models were used to predict the effect of the independent variables on daily microalgal production (rTSS) and microbial productivity (rAOB and rNOB).

2.3 Results and discussion

2.3.1 Microalgal productivity and community evolution

The growth of microalgae was monitored using total suspended solids (TSS) and algal counts as indicators. The trend of TSS with time is reported in Figure 1 as well as global radiation and temperature, which are major factors affecting microalgal growth. TSS concentration seems to have a similar trend as global radiation and this is very clear in the first period and during the last 30 days when the decrease of TSS concentration follows the decrease of radiation. Moreover, other factors, such as temperature and rainfall are known to affect algal growth, making it difficult to identify a simple relationship between TSS and radiation. On day 30 of continuous operation (June 30th), a clogging issue occurred on the recirculation pipe, causing the suspension to overflow and be wasted from the gas-transfer column (event hereafter referred to as "mishap"). Around 350 L of microalgal suspension were saved and used as a new inoculum; 50 % water and 50 % centrate mix was used to re-fill the raceway. That event clearly had a negative effect on microalgae, as the concentration of suspended solids reached back the pre-mishap levels only after two weeks. Afterwards, microalgae concentration stabilizes until the change of season. In September, starting from day 90, there was a substantial worsening of environmental conditions. Average temperature had rapidly dropped from 26°C in August to 17°C in September and the same trend was observed for average radiation that had dropped from 250 Wm^{-2} to 165 Wm^{-2}. Heavy rains also occurred at the beginning of September (day 96). Probably due to these multiple stresses, which on the other hand are common in pilot scale open air experiments, during the last month of the experimentation microalgae flocculated. That phenomenon led to sampling difficulties interfering with the productivity assessment. Considering the approaching of the winter season and the adverse environmental conditions, the trial was interrupted in mid-October.

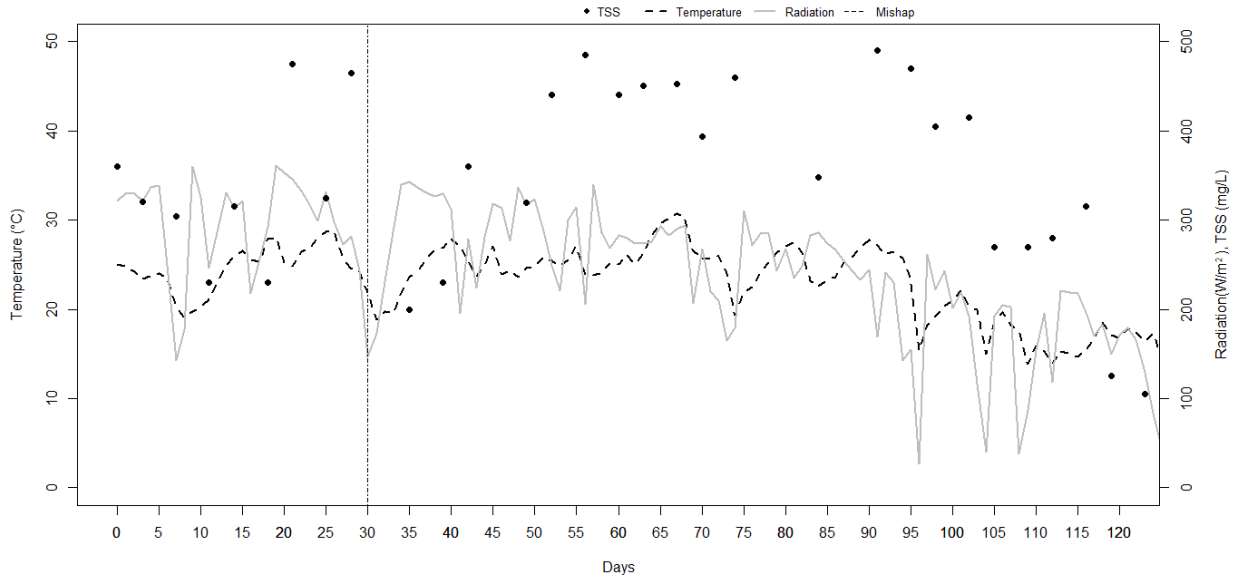

Figure 1. Trend of Total Suspended Solids, radiation and temperature during the continuous phase

As shown in Figure 2a, in the column reactor all the inoculated microalgae strains were present. In the raceway, during the batch phase (Figure 2b) *Scenedesmus* spp. and *Chlamydomonas* spp. increased gradually while *Chlorella* spp. slightly decreased starting from day 14. The situation changed when shifting to continuous mode as *Chlorella* spp. became dominant in the raceway while the other two populations rapidly declined (Figure 2c).

Most likely, changes in the environmental conditions and in light penetration influenced the evolution in the microalgal community. Some interesting laboratory scale studies concerning population dynamics of phytoplankton species claim that light competition is a very interesting phenomenon to be examined. Huisman et al., (1999) analyzed the competition for light between *Chlorella* spp. and *Scenedesmus* spp. by performing monoculture laboratory tests and competition tests and found that *Chlorella* spp. was a superior competitor with respect to *Scenedesmus* spp. in all the tests since it has a lower value of critical light intensity. In Bresso case no specific values were measured, but in the column the aeration flow was likely to ensure a more uniform exposition to sunlight even when the algal density was at its maximum. At the beginning of the batch phase of the raceway operation all the taxa might have grown rapidly because there was no severe light limitation due to the low algal suspension density. The increasing turbidity of the microalgal suspension in the continuous run led to a gradual decrease of light penetration through the raceway

water column. *Scenedesmus* spp. and *Chlamydomonas* spp. might have become less competitive upon denser culture conditions.

In spite of being open-air and thus exposed to contamination, the algal population remained quite stable and no predators were observed. In fact, apart from the above-mentioned mishap, no drop in the algal density was observed during the good season. The decline of the cell density observed at the end of the experimentation was the response to the decrease of light intensity and temperature.

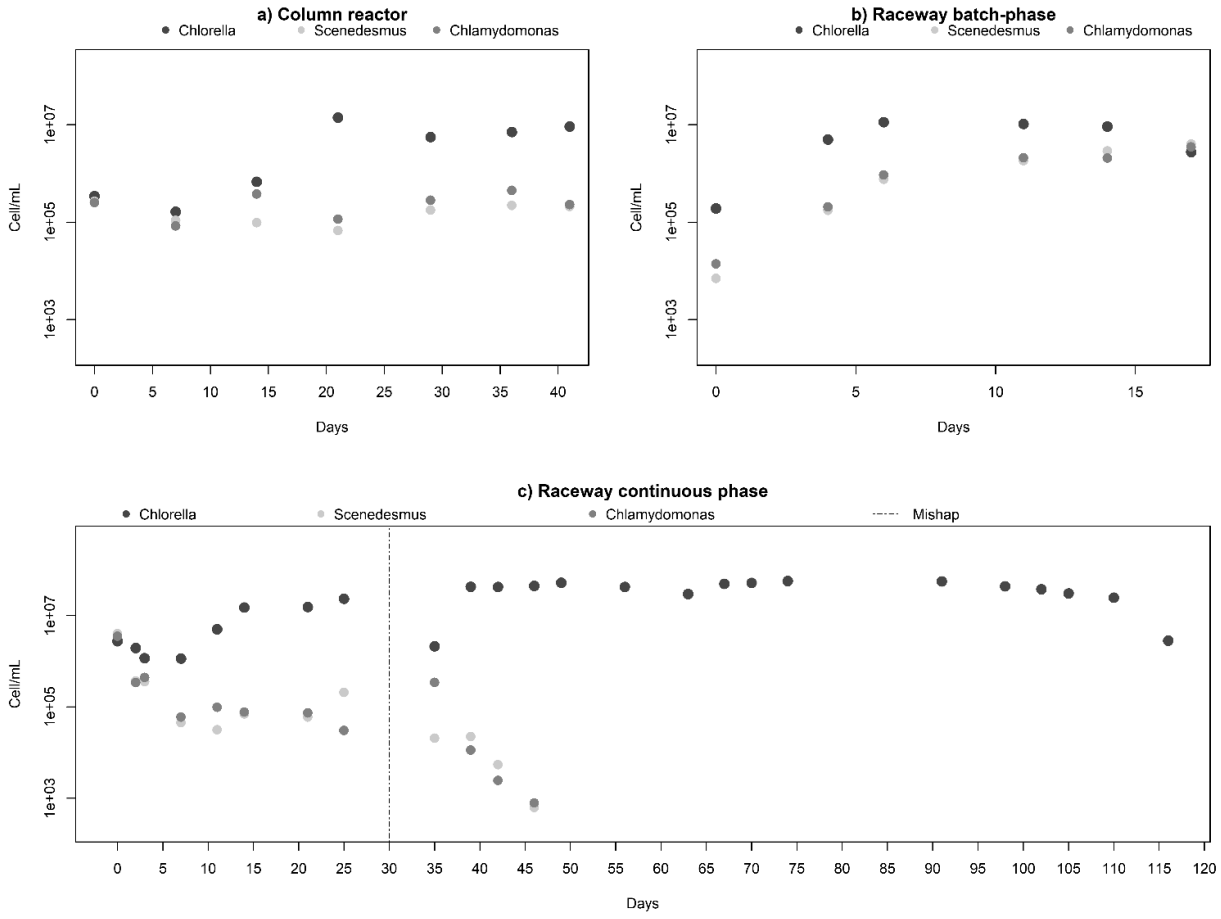

Figure 2. Microalgae counts during the preliminary phase in the column reactor (a); the batch phase (b) and continuous phase (c) of the raceway.

Optical density (680 nm), algal counts, turbidity, total suspended solids (TSS) and volatile suspended solids (VSS) have also been put in correlation to verify their reliability as indicators of microalgal biomass growth. The best correlations were found between algal counts and turbidity ($R^2 = 0.86$) and between counts and optical density ($R^2 = 0.87$). The correlations involving TSS and VSS were not so good, probably due to sampling problems, especially when flocculation

occurred, limiting the representativeness of the data. Moreover, TSS also include other particulate materials, such as salt precipitates, microbial biomass, residual suspended solids in the centrate, and cell debris.

Microalgal areal productivity obtained from experimental data was compared to the potential biomass productivity estimated by Park's model (Park, 2011) (Table 2).

Table 2. Main statistics on microalgae biomass areal production, monthly basis, and ratio between actual and optimal productivities (%)

		June	July	August	September
rTSS [g TSS m^{-2} d^{-1}]	Mean ± St.dev.	4.9 ± 9.3	8.4 ± 6.1	7.1 ± 5.6	3.4 ± 6.4
rTSS/rTSS_opt	%	30%	49%	47%	32%

The high standard deviation recorded in June is probably linked to the instability of the first days of the trial. In July and August, a similar areal production was recorded since the environmental conditions were quite stable and favorable. However, in September there was certainly a decrease in biomass production and the flocculation occurred in that phase led to sampling difficulties. In that period solar height had lowered with respect to the previous months, increasing the shadowing effect caused by the trees placed south of the raceway. The average overall microalgae areal productivity was 5.5 ± 7.4 g TSS m^{-2} d^{-1}. Apparently, there is not a defined ratio between actual and optimal productivities. Actual productivity was quite variable due to the uncontrolled outdoor conditions.

Other factors to be considered are the possible limitation by CO_2 and P (Marazzi et al., 2019), deriving from the competition between microalgae and nitrifying bacteria. In their turn, the presence and activity of nitrifying bacteria could have been fostered by the poor availability of degradable organic matter, preventing the development of a rich and oxygen competitive heterotrophic bacteria community. A further effect of the absence of available organic substrate is a reduced production of CO_2 from bacteria which could have helped microalgal development. The whole of such factors surely affected the growth rate of microalgae, preventing to adopt a shorter HRT which could make the process more cost-effective.

2.3.2 Nitrogen and phosphorus removal

Figure 3a reports the concentration of NH_4-N in the influent and the different nitrogen species in the effluent of the raceway. Ammonium, nitrite and nitrate trends at the outlet of the raceway are affected by nitrification, while the slow but notable decrease in NH_4-N inlet concentration is probably due to changes in digested sludge characteristics or centrifuge operation. Indeed, nitrification was observed starting from day 20. Nitrification was incomplete since nitrite instead of nitrate was the prevailing oxidized nitrogen. Nitrite concentration was very high until day 100, while the oxidation of nitrite to nitrate became relevant only from day 110. The trends of nitrite and nitrate suggest that Ammonia Oxidizing Bacteria (AOB) developed faster and were better adapted to the raceway condition than Nitrite Oxidizing Bacteria (NOB). The higher starting NH_4-N load in the pond probably promoted AOB over NOB. The occurring of nitrite oxidation in the final period of the trial might be due the seasonal change, when microalgae and AOB became less competitive with respect to NOB. Indeed, literature shows that free ammonia and nitrous acid concentration, dissolved oxygen, pH and temperature are the main aspects that can influence the nitrification process, leading to nitritation rather than a complete nitrification (Van Hulle et al., 2010). Figure 3b shows the concentration of PO_4-P in the influent and in the effluent of the raceway.

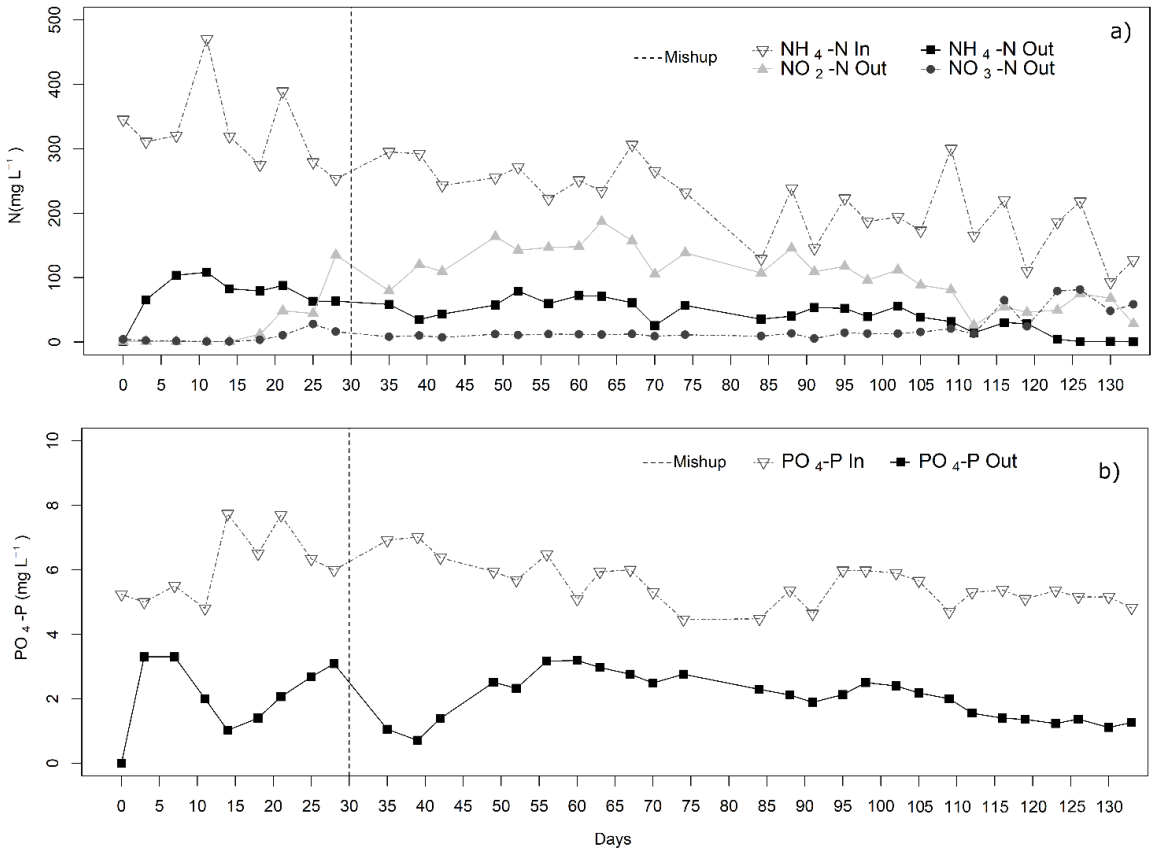

Figure 3. Nutrient evolution in time. Concentration of NH4-N in the influent is compared with the concentration of NH_4-N, NO_2-N and NO_3 -N in the effluent (a) while the concentration of PO_4-P in the influent is compared with the one of PO_4-P in the effluent (b).

The graphs highlight the potential of microalgal-bacteria consortia in wastewater treatment. In this experimentation satisfactory results were achieved: PO_4-P removal efficiency (η PO_4-P) was 71% ± 10% while NH_4-N removal (η NH_4-N) was 86% ± 7%.

Figure 4 reports the time trend of the total nitrogen apportioning and pH in the algal suspension. At the beginning of the trial the high microalgal activity strongly raised pH and this caused relevant nitrogen stripping. Starting from day 20, partial nitrification occurred. From that moment on, nitritation was a constant condition especially in July and August. Nitrogen assimilation by microalgae was low and quite stable. Nitrogen stripping, on the other end, was very relevant especially during the first and in the last part of the trial. Nitrogen stripping could be due either to NH_3 volatilization and to denitrification. Traditionally, denitrification was considered as an anoxic process and thus unlikely to occur in an algal pond where oxygen is always present due to photosynthesis. In fact, in Bresso pilot raceway the anoxic periods (at night) registered by the DO probe were too rare to make it contribute significantly to the nitrogen balance (see paragraph 3.3).

However, in the last years, aerobic denitrifiers have been found and identified (Ji et al., 2015; Lv et al., 2017). So, the contribution of N_2 produced by aerobic denitrification to the amount of stripped nitrogen cannot be excluded.

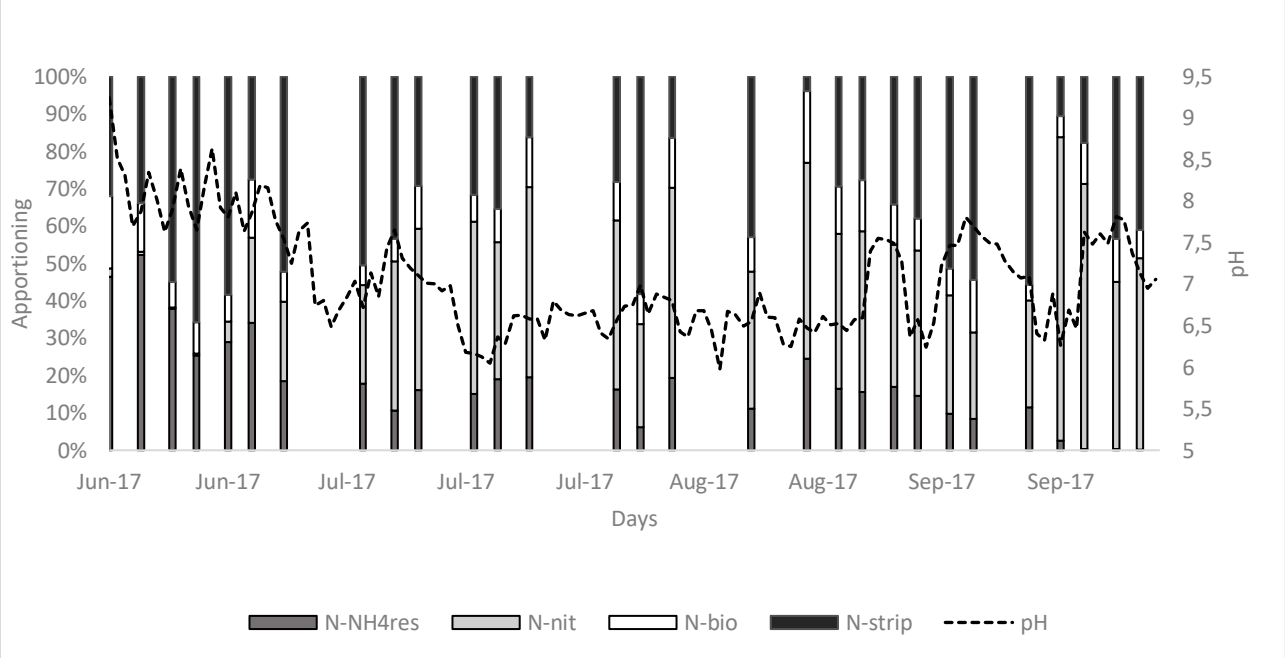

Figure 4. Nitrogen apportioning and raceway pH evolution in time: N-NH_4res represents the residual nitrogen, N-nitr is the nitrogen oxidized by nitrifying bacteria (as $N0_2$-N+NO_3-N), N-strip is the stripped nitrogen and N-bio is the fraction of biomass uptake.

Figure 5 summarizes these data as pie-charts. Data are presented for two different periods. The first one considers the entire trial, the second one starts from day 42 to exclude the time where pH was quite high promoting nitrogen stripping. Future experimentation will be performed by controlling pH to limit this issue. Considering the whole trial, the residual NH_4-N was, on average, 19%. Microalgal assimilated fraction was 10% while the sum of the oxidized forms accounted for 34%. The stripped fraction was quite relevant with a 37%. However, if we consider only the data from day 42 of continuous operation, deemed as representative of a well-established algae/nitrifiers community, the results are more encouraging. As described above, the increased activities of both AOB and NOB led to a different nitrogen apportioning. The nitrified nitrogen

increased to 45% while the residual ammonium and the stripped fraction decreased to 13% and 32%, respectively.

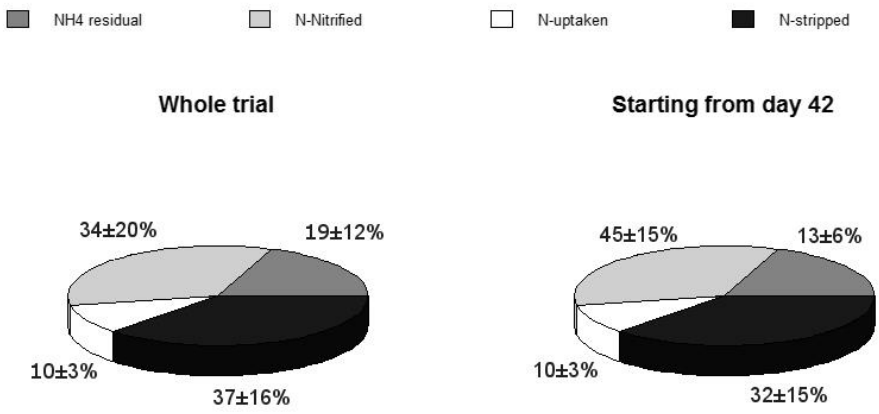

Figure 5. Pie-chart representations of the different contributions to nitrogen conversion. On the left the results computed on the whole trial. On the right, the same data are computed starting from day 42 when the raceway was on a quasi-steady state condition.

2.3.3 Nitrifying bacteria detection and quantification

FISH analyses were performed to confirm the presence of nitrifying bacteria and to quantify them. AOB were detected in all samples; colonies were mostly found over microalgal-aggregates as visible in Figure 6 and flocs or even in the biofilm attached to the raceway wall at water/air interface. The percentages of the AOB over the entire biomass (total bacteria plus microalgae) ranged between 0.5 and 5.2 % with a cell-specific ammonia oxidation rate from 0.07 to 5.6 fmol $cell^{-1}$ h^{-1} in line with previous studies focusing on the activity of AOB in efficiently performing nitrifying systems (Micol Bellucci, Ofiţeru, et al., 2011; Coskuner et al., 2005; Holger Daims et al., 2001). Although the quantification procedure was not performed with the standard protocol, which recommends the use of the Confocal Laser Scanning Microscope, the determined numbers were similar to the expected numbers of AOB, which was estimated considering nitrite production rate and the total VSS of the algal suspension (Figure 7). The only significant discrepancy was observed in the sample collected at day 42 when the microalgae/bacteria consortium could have still been in a recovery state after the accident occurred some days before. NOB could not be detected in any of the hybridized samples indicating that they were under the detection limit of the method. This is not surprising as at the beginning of the trial nitrite oxidation was not observed. Nitrate production occurred only during the last days of the trial, indicating NOB activity.

However, during these days the microalgal suspension was heavily flocculated causing some difficulties on collecting a representative biomass sample, as well as on the visualization of the NOB within the aggregates with the applied method.

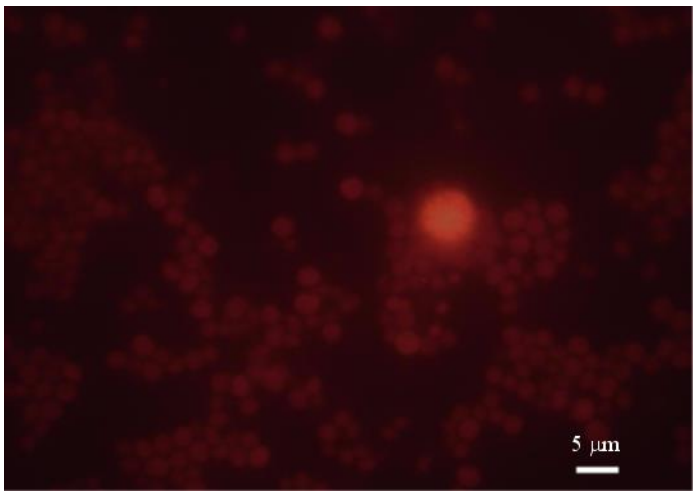

Figure 6. A colony of Ammonia Oxidizing Bacteria (bright red) hybridized with a mix of CY3-labelled probes in a microalgal aggregate (faint red) observed at 100x.

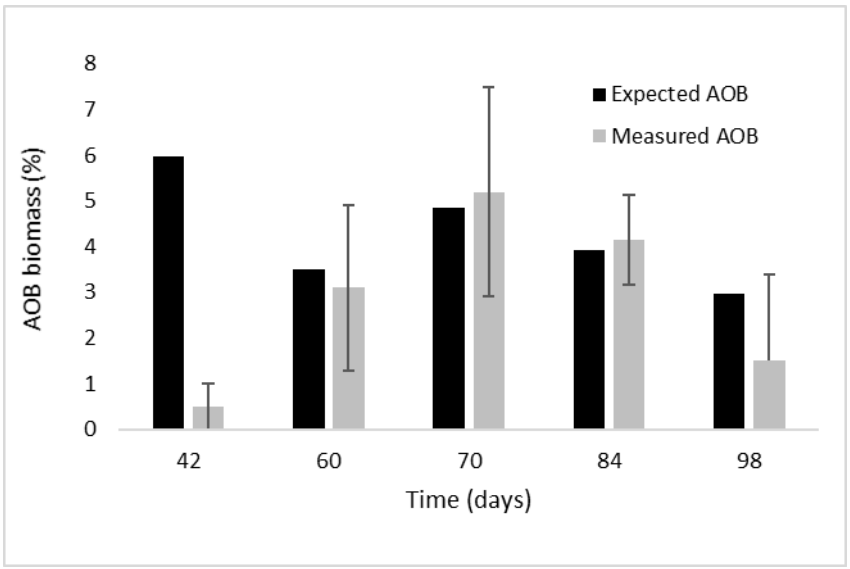

Figure 7. Comparison between the expected (black) and the empirical (gray) percentages of AOB biomass in the reactor suspension.

2.3.4 Oxygen balance

Microalgal growth promoted an aerobic environment in the raceway pond due to photosynthesis. Dissolved oxygen was monitored continuously. During the whole trial an average of 8.4 ± 2.3 mg O_2 L^{-1} was obtained with a maximum of 15 ± 2 mg O_2 L^{-1} and a minimum of 4.2 ± 2.2 mg O_2 L^{-1}. Minimum values were recorded during night hours when the consumption due to respiration and microbial activities was not compensated by photosynthesis. By considering the hourly data values we were able to rule out the presence of relevant anoxic periods.

Microalgal oxygen production was compared with the oxygen needed by nitrifying bacteria to sustain their activity. The results are shown in Table 3 indicating that photo-oxygenation was enough to support nitrification during the trial. The only gap seems to have occurred in September. However, as previously explained, in that phase of the raceway operation microalgal flocculation occurred. rTSS and therefore OPR might have been underestimated due to the difficulties in collecting representative samples.

Table 3. Oxygen balance main statistics (Mean ± st.dev.)

	rTSS	***rAOB***	***rNOB***	***OPR***	***OR***
	g $m^{-2}d^{-1}$	***g $m^{-2}d^{-1}$***	***g $m^{-2}d^{-1}$***	***g $m^{-2}d^{-1}$***	***g $m^{-2}d^{-1}$***
June	*4.9 ± 9.3*	*1.8 ± 2.4*	*0.2 ± 0.5*	*7.6 ± 14.9*	*6.2 ± 8.0*
July	*8.4 ± 6.1*	*3.2 ± 2.0*	*0.2 ± 0.1*	*13.2 ± 11.4*	*11.1 ± 6.7*
August	*7.1 ± 2.6*	*1.3 ± 2.4*	*0.09 ± 0.29*	*11.1 ± 8.8*	*4.4 ± 8.3*
September	*3.4 ± 6.4*	*1.4 ± 2.9*	*1.1 ± 1.9*	*5.2 ± 11.9*	*5.9 ± 11.5*
Average	*5.5 ± 7.4*	*1.9 ± 2.5*	*0.5 ± 1.2*	*8.6 ± 11.3*	*7 ± 9*

2.3.5 Statistical analyses

Table 4 summarizes those parameters that were identified as significant according to the GLM models. The results are also shown in Figure 8. Microalgal growth rate (rTSS) and AOB activity (rAOB) were positively correlated to the PO_4-P inlet concentration. Competition for PO_4-P might have affected microalgae and AOB more than the environmental conditions such as light and temperature. This might be odd since environmental conditions should affect microalgal growth, but the raceway operation period (from June to October) run during the best environmental conditions for microalgae growth. At the same time this result confirms the key role of PO_4-P in the microalgae-based system and its limiting effect on microalgae growth due to the low concentration of PO_4-P in the inlet (5.7 ± 0.8 mg L^{-1}).

On the other hand, as the substrate for nitrification is ammonium, NH_4-Nin was positively related to the nitrite oxidizing bacteria growth rate (rNOB) as already presented in Marazzi et al (2017). rNOB shows also a negative correlation with cumulative rain and cumulative radiation. When no rain occurred in the 4 days prior the sampling, NOB were more relevant. Furthermore, according to Merbt et al. (2012) nitrite oxidizers are more photosensitive than ammonia oxidizers and this could explain the incomplete nitrification. At the same time rNOB activity appeared at the end of the experimental period (as shown in Figure 3) when the solar radiation became lower. However, the complexity of the system is such as to make it difficult to define strong correlations.

Table 4. Summary of significant correlations (+ for positive and – for negative) on data from the raceway continuous operation

	Independent variable							
Dependent variables	NH_4-N_{in} (mg/L)	PO_4-P_{in} (mg/L)	TSS_{in} (mg/L)	COD_{in} (mg/L)	Temp (°C)	Rain (yes/no)	Radiation (W/m^2 d)	**Distribution**
rAOB (g/m^2 d)		+						Lognormal
rNOB (g/m^2 d)	+					-	-	Gamma
rTSS (g/m^2 d)		+						Normal

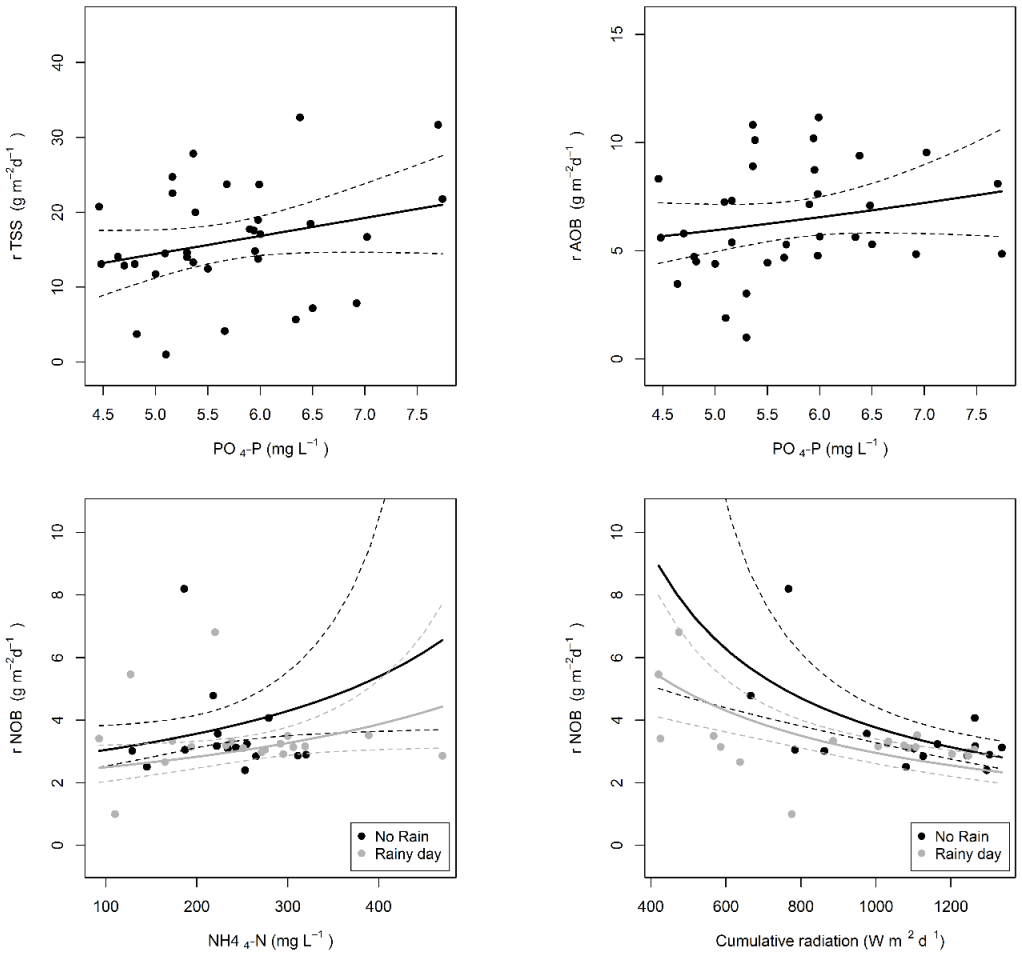

Figure 8. Effect plot for the predictor of the rTSS, rAOB and rNOB obtained with the GLMs. Dots are experimental data, solid lines represent the prediction models, dashed lines represent the 95th-percent confidence interval.

2.3.6 Expected energy savings

Considering a full-scale application in Bresso WWTP an energetic balance can be conceived based on the experimental data and the assumptions listed in table 5.

An experimental productivity of 7.2 g TSS m^{-2} d^{-1} was considered for the computation. This value is 20% higher than the one obtained during the trial. However, working with a more efficient source of carbon supply such as the off-gas a higher productivity should be expected.

The energetic balance considers the reduced demand of oxygen for nitrification (the ammonia nitrogen in the centrate that is redirected to the waterline will be mostly oxidized using the oxygen produced by microalgae) and the extra energy production obtained sending the microalgal biomass to anaerobic digestion.

A net energy saving of 0.382 Wm^{-2} would be achieved as indicated in table 6. The data already includes the energy consumption for the paddlewheel and the extra costs in the sludge line.
This energetic balance must be considered as approximate. Additive costs or saving concerning COD and phosphorus removal in the raceway were not considered. Anaerobic digestion was chosen as the main biomass valorization. Bio-methane potential (BMP) tests were performed (data not shown) highlighting similar results compared to previous studies (Francesca Marazzi et al., 2017). Specific research on different potential biomass valorization are currently ongoing since higher value products other than biogas are needed to achieve a positive economic assessment (i.e. bio-stimulant and bioplastics). Also, an accurate life cycle assessment is clearly needed in order to prove the overall sustainability of the full-scale application.

Table 5. Assumptions list for the energy balance

Parameters	Symbol	Value	Units	Reference
Operational days of the pond	d_{op}	275	d/y	Working assumption
HRT		9	D	Working assumption
Water height	H	0.1	M	Working assumption
Experimental Productivity	rTSS	7.2	g TSS m^{-2} d^{-1}	Experimental data
Shadowing effect	S	30%		Working assumption
N content in algae biomass	N_{TSS}	0.07	g N TSS^{-1}	Experimental data
N-Uptaken	N_{bio}	11%		Fig.5
N-Nitrified	N_{nit}	44%		Fig.5
Stripping	N_{str}	30%		Fig.5
N residual	N_{res}	15%		Fig.5
Energy consumption for N removed at Bresso	E_{WWTP}	2.4	kWh kg^{-1} N_{in}	Milano-Bresso WWTP data
Energy consumption in sludge line	E_{sludge}	0.17	kWh kg^{-1} TSS	Milano-Bresso WWTP data
Biomethane potential	BMP	0.18	LCH_4 g^{-1} TSS	Previously studies (Marazzi et al., 2017)
CHP efficiency	η_{CHP}	0.34		Milano-Bresso WWTP data
Lower Heating Value methane	LHV	9.96	kWh m^{-3}	
Centrifuge efficiency	H_{sep}	0.9		Lab centrifuge
Paddlewheel power	W_p	2	W m^{-3}	

Table 6. Energy calculation

Parameters	Formula	Value	Units
Productivity without shadow (Ps)	rTSS x (1+s)	9.36	g TSS $m^{-2}d^{-1}$
N assimilated (a)	Ps x N_{TSS}	0.66	g N $m^{-2}d^{-1}$
N-Nitrified (b)	(a/N_{bio}) x N_{nit}	2.69	g N $m^{-2}d^{-1}$
N-Stripped (c)	(a/N_{bio}) x N_{str}	1.84	g N $m^{-2}d^{-1}$
Tot N not to be oxidized (e)	a+b+c	5.19	g N $m^{-2}d^{-1}$
Extra Biomethane ($CH_{4\ Algae}$)	η_{sep} x Ps x BmP x d_{op}/365	1.14	L $m^{-2}d^{-1}$
O_2 saved	e x 3.43 x d_{op}/365	13.4	g $m^{-2}d^{-1}$
Aeration savings (F)	(e x E_{WWTP} x d_{op}/365)/24	0.40	W m^{-2}
Extra energy from anaerobic digestion (G)	$CH_{4\ Algae}$ x LHV/24 x η_{CHP}	0.179	W m^{-2}
Energy consumption for paddlewheel (H)	W_p x h x d_{op}/365	0.150	W m^{-2}
Extra costs for sludge line (I)	Ps x E_{sludge}/24 x d_{op}/365	0.049	W m^{-2}
Net energy saved	F+G-(H+I)	0.382	W m^{-2}

2.4 Discussion

During the pilot test a stable microalgal community was maintained from May to the end of September, as the tested culturing conditions were suitable.

Comparisons with other studies are quite complicated since the environmental conditions depend on the specific site. Similar applications are not even that widespread and chiefly based on different climate areas such as Spain and New Zealand. The climate in Northern Italy is certainly not optimal for microalgal cultivation. Winter seasons are far too cold for the microalgae-bacteria based treatment as described in the previous pages.

The measured microalgal productivity was 5.5 ± 7.4 g TSS $m^{-2}d^{-1}$ (20.8 ± 28.1 mg TSS $L^{-1}d^{-1}$), slightly lower than the one obtained by Pizzera et al. (2019) (8.2 ± 8.5 g TSS $m^{-2}d^{-1}$) growing microalgae on the centrate from a piggery WWTP in the Cremona Province (Northern Italy). Even if the environmental conditions in Cremona could be considered similar to the ones in Bresso, the wastewater was clearly different, having higher nutrient concentrations and N/P ratio closer to Redfield value. This could have allowed a higher microalgal productivity which was also supported by the addition of CO_2 to ensure an extra carbon source. A review citing productivities in wastewaters reports slightly higher values (23–40 mg TSS L^{-1} d^{-1}) but does not give any specific indication about centrates (Pittman et al. 2011). Our previous studies, based on the outdoor cultivation of microalgae in Bresso WWTP, provided higher productivities but were performed in different conditions: a column reactor was used instead of the raceway pond and the off-gas from the CHP unit was bubbled to ensure mixing and CO_2 (Marazzi et al., 2017; Marazzi et al., 2019).

In full-scale applications, an important item would be the reduction of HRT. This could only be obtained by improving algal productivity.

In the future, the off-gas from the cogeneration unit of the WWTP will be used instead of air with the double aim to control the pH and provide an extra supply of CO_2 thus improving algal growth.

The use of selected, fast-growing strains could also be considered, but, in a full-scale application within a WWTP this would involve a significant increase of complexity and cost. In fact, a specific side-stream culture to be used for re-inoculum should be maintained to control the microalgal community. This could be affordable if the advantages of such solutions (i.e. in terms of biogas production from microalgae or from higher bio-stimulating properties in the produced biomass) could be assessed and quantified.

It is likely that attached microalgae cultivation systems could provide higher algal densities and allow shorter HRT. However, the same considerations made for the selection of fast-growing strains apply to this possibility: the capital and operation costs of a raceway system are surely lower than the costs for more complex systems.

The observed stripping was certainly high, but the available data do not allow to understand if it was due to NH_3 volatilization (as the high pH could lead to suppose) or to denitrification. Anyway, the pH control deriving from the supply of CO_2 from the off-gas would also reduce the risks of NH_3 volatilization.

Photo-oxygenation was enough to sustain nitrification in the raceway leading to the conversion of ammonium to nitrogen oxidized species. Considering the oxygen demand indicated in Daigger (2014) for the biological nitrogen oxidation and assuming for the raceway an average areal productivity of 5 g TSS $m^{-2}d^{-1}$, the production of oxygen by microalgal photosynthesis would be higher than needed to sustain nitrification.

2.5 Conclusions

The technical feasibility of integrating a microalgae-bacteria based system within an existing WWTP in Northern Italy was confirmed even if variable productivities were obtained (5.5 ± 7.4 g TSS m^{-2} d^{-1}). Despite the overall non optimal conditions related to climate and to the feed properties, the obtained productivity was comparable to the literature values in more favorable situations.

The microalgal photo-oxygenation supported the activity of nitrifying bacteria and the overall removal of NH_4-N was very high. This is enough to say that, in the scale-up hypothesis, the

microalgal treatment of centrate could lead to a relevant decrease of energy demand for nitrification in the WWTP.

The process efficiency could probably be improved supplying CO_2 by bubbling off-gas from the co-generation unit in order to limit pH variations and to increase microalgal growth. In fact, in the present conditions, where nitrification was relevant, it is likely that competition between nitrifying bacteria and microalgae for CO_2 resulted in carbon limitation for these ones. This sounds particularly important considering that the absence of degradable organic substrate did not allow the production of CO_2 from bacteria.

Further investigations will be carried out to understand the respective role of denitrification and NH_3 production and stripping: of course, the environmental impact would be much better if the stripped fraction of nitrogen was made of N_2 rather than of NH_3.

Process modifications to decrease HRT could be considered if the value of the produced microalgal biomass could justify the additional costs involved.

2.6 References

Abdel-Raouf, N., Al-Homaidan, A.A., Ibraheem, I.B.M., 2012. Microalgae and wastewater treatment. Saudi J. Biol. Sci. https://doi.org/10.1016/j.sjbs.2012.04.005

Amann, R.I., 2011. In situ identification of micro-organisms by whole cell hybridization with rRNA-targeted nucleic acid probes, in: Molecular Microbial Ecology Manual. https://doi.org/10.1007/978-94-011-0351-0_23

Amann, R.I., Binder, B.J., Olson, R.J., Chisholm, S.W., Devereux, R., Stahl, D.A., 1990. Combination of 16S rRNA-targeted oligonucleotide probes with flow cytometry for analyzing mixed microbial populations. Appl. Environ. Microbiol.

APHA/AWWA/WEF, 2012. Standard Methods for the Examination of Water and Wastewater. Stand. Methods 541. https://doi.org/ISBN 9780875532356

Bellucci, M., Curtis, T.P., 2011. Ammonia-oxidizing bacteria in wastewater, 1st ed, Methods in Enzymology. Elsevier Inc. https://doi.org/10.1016/B978-0-12-386489-5.00011-7

Bellucci, M., Ofiţeru, I.D., Graham, D.W., Head, I.M., Curtis, T.P., 2011. Low-Dissolved-Oxygen Nitrifying Systems Exploit Ammonia-Oxidizing Bacteria with Unusually High Yields. Appl. Environ. Microbiol. https://doi.org/10.1128/aem.00330-11

Bellucci, M., Ofiţeru, I.D., Head, I.M., Curtis, T.P., Graham, D.W., 2013. Nitrification in hybrid bioreactors treating simulated domestic wastewater. J. Appl. Microbiol. https://doi.org/10.1111/jam.12233

Coskuner, G., Ballinger, S.J., Davenport, R.J., Pickering, R.L., Solera, R., Head, I.M., Curtis, T.P., 2005. Agreement between theory and measurement in quantification of ammonia-oxidizing bacteria. Appl. Environ. Microbiol. https://doi.org/10.1128/AEM.71.10.6325-6334.2005

Daigger, G.T., 2014. Oxygen and Carbon Requirements for Biological Nitrogen Removal Processes Accomplishing Nitrification, Nitritation, and Anammox. Water Environ. Res. 86, 204–209. https://doi.org/10.2175/106143013X13807328849459

Daims, H., A.Brühl, R.Amann, K.-H.Schleifer, M.Wagner, and, 1999. The domain- Bacteria: Development and evaluation of a more comprehensive probe set. Syst. Appl. Microbiol. https://doi.org/Doi 10.1016/S0723-2020(99)80053-8

Daims, H., Ramsing, N.B., Schleifer, K.H., Wagner, M., 2001. Cultivation-Independent, Semiautomatic Determination of Absolute Bacterial Cell Numbers in Environmental Samples by Fluorescence in Situ Hybridization. Appl. Environ. Microbiol. https://doi.org/10.1128/AEM.67.12.5810-5818.2001

Delgadillo-Mirquez, L., Lopes, F., Taidi, B., Pareau, D., 2016. Nitrogen and phosphate removal from wastewater with a mixed microalgae and bacteria culture. Biotechnol. Reports 11, 18–26. https://doi.org/10.1016/j.btre.2016.04.003

Ficara, E., Uslenghi, A., Basilico, D., Mezzanotte, V., 2014. Growth of microalgal biomass on supernatant from biosolid dewatering. Water Sci. Technol. 69, 896–902. https://doi.org/10.2166/wst.2013.805

Franchino, M., Tigini, V., Varese, G.C., Mussat Sartor, R., Bona, F., 2016. Microalgae treatment removes nutrients and reduces ecotoxicity of diluted piggery digestate. Sci. Total Environ. https://doi.org/10.1016/j.scitotenv.2016.06.100

Huisman, J., Jonker, R.R., Zonneveld, C., Weissing, F.J., 1999. Competition for light between phytoplankton species: Experimental tests of mechanistic theory. Ecology 80, 211–222. https://doi.org/10.1890/0012-9658(1999)080[0211:CFLBPS]2.0.CO;2

Ji, B., Yang, K., Zhu, L., Jiang, Y., Wang, H., Zhou, J., Zhang, H., 2015. Aerobic denitrification: A review of important advances of the last 30 years. Biotechnol. Bioprocess Eng. https://doi.org/10.1007/s12257-015-0009-0

Jones, C.S., Mayfield, S.P., 2012. Algae biofuels: Versatility for the future of bioenergy. Curr. Opin. Biotechnol. https://doi.org/10.1016/j.copbio.2011.10.013

Karya, N.G.A.I., van der Steen, N.P., Lens, P.N.L., 2013. Photo-oxygenation to support nitrification in an algal-bacterial consortium treating artificial wastewater. Bioresour. Technol. https://doi.org/10.1016/j.biortech.2013.02.005

Lv, P., Luo, J., Zhuang, X., Zhang, D., Huang, Z., Bai, Z., 2017. Diversity of culturable aerobic denitrifying bacteria in the sediment, water and biofilms in Liangshui River of Beijing, China. Sci. Rep. https://doi.org/10.1038/s41598-017-09556-9

Marazzi, F., Bellucci, M., Rossi, S., Fornaroli, R., Ficara, E., Mezzanotte, V., 2019. Outdoor pilot trial integrating a sidestream microalgae process for the treatment of centrate under non optimal climate conditions. Algal Res. 39, 101430. https://doi.org/10.1016/j.algal.2019.101430

Marazzi, F., Ficara, E., Fornaroli, R., Mezzanotte, V., 2017. Factors Affecting the Growth of Microalgae on Blackwater from Biosolid Dewatering. Water. Air. Soil Pollut. 228. https://doi.org/10.1007/s11270-017-3248-1

Merbt, S.N., Stahl, D.A., Casamayor, E.O., Martí, E., Nicol, G.W., Prosser, J.I., 2012. Differential photoinhibition of bacterial and archaeal ammonia oxidation. FEMS Microbiol. Lett. 327, 41–46. https://doi.org/10.1111/j.1574-6968.2011.02457.x

Muñoz, R., Guieysse, B., 2006. Algal-bacterial processes for the treatment of hazardous contaminants: A review. Water Res. 40, 2799–2815. https://doi.org/10.1016/j.watres.2006.06.011

Park, J.B.K., Craggs, R.J., Shilton, A.N., 2011. Wastewater treatment high rate algal ponds for biofuel production. Bioresour. Technol. 102, 35–42. https://doi.org/10.1016/j.biortech.2010.06.158

Penman, A.H.L., 2013. Natural Evaporation from Open Water, Bare Soil and Grass 193, 120–145.

Pittman, J.K., Dean, A.P., Osundeko, O., 2011. The potential of sustainable algal biofuel production using wastewater resources. Bioresour. Technol. 102, 17–25. https://doi.org/10.1016/j.biortech.2010.06.035

Pizzera, A., Scaglione, D., Bellucci, M., Marazzi, F., Mezzanotte, V., Parati, K., Ficara, E., 2019. Digestate treatment with algae-bacteria consortia: A field pilot-scale experimentation in a sub-optimal climate area. Bioresour. Technol. 274, 232–243. https://doi.org/10.1016/j.biortech.2018.11.067

R Core Team, 2018. R: A language and environment for statistical computing.

Ramanan, R., Kim, B.H., Cho, D.H., Oh, H.M., Kim, H.S., 2016. Algae-bacteria interactions: Evolution, ecology and emerging applications. Biotechnol. Adv. 34, 14–29. https://doi.org/10.1016/j.biotechadv.2015.12.003

Rasband, W., 2016. ImageJ. U. S. Natl. Institutes Heal. Bethesda, Maryland, USA.

Rittmann, B.E., McCarty, P.L., 2001. Environmental biotechnology : principles and applications, (Boston Mass): McGraw-Hill. Boston (Mass.) : McGraw-Hill, 2001.

Rosso, D., Larson, L.E., Stenstrom, M.K., 2008. Aeration of large-scale municipal wastewater treatment plants: State of the art. Water Sci. Technol. https://doi.org/10.2166/wst.2008.218

Shuttleworth, W.J., 2007. Putting the "vap" into evaporation. Hydrol. Earth Syst. Sci. 11, 210–244. https://doi.org/10.5194/hess-11-210-2007

Van Hulle, S.W.H., Vandeweyer, H.J.P., Meesschaert, B.D., Vanrolleghem, P.A., Dejans, P., Dumoulin, A., 2010. Engineering aspects and practical application of autotrophic nitrogen removal from nitrogen rich streams. Chem. Eng. J. 162, 1–20. https://doi.org/10.1016/J.CEJ.2010.05.037

van Loosdrecht, M.C.M., Nielsen, P.H., Lopez-Vazquez, C. M. Brdjanovic, D., 2016. Experimental methods in wastewater treatment. IWA.

Vargas, G., Donoso-Bravo, A., Vergara, C., Ruiz-Filippi, G., 2016. Assessment of microalgae and nitrifiers activity in a consortium in a continuous operation and the effect of oxygen depletion. Electron. J. Biotechnol. https://doi.org/10.1016/j.ejbt.2016.08.002

Wagner, M., Rath, G., Koops, H.P., Flood, J., Amann, R., 1996. In situ analysis of nitrifying bacteria in sewage treatment plants, in: Water Science and Technology. https://doi.org/10.1016/0273-1223(96)00514-8

Walker, D.A., 2009. Biofuels, facts, fantasy, and feasibility. J. Appl. Phycol. 21, 509–517. https://doi.org/10.1007/s10811-009-9446-5

Wang, L., Min, M., Li, Y., Chen, P., Chen, Y., Liu, Y., Wang, Y., Ruan, R., 2010. Cultivation of green algae Chlorella sp. in different wastewaters from municipal wastewater treatment plant. Appl. Biochem. Biotechnol. 162, 1174–1186. https://doi.org/10.1007/s12010-009-8866-7

Chapter 3

3. Hydrothermal carbonization of microalgal biomass: an eco-sustainable process to improve properties and effectiveness of microalgae in different applications

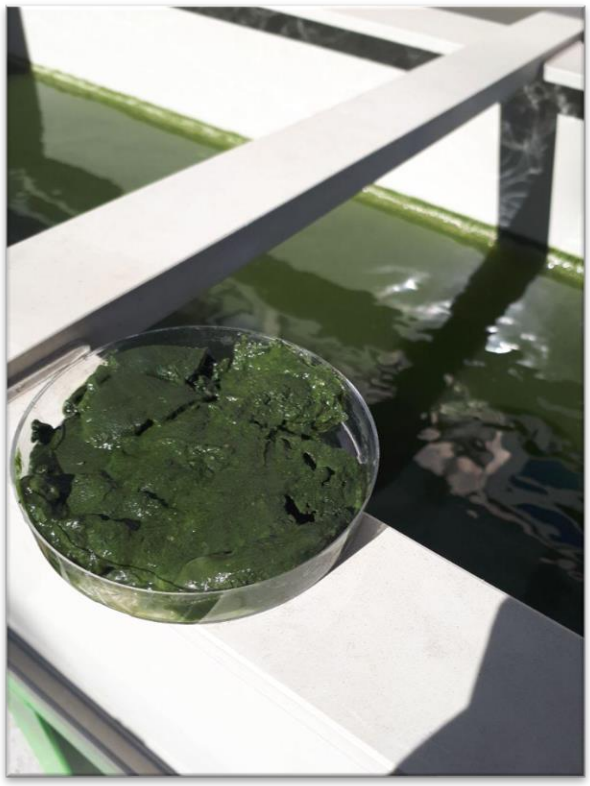

3.1 Introduction

Nowadays, biomasses have a leading role in the definition of sustainable consumption strategies since they can be used in a wide range of applications involving energy production, carbon sequestration and environmental remediation. Even if their heterogeneity in terms of chemical composition, water content and seasonal availability, as well as potential transport and storing issues, represents a real challenge during the standardization of many applications, the advantages are still very likeable as they are renewable and abundant (Cherubini, 2010). Among biomass sources, microalgae are quite interesting. These eukaryotic photosynthetic organisms can transform solar energy and inorganic compounds into new biomass and oxygen. They are very versatile as they have simple growing requirements, and they can be found both in fresh and marine water. Microalgae can produce valuable molecules such as proteins, carbohydrates and lipids which are accumulated within the cells under certain environmental condition (Chisti, 2007). The possibility to cultivate microalgae on different substrates with the final aim of extracting specific compounds was largely investigated by the scientific community. Microalgal cultivation, in fact, does not require arable lands and pesticides and could potentially be performed on poor quality growth medium like wastewaters, as that they contain inorganic nutrients (Spolaore et al., 2006; Yaakob et al., 2014). The end-use of the biomass is crucial for every application involving microalgae and is strictly dependent on their growth medium. Identifying a highly profitable exploitation would allow to reduce the costs related to cultivation which are still too high at real scale. Since microalgae are not classified as conventional food and some species are known to accumulate lipids and fatty acids, biofuels extraction was a popular theme among the scientific community. However, not every microalgal strains seems suitable and the selection and maintenance of pure cultures involves high costs especially working with outdoor large-scale cultivation. Moreover, extraction costs and yields have dampened this field of research (Mercer and Armenta, 2011).

Similar considerations can be made for biogas production using microalgae as the substrate for anaerobic digestion or co-digestion with another feedstock. The cell wall of microalgae is very resistant, limiting its degradation by microbial activity and the consequent biogas yield. Literature testifies a lipid and carbohydrates accumulation within microalgal cells when they are under nutrient famine. This phenomenon is referred to as “starvation” (Sharma et al., 2012). The lipid content is directly correlated to biogas production through anaerobic digestion (Montingelli et al., 2015). However, lipid accumulation can also be species dependent, so the input of nutrients is not

the only condition to be considered. A different approach to foster the biogas production involves pretreatment process on the biomass, to damage the cell wall and increase the bioavailability of the feedstock for bacteria. Chemical treatments with alkali or with acids and physical treatment are the most common ones (Passos et al., 2014).

Even if it is not an easy task, finding the best strategies for the valorization of the microalgal biomass is still crucial to make microalgal applications more appealing for scale up implementations. For that reason, during the last decades new approaches have been proposed: pretreatment steps like thermochemical processes, for example, can upgrade diverse raw feedstocks, leading to valuable products with improved characteristics (Xiao et al., 2012). Biochars and hydrochars for example, are solid carbon-made residues that can be obtained during the thermal decomposition of organic materials under low (or no) supply of oxygen and high temperature. Depending on the technology and the feedstock used for their production, these compounds have different but interesting physico-chemical features. Slow pyrolysis, torrefaction, gasification and hydrothermal treatments are the most common processes used to obtain chars usually starting from wood, municipal solid wastes, sewage sludges, agricultural wastes, energy crops and many others (Cha et al., 2016; Kambo and Dutta, 2015).

The term “biochar” was firstly distinguished from “charcoal” mainly for the different use, since the first one indicates all carbonized organic materials used as a soil enhancers to promotes fertility while the second indicates charred residues used mainly for energy production. However, definition and terminology have evolved and nowadays biochar is commonly used to indicate carbon-made residues obtained via dry carbonization process, while “hydrochar” refers to materials produced in a wet environment (Fuertes et al., 2010). However, authors do not always respect this distinction making it difficult to have a standardized definition.

3.2 Hydrothermal carbonization

As the name might suggest, water is a crucial factor in hydrothermal processes of biomasses as it is cheap, highly available and nontoxic. However, water is particularly interesting due to its tendency of acting as a catalyst when thermally treated in a compressed environment: important properties such as polarity, acidity and dielectric constant change under such conditions, lowering the activation energy of different chemical reactions. Depending on the temperature reached during the heating phase, Hydrothermal Carbonization (HTC) is distinguished from Hydrothermal Liquefaction (HTL) and Hydrothermal Gasification (HTG). The temperature of 374°C, that

corresponds to water critical point, marks the border between HTL and HTG, while HTC occurs under milder conditions (in the range between 150°C and 250°C, according to Libra et al., 2011). During HTC, the carbon content of the feedstock is enhanced while oxygen and mineral matter are subsequently reduced due to the hydrolysis of the biomass and to other chained liquid-phase reactions like dehydration, decarboxylation, condensation, polymerization and aromatization (Funke and Ziegler, 2010; Libra et al., 2011). When temperature and pressure are still moderate, the gaseous fraction is low and the most abundant product is the solid one, the hydrochar, resulting from the carbonization of carbon compounds. With increasing temperature and pressure, shifting from HTC to HTL, the relative composition of the products changes. During HTL, the biomass is decomposed to smaller fractions, forming chiefly oils. However, under HTG the most abundant products are syngas and other gas traces such as CO, CO_2 and CH_4.

3.3 Microalgal hydrochar as fuel

According to Heilmann et al. (2010), even if microalgae can be renewable sources of energy, burning them as such does not seem the best available option as they usually have a low heating value (HV). The authors inquired about the possibility to treat the biomass with the HTC process in order to improve the heat of combustion. A mixture made with 16 g of freeze-dried biomass of *Chlamydomonas reinhardtii*, 0.37 g of oxalic acid and 500 mL of distilled water was prepared and treated in an autoclave reactor at 203 °C for 2 h with an autogenous pressure of 1.65 MPa. When the reactor had cooled down, the insoluble solid product was separated from the liquid phase through vacuum filtration, washed with water and freeze-dried.

The algal hydrochar was characterized in terms of elemental composition, heat of combustion and ash content and the data were compared with the ones of natural coal and a char made from a lignocellulosic biomass. The sample had a 31.58 MJ kg^{-1} heat of combustion which is very similar to the one reported in the paper for natural coal (28.59 MJ kg^{-1}) and almost twice higher than the values reported for freeze-dried *Chlamydomonas* (18.04 MJ kg^{-1}). This can be explained by comparing the elemental analysis of the raw microalgae and the hydrochar: the higher carbon and hydrogen content in the latter is the result of the liquid phase reactions occurring during the HTC process (Heilmann et al., 2010). A similar heat of combustion was also reported in Heilmann et al. (2010): 22.56 g of dried *Chlamydomonas reinhardtii* was resuspended in 277.5 mL and were heated to 200 °C for 2 h. The authors highlighted the importance of the high fatty acid content in the starting biomass: the heat of combustion of the hydrochar was 30.11 MJ kg^{-1}. However, when

the fatty acids were extracted from the hydrochar by using Methyl t-butyl ether (MTBE) as solvent the heating values decrease by 20%.

The same considerations were recently confirmed by Liu et al., (2019) working with hydrochar made from *Scenedesmus* spp. through the HTC process. Different syntheses were performed changing the process temperature (180, 220 and 260 °C) but always maintaining 4 h residence time in the reactor. The microalgae suitability as fuel was improved by HTC treatment, and the optimal temperature was 220 °C, resulting in the maximum energy recovery efficiency. The HV of the *Scenedesmus* derived hydrochar were around 20.91–26.70 MJ kg^{-1}, lower range than reported by Heilmann et al. (2010) but still comparable with the one of lignite (15–20 MJ kg^{-1}) (Liu et al., 2019).

The main results found in literature about the properties of microalgal hydrochar as fuel are reported in Table 1.

Table 1 – Summary of the results found in literature on the use of microalgal hydrochar as fuel

Species	HTC Process conditions	Results	References
Chlamydomonas reinhardtii	T =203 °C, autogenous pressure=1.65 MPa, 2 h residence time, addition of oxalic acid and distilled water	HV =31.58 MJ kg^{-1}	Heilmann et al., 2010
Chlamydomonas reinhardtii	T =200 °C, 2 h residence time	HV = 30.11 $MJkg^{-1}$	Heilmann et al., 2011
***Scenedesmus* sp.**	T =180, 220 and 260 °C, 4 h residence time	HV =20.91–26.70 $MJkg^{-1}$	Liu et al., 2019

The HTC process could also be considered an interesting pretreatment step on microalgae to facilitate lipid extraction, increasing the final yields of biofuels like biodiesel. In fact, during the hydrothermal treatment not only the carbon component of carbohydrates and proteins in the algal cells are carbonized but also the microalgal cell walls are weakened due to the high temperature and pressure. Furthermore, hydrolysis reactions do occur converting the typical bound fatty acids of microalgae into free fatty acids which are easier to be extracted by methanol (Phuoc et al., 2017). Within this context, Phuoc et al. (2017) compared the transesterification process involving *Chlorella* spp. and the hydrochar produced from the same microalgae. 3 g of dried biomass were resuspended in 17 g of water. The prepared mixtures were used to test different HTC temperatures (200, 210 and 220°C) for 30 minutes. Argon gas was purged in the reactor. Total fatty acid content

was determined both in microalgae (11.6 % on dry weight basis) and in hydrochars (25.4, 25.7 and 25.9 % on dry weight basis). The hydrochar produced at 200°C which possessed the highest retention of fatty acids (95% on dry weight) was selected for the transesterification process. To test biodiesel production, fatty acid equivalent masses of hydrochar and microalgae were selected for methanol extraction. Therefore, 100, 200, 300 and 400 mg of microalgae per mL of methanol were compared with 45.5, 91.0, 136.5, 182.1 and 227.6 mg of hydrochar per mL of methanol. At the lower ratio, no significant difference was detected between microalgae and microalgal hydrochar. The biodiesel yield was 95.9 % on dry basis after 90 minutes. At higher ratios, significant improvements were obtained with hydrochar, as indicated in Table 2. Lipid extraction on microalgae was less efficient with increasing biomass concentration. In fact, the biomass was not fully covered by methanol when 400 mg mL^{-1} ratio was used, and this explains the low biodiesel yield. On the other hand, changes on the fatty acid composition and on the cell wall integrity due to the hydrothermal process are responsible for the better results on the hydrochar samples.

Table 2 – Summary of the results comparing the biodiesel yield by transesterification of microalgae (%) and microalgal-based hydrochar (Phuoc et al., 2017)

Microalgae (mg)		**Hydrochar (mg)**	
mg Hydrochar on mL of ethanol	**Biodiesel yield %**	**mg Hydrochar on mL of ethanol**	**Biodiesel yield %**
100	95.9	45.5	95.9
200	88.8	91.0	98.6
300	60.5	136.5	96.4
400	65	182.1	91.1
500	41.1	227.6	81.5

The transesterification process was also tested by Ennis et al. 2017 on microalgal-based hydrochar. HTC was performed by resuspending 4 g of freeze-dried *Phaeodactylum tricornutum* in 50 mL of 0.1 M citric acid solution. The temperature of the HTC reactor was 210°C for 2 h. GC-MS analysis was performed on the transesterified extracts showing peaks that were typical of either saturated or unsaturated fatty acid methyl esters which are valuable biodiesel precursors.

3.4 Microalgae and microalgal hydrochar as soil amendment

Soil loss and degradation are severe global problems that are occurring at alarming rates (Verheijen et al., 2009). Intensive agricultural activities as well with other anthropogenic pressures are leading to loss in soil productivities that have been firstly managed using chemical fertilizers. However, their introduction to compensate the lack of nitrogen and phosphorus has created not negligible environmental problems as these substances can seep through the treated soil and contaminate freshwater and groundwater, affecting different ecosystems in many ways (i.e. drinking water contaminations, toxicity for aquatic fauna and flora). New strategies to limit the load of fertilizers have been proposed, decreasing the application doses while coupling those substances with soil amendments. Since microalgae can uptake nitrogen from their growth medium, the possibility of using them as a slow-release fertilizer in agriculture have been investigated.

Coppens et al., 2016 focused on the positive effect of *Nannochloropsis oculata* and microalgal-bacteria flocs (MaB-flocs) grown on an aquaculture wastewater as a biofertilizer for tomato cultivation. During the study, an organic growing medium was used for the cultivation experiments. The medium consisted in a nutrient-poor blend of sod peat, Irish peat and coconut fiber with the addition of calcium and magnesium carbonate to ensure a pH of 5.5. Then, a mixture of the chosen microalgal biomass and the growing medium was made to obtain a soil with a 555 mg biomass-TN L^{-1} concentration. Tomato cultivations were then prepared as follows: two different sets of plants were treated with the organic medium and an inorganic medium, acting as controls, and two others were treated with *Nannochloropsis* biomass and MaB-flocs addition, respectively.

Even if no significant difference in terms of plant growth and plant size were highlighted between the microalgal treated plants and the controls, the sugar content and carotenoid concentrations were higher in the first ones. Fruits grown on MaB-flocs had a 70% carotenoid increase than in the inorganic fertilizer control and a 44% increase than in the organic control. Tomatoes grown under the *Nannochloropsis* amendment also had a 36% higher carotenoid concentration compared to the inorganic control.

Microalgae can also be used to produce a nutrient rich hydrochar as a valuable material for carbon sequestration and agricultural applications (Marris, 2006; Torri et al., 2011), showing interesting potential as a slow-release fertilizer in soil. This could be an interesting valorization as the

hydrochar can modify the physicochemical properties of the soil, increasing its cation exchange capacity (CEC) and affecting the nutrient bioavailability (Deluca et al., 2015). Properties such as the high surface area and porosity of hydrochar also cause an enhanced complexity of the soil texture, providing a better aeration and valuable effects on microorganisms (i.e. bacteria and fungi that can form symbiotic relationship with plant roots). That could probably be the major positive effect of the use of microalgal hydrochar with respect to raw biomass. Applications of hydrochar alone in agriculture usually does not increase crop yields, as also shown by the above-mentioned experience of Coppens et al. (2016). However, when coupled with N fertilizers the hydrochar improves plant nutrients uptake. This was observed on radish, with a yield increase of 42% and 96% with a dose application at 10 and 50 t ha^{-1} respectively (Chan et al., 2007). Zhang et al. (2010) indicated that a biochar application at 40 t ha^{-1} increased rice yield by 12.1% in soil with N fertilization (Zhang et al., 2010). However, the final effect may depend on the operative parameters chosen to produce the hydrochar as well as the starting feedstock.

Microalgal hydrochar can retain up to 30-50% and 40% of the N and P, respectively, of the original biomass but this may change with the microalgal species and the process temperature (Yu et al., 2018). *Chlorella* was investigated as a potential species to produce a microalgal-based char with high N and mineral content (Chang et al., 2015). Microalgal hydrochar can be used as soil enhancer, promoting its fertility while giving an alternative strategy in the management and recycle of nutrient from wastewater.

The already cited work of Ennis et al. 2017 had also the goal to investigate the feasibility to use the produced hydrochar as soil amendment. Indeed, the extraction of lipids (which was the first step of the study) determined the formation of the so called delipidated hydrochar which was tested as well as the raw hydrochar to determine their effects on cress seeds. Germination tests were performed on 50 mg of delipidated hydrochar, 50 mg of raw non-delipidated hydrochar and 50 g of ground non-delipidated hydrochar, put on filter paper and transferred in Petri dishes. 20 cress seeds were added in each Petri dish. Three Petri dishes were used as control, containing only moisty filter paper and 20 seeds. Each filter was water saturated, and 5 water drops were added each day for seven days. The germinated seeds were counted, and the lengths of radicles were measured after the seventh day. The germination index (GI), the relative seed growth (RSG) and relative root growth (RRG) were also calculated. No difference was detected among the three conditions for the number of germinated seeds. Root length and GI were higher for raw non-delipidated hydrochar (GI =102%) and ground non-delipidated hydrochar (GI =126%) than for

the controls but dropped for the raw hydrochar. Such results suggested a phytotoxic effect of the lipidic component.

Arun et al. (2020), performed pot experiments on the cultivation of tomato plants, testing exhausted microalgal-based hydrochar as fertilizer. The hydrochar was produced from *Scenedesmus* spp. biomass treated at 350°C and 5Mpa pressure for 1 hour. The authors define their process as HTC, but the operative conditions seem more consistent with hydrothermal liquefaction. The hydrochar was first used for removing phosphorus from a synthetic wastewater (60 min adsorption time, 150 rpm mixing speed, 1 g L^{-1} hydrochar dose and 60°C temperature) and then, when exhausted, for the pot experiments. "Fresh" (not exhausted) hydrochar and the spent hydrochar having a 2,505 mg g^{-1} phosphorus adsorption capacity was recovered. Three different pots containing 250 g of agricultural soil were prepared with the addition of 0.5 g of raw hydrochar, 0.5 g of spent hydrochar and a commercial fertilizer (DAP) to reach a dose of 2 mg g^{-1}. A fourth pot was filled with the same agricultural soil, with no addition, and used as control. Tomato seeds were planted and cultivated for 30 days after which plant height and chlorophyll content were measured. The best results were obtained with the spent hydrochar: the plants reached a height of 22 ± 0.5 cm and a chlorophyll concentration of 24.5 ± 0.42 mg g^{-1}, better than in the control and in the commercial fertilizer pots. Also, raw hydrochar gave better results than the control, but the improvements in the chlorophyll content and plant height were smaller than in the case of the commercial fertilizer. The experiments suggest that hydrochar could have a double and subsequent use for phosphorus recovery from wastewater, and for the amendment of agricultural soil. The accumulation of phosphorus due to the first use of the hydrochar improves its quality for soil making it both an amendment and a fertilizer.

The main experiences found in literature on the agricultural use of microalgae and microalgal hydrochar are summarized in Table 3.

Table 3 – Microalgae and microalgal hydrochar as soil amending

Species	Amendent	Crops	Results	References
Nannochloropsis oculata	Microalgal-bacteria flocs (MaB-flocs)	Tomato	70% and 44% carotenoid increase than inorganic and organic fertilizer	Coppens et al., 2016
Phaeodactylum tricornutum	Raw delipidated hydrochar	Cress seeds	GI= 102%	Ennis et al. 2017
	Grounded delipided hydrochar		GI= 126%	
	Raw hydrochar		GI=78%	
Scenedesmus spp.	Spent hydrochar	Tomato	Chlorophyll: 24.5 ± 0.4 mg g^{-1}	Arun et al. 2020
	Raw hydrochar		Chlorophyll: 13.5 ± 0.4 mg g^{-1}	

3.5 Hydrochar as adsorbent material as such and combined with iron nanoparticles

The possible use of hydrochar and biochar for wastewater treatment is justified by the low production costs and by the intrinsic properties of this material. The high specific surface (S_{bet}), the porosity and the presence of functional groups that can bind many molecules are important properties of effective adsorbent (Titirici et al., 2007). The use of microalgae as feedstock for HTC in this field was recently proposed by Sun et al. (2018). This study concerned the production of a porous carbon-made adsorbent using *Chlorococcum* spp. to remove Cr (VI) from water solution. A mixture made of 2.25 g of dried microalgae and 0.7 g of oxalic acid was resuspended in 0.3 L of deionized water and heated at 200°C for three hours. The obtained hydrochar was collected by filtration and dried at 110°C. Then the sample was post-treated via KOH or NH_3 activation, following heating ramps at 650°C, 700°C, 750 °C or 900 °C under a N_2 stream (120 mL min^{-1}). Undoubtedly the activation step is crucial in this study in order to achieve a higher specific surface area and a higher sorbent capacity. The activation via KOH at 750°C allowed a

S_{bet} increase of two orders of magnitude (from 11 $m^2 g^{-1}$ to 1784 $m^2 g^{-1}$). The adsorption isotherms on Cr (VI) were determined for all the obtained hydrochars and different results were obtained among the tested samples. The KOH activated hydrochar showed the best adsorption capacity (Q_e) (370.37 $m^2 g^{-1}$). The NH_3 activated hydrochar and the non-activated hydrochar had Q_e = 95.60 mg g^{-1} and 17.60 mg g^{-1}, respectively.

The effectiveness of the adsorbent was clearly increased by post treatment, however energy consumption, use of solvents, cleaning steps and N_2 consumption also increase the overall cost in the view of a scale up. This is also a limit for similar applications. That is the reason why the scientific community is now focusing on alternatives to produce new low-cost materials with suitable characteristics for the adsorption of contaminants from water.

A similar research was carried out by Saber et al. 2018, working with microalgal-based hydrochar obtained by hydrothermal liquefaction to remove Cu (II) ions from aqueous solution. 10 g of dried *Nannochloropsis* spp. were used and resuspended in 150 mL deionized water. Then, the obtained suspension was heated in autoclave at 210 and 250 °C for 60 minutes. Argon was used to create anoxic condition in the reactor vessel. The used thermal treatment should have favored the formation of the liquid byproduct at the expense of the hydrochar, however the temperature conditions are still considered by some authors as typical of hydrothermal carbonization. The obtained hydrochars had BET surface area of 1.38 and 12.56 $m^2 g^{-1}$, respectively. Both samples were tested for the removal of copper, using 5g L^{-1} dose, studying the effect of pH, initial Cu (II) concentration and contact time. Experiments were performed in the pH range 2-6 with a Cu (II) starting concentration of 100 mg L^{-1}. The maximum adsorption capacity was obtained at pH 5 and the best performances were provided by the hydrochar produced at 250°C (19.7 mg g^{-1} against the 14.7 mg g^{-1} of the other one). Furthermore, by increasing the starting copper concentration (up to 300 mg L^{-1}) a higher adsorption was achieved with a maximum value of 35 mg g^{-1} after 24h.

The already cited work of Aron at al. (2020) focused on nutrient recovery from wastewater using microalgal-based hydrochar as adsorbent prepared at 350°C. The factors affecting adsorption were studied, testing different contact times (10–60 min), speed (50–250 rpm), temperature (10-60°C) and adsorbent dose (0.3–1.5 g L^{-1}). The adsorption tests were performed on a synthetic solution having a COD, phosphorus and ammoniacal nitrogen concentration of 5000, 150 and 80 mg L^{-1}, respectively. Phosphorus and ammoniacal nitrogen removal were high (90 and 73% respectively) at 60 min at 1g L^{-1} dose.

The same hydrothermal process used by the previous authors was adapted to prepare a magnetic adsorbent material using blue-green microalgae as carbonaceous substrate under different

loadings of iron (Peng et al., 2014). The aim was to obtain a porous material to remove Tetracycline (TC) from aqueous systems. Tetracycline is a common antibiotic that shows bacteriostatic activity against a wide range of gram-positive and gram-negative bacteria. 3 g of dried microalgae were mixed with different amounts of an iron salt (0.6, 1.2, 2.4, 3.5 g of $(NH_4)_2SO_4 \cdot FeSO_4 \cdot 6H_2O$) and homogenized in 0.1 L of distilled water. The obtained mixture was put in a stainless-steel reactor and heated in an electric oven for 6 h, setting a temperature of 170°C. Once the reactor had cooled, the mixture products were centrifuged to recover the solid fraction, then washed with distilled water and ethanol (99 %) solution and finally dried in a vacuum oven at 60°C for 24h. The SEM analysis showed the presence of Fe_3O_4 nanoparticles dispersed in the carbonaceous substrate. The starting iron concentration used for the synthesis emerged as a leading factor in the morphology and properties of the samples. Not only the presence of iron made easier the magnetic separation and recovery of the particles after treatment, but also hydrochar conformation changed from sheets to particles with increasing iron load. The authors refer to that tendency as the "separation effect": the iron ions in the reactor vessels modify the carbon structure aggregation, creating more defective sites and structural complexity in the matrix. This was confirmed also by surface area data (Table 4) which showed a positive correlation with the starting iron concentration.

Table 4 – Specific Surface area and pore volume of the samples as a function of the added iron dose (Peng et al (2014), modified)

$(NH_4)_2SO_4 \cdot FeSO_4 \cdot 6H_2O$) (g)	**mg Fe/g dried microalgae**	**Surface Area ($g\ m^{-2}$)**	**Pore Volume ($cm^3 g^{-1}$)**
0.6	28	38.3	0.012
1.2	56	96.5	0.026
2.4	112	122.8	0.027
3.5	168	128.3	0.029

The different iron doped biochar prototypes were tested at the dose of 2 $g\ L^{-1}$ for the removal of TC, running some jar tests on a 50 $mg\ L^{-1}$ water solution of TC. The samples were analyzed with UV–vis spectroscopy at 360 nm wavelength. The greater TC removal efficiency (97.8 %) was obtained using the sample made with 3.5 g of $(NH_4)_2SO_4 \cdot FeSO_4 \cdot 6H_2O$ (6 mmol).

During the hydrothermal carbonization, the iron salt interactions with the carbonaceous matrix has resulted in the formation of iron oxides nanoparticles. This was certainly a great advantage with respect to the work of Sun et al (2018). In fact, positive correlations were highlighted between the starting iron amount and the specific surface area as well as between the starting iron amount and the sorption capacity of the final product. The results suggest that iron leads to valuable hydrogen bonding and other chemical-physical interactions with the TC.

The use of iron for wastewater purpose is historically well known (Fu et al., 2014), but more recently iron oxide and zerovalent iron nanoparticles have created a great deal of interest in wastewater treatment field because of their high potential. Zero-Valent Iron (ZVI) is a quite abundant chemical element, it is not toxic, cheap and easy to produce. In the past it was tested for wastewater treatment applications. However, the rise of nanotechnologies shifted the focus of the scientific community as the nanomaterials often show very different and more interesting physical, chemical, and biological properties compared to their macroscopic counterpart. This results from their larger surface area per unit of volume and from the quantum effects (Khan et al., 2019). Promising nanoscale solutions, which can be applied to water treatment, already exist. However, the current cost of these materials commonly prevents their use for large-scale applications. Thus, developing a low-cost nanotechnology to remove pollutants from water is still an important goal.

Within this context, zerovalent iron nanoparticles (nZVI) have been tested in the last years as an interesting technology to remove several classes of contaminant from wastewaters. Since they are characterized by a high reductive potential, they can offer a new perspective to water treatment (Kharisov et al., 2012). In the last twenty years lot of reports on different ways to synthesize iron nanoparticles have been described, following two different general approaches: the top-down synthesis involves a starting macro or microscopic substrate which is broken down using physical or chemical methods to obtain nanostructures. The bottom-up synthesis produces nanomaterials by building-up atoms or molecules onto each other. The most used methods are thermal reduction and/or decomposition of iron salts with sodium borohydride, carbothermal synthesis, vapor-solid growth synthesis and sol-gel techniques (Ahmmad et al., 2013; Crane and Scott, 2012).

The chemical reduction of iron salts in water solution is probably the most common methods for the synthesis of iron nanoparticles. Sodium borohydride ($NaBH_4$) is used as the reducing agent according to the following reactions:

$$Fe(H_2O)_6{}^{3+} + 3BH_4^- + 3H_2O \rightarrow Fe^0_{(s)} \downarrow + 3B(OH)_3 + 10.5H_{2(g)} + 3H^+ \quad (1)$$

$$Fe(H_2O)_6{}^{2+} + 2BH_4^- \rightarrow Fe^0_{(s)} \downarrow + 2B(OH)_3 + 7H_{2(g)} \quad (2)$$

This technique produces very small particles with homogeneous structure, showing high reactivity and high specific surface area. The drawbacks include the use of sodium borohydride and other organic solvents, that increase the costs of the process making it difficult to scale-up to an industrial level (Li et al., 2009).

The carbothermal synthesis of nanoparticles consists in the reduction of metal oxides using a gaseous stream of H_2 or CO_2 to achieve reducing conditions in the reaction vessel. The gas could also be CO produced directly in the reactor through the thermal decomposition of a carbonaceous substrate under high temperature (> 500°C) (Stefaniuk et al., 2016).

The vapor-solid growth synthesis consists in the deposition of a gas onto a solid support allowing the formation of crystals and the condensation of metal nanoparticles (Pandey et al., 2011). The Sol-gel method involves three subsequent steps: a solution containing the precursor metal is first hydrolyzed to obtain a hydroxide solution which is converted into a gel phase through condensation. Finally, the drying process favors the formation of ultrafine powders (Qi et al., 2010).

However, these methods are quite expensive and usually require advanced equipment to reach high temperature and pressure. Furthermore, a separation procedure is usually needed in order to recover the final product from the reaction medium as well as a post treatment to remove impurities deriving from the use of solvents and chemical additives.

Moreover, the application of nZVI for wastewater treatment also involves other problems. In fact, their rapid oxidation, the difficulty to separate nZVI from the treated media as they tend to aggregate in water solution and the “ageing effect” are serious issues that limit their efficiency (Calderon and Fullana, 2015). Considering the agglomeration tendency of nZVI in water solution, a recent but promising strategy consists in the combination of the nanoparticles with porous material acting as a physical support.

In the last years, the scientific community focused on new strategies for the synthesis of iron nanoparticles, aiming at reducing the costs while overcoming the above described limitations. An important turning point is certainly the possibility of using compounds deriving from renewable sources. Biomasses are rich in antioxidants which can be exploited as reducing agents, modifying the conventional synthesis of nanoparticles. The entire production can take a new eco-friendly

perspective by replacing chemical additives like $NaBH_4$ with the antioxidants naturally found in the biomass. The study of Peng et al. (2014), previously described, fits perfectly that framework. Furthermore, in order to improve the effectiveness of nZVI, also modification of iron nanoparticles have been investigated, improving their chemical-physical characteristics and their potential for wastewater treatment purposes. Various publications deal with different strategies involving the addition of alumina (Karabelli et al., 2011), polymers (Jiang et al., 2011,) and carbonaceous materials (Vadahanambi et al., 2013; Wildgoose et al., 2006). Many waste biomasses are quite rich in carbon and can be used as such but can also be pretreated and used to produce modified nanoparticles.

A different concept was proposed by Lalhmunsiama et al. (2017), who produced a sorbent magnetic material combining some already synthesized iron oxides nanoparticles (Fe_3O_4) with microalgae. The process was carried out in two different steps: the iron nanoparticles were initially produced with the coprecipitation methods consisting in the dispersion of iron oxides (Fe^{2+} and Fe^{3+}) in an ammonium hydroxide water solution. The suspension was stirred and heated at 80°C until the formation and precipitation of the nanoparticles was achieved. Then, 1 g of Fe_3O_4 nanoparticles was dispersed in 0.2 L of distilled water with 5 g of dried microalgae (*Chlorella vulgaris)*. The mixture was stirred for 24h to allow the deposition and incorporation of the iron nanoparticles on the biomass surface. As a result of that protocol it was possible to limit the agglomeration of the nanoparticles in water as well as the decrease of the active sites. The effect of various physico-chemical parameters like pH, initial concentration, contact time, and background electrolyte concentrations were studied under the batch reactor studies .The obtained material was found to be efficient in the rapid up- take of Cd (II) and Pb (II) from aqueous solutions. Table 5 summarizes the main literature findings concerning the use of microalgal-based hydrochar as adsorbent.

Table 5 – Use of microalgal hydrochar as adsorbent, as such and doped, for the removal of pollutants from water.

Microalgal species	Production process	Application rate	Pollutant removal	Reference
***Chlorococcum* spp.**	HTC, T=200 °C, 3h residence time, post treatment with KOH at 750 °C under N2 stream	0.2 g L^{-1}	Cr (VI)	Sun et al.,2018
***Nannochloropsis* spp.**	HTC/HTL, T=200 and 250°C, 1h residence time	5 g L^{-1}	Cr (VI)	Saber et al., 2018
Scenedesmus spp.	HTC/HTL, T=350°C, 1h residence time	1 g L^{-1}	Phorpsohurs And Ammoniacal Nitrogen	Aron at al., 2020
Blue-green microalgae	HTC, T =170 °C, 6 h residence time	2 g L^{-1}	Tetracycline	Peng et al., 2014
Chlorella vulgaris	Coprecipitation method at 80°C + deposition on algal biomass	2 g L^{-1}	Cd (II) and Pb (II)	Lalhmunsiama et al., 2017

3.6 Conclusions

In the last twenty years the growing concern in eco-sustainability have inspired researchers from all around the world to study microalgae. In fact, they are quite appealing due to their fast growth rate and their ability to growth even on poor quality media like municipal wastewater or other waste streams from various kinds of industry. However, the identification of the best profitable way to valorize the microalgal biomass is still an important issue that is slowing down the scale up of many studies. The thermochemical conversion of microalgal biomass was recently proposed in order to upgrade many of its properties leading to more appealing and cost-effective products. The hydrothermal carbonization (HTC) is considered an eco-sustainable process that could be easily scaled up as it does not involve the use of expensive solvents or toxic compounds. However, most of the HTC applications involving microalgae are still at laboratory scale. The microalgal derived hydrochars have intrinsic characteristics making them very versatile.

According to the works analyzed in this review, using hydrochar as soil amendment could be very promising mostly starting with microalgae grown on municipal wastewater. Thinking about the wider context of circular economy, nutrients and material could be recovered from wastewater while obtaining a low-cost solid product giving better qualities to soils and crops. Of course, the starting properties and chemical characteristics of the original biomass must be assessed first, as the microalgae can adsorb and uptake metals and contaminant from their growth media. This must be seriously considered as the accumulation of hazardous substances in the hydrochar could led to potential release to soil and crops.

HTC is also deemed useful to increase the heating value of microalgae, improving the potential generation of energy through combustion, being an efficient way to concentrate carbon and hydrogen from the microalgal cells. Furthermore, the HTC process could also be considered an effective pretreatment strategy for microalgae as the high temperature and pressure can weaken the microalgal cells wall and favor the chemical extraction of valuable substances.

Recently, the rise of nanotechnology also promotes the interest in the synthesis of porous material with high sorption capacity to be used for bioremediation. Microalgal-based hydrochar was used as a solid material to be dispersed in water solution to adsorb heavy metals and organic compounds but also to act as a physical support in the combination with nanoparticles. Again, this could be very interesting especially thinking about the introduction of microalgae in a real wastewater treatment plant. The exploitation of their metabolism would allow the removal of inorganic nutrient from wastewater, and later the obtained biomass could be used to adsorb and remove emerging compounds and other targets compound during tertiary treatment. Among the critical issues involving hydrothermal carbonization of microalgae, the byproducts must be studied to identify the best option for a sustainable management solution.

3.7 References

Ahmmad, B., Leonard, K., Shariful Islam, M., Kurawaki, J., Muruganandham, M., Ohkubo, T., Kuroda, Y., 2013. Green synthesis of mesoporous hematite (α-Fe2O3) nanoparticles and their photocatalytic activity. Adv. Powder Technol. 24, 160–167. https://doi.org/10.1016/J.APT.2012.04.005

Arun, J., Gopinath, K.P., Vigneshwar, S.S., Swetha, A., 2020. Sustainable and eco-friendly approach for phosphorus recovery from wastewater by hydrothermally carbonized microalgae: Study on spent bio-char as fertilizer. J. Water Process Eng. 38, 101567. https://doi.org/10.1016/j.jwpe.2020.101567

Calderon, B., Fullana, A., 2015. Heavy metal release due to aging effect during zero valent iron nanoparticles remediation. Water Res. 83, 1–9. https://doi.org/10.1016/j.watres.2015.06.004

Calderon, B., Smith, F., Aracil, I., Fullana, A., 2018. Green Synthesis of Thin Shell Carbon-Encapsulated Iron Nanoparticles via Hydrothermal Carbonization. ACS Sustain. Chem. Eng. 13, 24. https://doi.org/10.1021/acssuschemeng.8b01416

Cha, J.S., Park, S.H., Jung, S.C., Ryu, C., Jeon, J.K., Shin, M.C., Park, Y.K., 2016. Production and utilization of biochar: A review. J. Ind. Eng. Chem. https://doi.org/10.1016/j.jiec.2016.06.002

Chan, K.Y., Van Zwieten, L., Meszaros, I., Downie, A., Joseph, S., 2007. Agronomic values of greenwaste biochar as a soil amendment. Aust. J. Soil Res. 45, 629–634. https://doi.org/10.1071/SR07109

Chang, Y.-M., Tsai, W.-T., Li, M.-H., 2015. Chemical characterization of char derived from slow pyrolysis of microalgal residue. J. Anal. Appl. Pyrolysis 111, 88–93. https://doi.org/10.1016/J.JAAP.2014.12.004

Cherubini, F., 2010. The biorefinery concept: Using biomass instead of oil for producing energy and chemicals. Energy Convers. Manag. https://doi.org/10.1016/j.enconman.2010.01.015

Chisti, Y., 2007. Biodiesel from microalgae. Biotechnol. Adv. https://doi.org/10.1016/j.biotechadv.2007.02.001

Coppens, J., Grunert, O., Van Den Hende, S., Vanhoutte, I., Boon, N., Haesaert, G., De Gelder, L., 2016. The use of microalgae as a high-value organic slow-release fertilizer results in tomatoes with increased carotenoid and sugar levels. J. Appl. Phycol. 28, 2367–2377. https://doi.org/10.1007/s10811-015-0775-2

Crane, R.A., Scott, T.B., 2012. Nanoscale zero-valent iron: Future prospects for an emerging water treatment technology. J. Hazard. Mater. 211–212, 112–125. https://doi.org/10.1016/j.jhazmat.2011.11.073

Deluca, T.H., Gundale, M.J., MacKenzie, M.D., Jones, D.L., 2015. Biochar effects on soil nutrient transformations. Biochar Environ. Manag. Sci. Technol. Implement. 421–454. https://doi.org/10.4324/9781849770552

Ennis, C.J., Clarke, J., Neate, K., Cerejeira, J., Tull, L., 2017. Hydrothermal extraction of microalgae fatty acid Influences hydrochar phytotoxicity. Front. Environ. Sci. 5, 1–8. https://doi.org/10.3389/fenvs.2017.00047

Fu, F., Dionysiou, D.D., Liu, H., 2014. The use of zero-valent iron for groundwater remediation and wastewater treatment: A review. J. Hazard. Mater. https://doi.org/10.1016/j.jhazmat.2013.12.062

Fuertes, A.B., Arbestain, M.C., Sevilla, M., Maclá-Agulló, J.A., Fiol, S., López, R., Smernik, R.J., Aitkenhead, W.P., Arce, F., MacIas, F., 2010. Chemical and structural properties of carbonaceous products obtained by pyrolysis and hydrothermal carbonisation of corn stover, in: Australian Journal of Soil Research. https://doi.org/10.1071/SR10010

Funke, A., Ziegler, F., 2010. Hydrothermal carbonization of biomass: A summary and discussion of chemical mechanisms for process engineering. Biofuels, Bioprod. Biorefining. https://doi.org/10.1002/bbb.198

Heilmann, S.M., Davis, H.T., Jader, L.R., Lefebvre, P.A., Sadowsky, M.J., Schendel, F.J., von Keitz, M.G., Valentas, K.J., 2010. Hydrothermal carbonization of microalgae. Biomass and Bioenergy 34, 875–882. https://doi.org/10.1016/j.biombioe.2010.01.032

Jiang, Z., Lv, L., Zhang, W., Du, Q., Pan, B., Yang, L., Zhang, Q., 2011. Nitrate reduction using nanosized zero-valent iron supported by polystyrene resins: Role of surface functional groups. Water Res. https://doi.org/10.1016/j.watres.2011.01.005

Kambo, H.S., Dutta, A., 2015. A comparative review of biochar and hydrochar in terms of production, physico-chemical properties and applications. Renew. Sustain. Energy Rev. https://doi.org/10.1016/j.rser.2015.01.050

Karabelli, D., Ünal, S., Shahwan, T., Eroĝlu, A.E., 2011. Preparation and characterization of alumina-supported iron nanoparticles and its application for the removal of aqueous Cu2+ ions. Chem. Eng. J. https://doi.org/10.1016/j.cej.2011.01.015

Khan, Ibrahim, Saeed, K., Khan, Idrees, 2019. Nanoparticles: Properties, applications and toxicities. Arab. J. Chem. https://doi.org/10.1016/j.arabjc.2017.05.011

Kharisov, B.I., Rasika Dias, H. V., Kharissova, O. V., Manuel Jiménez-Pérez, V., Olvera Pérez, B., Muñoz Flores, B., 2012. Iron-containing nanomaterials: synthesis, properties, and environmental applications. RSC Adv. 2, 9325. https://doi.org/10.1039/c2ra20812a

Lalhmunsiama, Gupta, P.L., Jung, H., Tiwari, D., Kong, S.-H., Lee, S.-M., 2017. Insight into the mechanism of Cd(II) and Pb(II) removal by sustainable magnetic biosorbent precursor to Chlorella vulgaris. J. Taiwan Inst. Chem. Eng. 71, 206–213. https://doi.org/10.1016/J.JTICE.2016.12.007

Leng, S., Li, W., Han, C., Chen, L., Chen, J., Fan, L., Lu, Q., Li, J., Leng, L., Zhou, W., 2020. Aqueous phase recirculation during hydrothermal carbonization of microalgae and soybean straw: A comparison study. Bioresour. Technol. 298, 122502. https://doi.org/10.1016/j.biortech.2019.122502

Li, S., Yan, W., Zhang, W., 2009. Solvent-free production of nanoscale zero-valent iron (nZVI) with precision milling. Green Chem. 11, 1618. https://doi.org/10.1039/b913056j

Libra, J.A., Ro, K.S., Kammann, C., Funke, A., Berge, N.D., Neubauer, Y., Titirici, M.M., Fühner, C., Bens, O., Kern, J., Emmerich, K.H., 2011. Hydrothermal carbonization of biomass residuals: A comparative review of the chemistry, processes and applications of wet and dry pyrolysis. Biofuels 2, 71–106. https://doi.org/10.4155/bfs.10.81

Liu, H., Chen, Y., Yang, H., Gentili, F.G., Söderlind, U., Wang, X., Zhang, W., Chen, H., 2019. Hydrothermal carbonization of natural microalgae containing a high ash content. Fuel. https://doi.org/10.1016/j.fuel.2019.03.004

Marris, E., 2006. Putting the carbon back: Black is the new green. Nature. https://doi.org/10.1038/442624a

Mercer, P., Armenta, R.E., 2011. Developments in oil extraction from microalgae. Eur. J. Lipid Sci. Technol. https://doi.org/10.1002/ejlt.201000455

Montingelli, M.E., Tedesco, S., Olabi, A.G., 2015. Biogas production from algal biomass: A review. Renew. Sustain. Energy Rev. https://doi.org/10.1016/j.rser.2014.11.052

Pandey, P.A., Bell, G.R., Rourke, J.P., Sanchez, A.M., Elkin, M.D., Hickey, B.J., Wilson, N.R., 2011. Physical vapor deposition of metal nanoparticles on chemically modified graphene: Observations on metal-graphene interactions. Small. https://doi.org/10.1002/smll.201101430

Passos, F., Uggetti, E., Carrère, H., Ferrer, I., 2014. Pretreatment of microalgae to improve biogas production: A review. Bioresour. Technol. https://doi.org/10.1016/j.biortech.2014.08.114

Peng, L., Ren, Y., Gu, J., Qin, P., Zeng, Q., Shao, J., Lei, M., Chai, L., 2014. Iron improving bio-char derived from microalgae on removal of tetracycline from aqueous system. Environ. Sci. Pollut. Res. 21, 7631–7640. https://doi.org/10.1007/s11356-014-2677-2

Phuoc, V.T., Yoshikawa, K., 2017. Comparison between direct transesterification of microalgae and hydrochar. AIMS Energy 5, 652–666. https://doi.org/10.3934/energy.2017.4.652

Qi, H., Yan, B., Li, C., 2010. Preparation and magnetic properties of magnetite nanoparticles by Sol-gel method, in: INEC 2010 - 2010 3rd International Nanoelectronics Conference, Proceedings. https://doi.org/10.1109/INEC.2010.5425143

Saber, M., Takahashi, F., Yoshikawa, K., 2018. Characterization and application of microalgae hydrochar as a low-cost adsorbent for Cu(II) ion removal from aqueous solutions. Environ. Sci. Pollut. Res. 25, 32721–32734. https://doi.org/10.1007/s11356-018-3106-8

Sharma, K.K., Schuhmann, H., Schenk, P.M., 2012. High lipid induction in microalgae for biodiesel production. Energies. https://doi.org/10.3390/en5051532

Spolaore, P., Joannis-Cassan, C., Duran, E., Isambert, A., 2006. Commercial applications of microalgae. J. Biosci. Bioeng. https://doi.org/10.1263/jbb.101.87

Stefaniuk, M., Oleszczuk, P., Ok, Y.S., 2016. Review on nano zerovalent iron (nZVI): From synthesis to environmental applications, Chemical Engineering Journal. Elsevier. https://doi.org/10.1016/j.cej.2015.11.046

Sun, Y., Liu, C., Zan, Y., Miao, G., Wang, H., Kong, L., 2018. Hydrothermal Carbonization of Microalgae (Chlorococcum sp.) for Porous Carbons With High Cr(VI) Adsorption Performance. Appl. Biochem. Biotechnol. 186, 414–424. https://doi.org/10.1007/s12010-018-2752-0

Titirici, M.M., Thomas, A., Antonietti, M., 2007. Back in the black: Hydrothermal carbonization of plant material as an efficient chemical process to treat the CO2 problem? New J. Chem. https://doi.org/10.1039/b616045j

Torri, C., Samorì, C., Adamiano, A., Fabbri, D., Faraloni, C., Torzillo, G., 2011. Preliminary investigation on the production of fuels and bio-char from Chlamydomonas reinhardtii biomass residue after bio-hydrogen production. Bioresour. Technol. 102, 8707–8713. https://doi.org/10.1016/J.BIORTECH.2011.01.064

Usman, M., Chen, H., Chen, K., Ren, S., Clark, J.H., Fan, J., Luo, G., Zhang, S., 2019. Characterization and utilization of aqueous products from hydrothermal conversion of biomass for bio-oil and hydro-char production: A review. Green Chem. 21, 1553–1572. https://doi.org/10.1039/c8gc03957g

Vadahanambi, S., Lee, S.H., Kim, W.J., Oh, I.K., 2013. Arsenic removal from contaminated water using three-dimensional graphene-carbon nanotube-iron oxide nanostructures. Environ. Sci. Technol. https://doi.org/10.1021/es401389g

Verheijen, F.G.A., Jones, R.J.A., Rickson, R.J., Smith, C.J., 2009. Tolerable versus actual soil erosion rates in Europe. Earth-Science Rev. https://doi.org/10.1016/j.earscirev.2009.02.003

Wildgoose, G.G., Banks, C.E., Compton, R.G., 2006. Metal nanoparticles and related materials supported on Carbon nanotubes: Methods and applications. Small. https://doi.org/10.1002/smll.200500324

Xiao, L.P., Shi, Z.J., Xu, F., Sun, R.C., 2012. Hydrothermal carbonization of lignocellulosic biomass. Bioresour. Technol. https://doi.org/10.1016/j.biortech.2012.05.060

Yaakob, Z., Ali, E., Zainal, A., Mohamad, M., Takriff, M.S., 2014. An overview: Biomolecules from microalgae for animal feed and aquaculture. J. Biol. Res. https://doi.org/10.1186/2241-5793-21-6

Yu, K.L., Show, P.L., Ong, H.C., Ling, T.C., Chen, W.H., Salleh, M.A.M., 2018. Biochar production from microalgae cultivation through pyrolysis as a sustainable carbon sequestration and biorefinery approach. Clean Technol. Environ. Policy 20, 2047–2055. https://doi.org/10.1007/s10098-018-1521-7

Zhang, A., Cui, L., Pan, G., Li, L., Hussain, Q., Zhang, X., Zheng, J., Crowley, D., 2010. Effect of biochar amendment on yield and methane and nitrous oxide emissions from a rice paddy from

Tai Lake plain, China. Agric. Ecosyst. Environ. 139, 469–475. https://doi.org/10.1016/j.agee.2010.09.00

Chapter 4

4. Microalgal-based carbon-encapsulated iron nanoparticles (ME-nFe) to remove heavy metals in wastewater

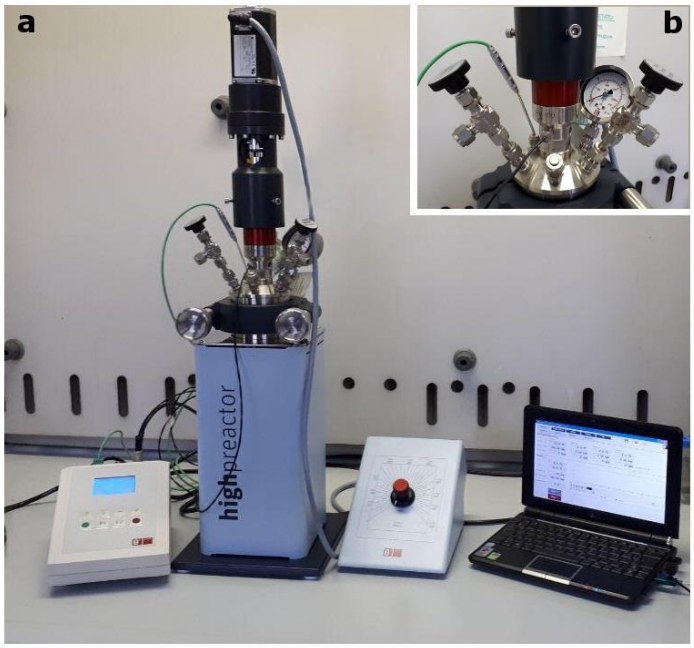

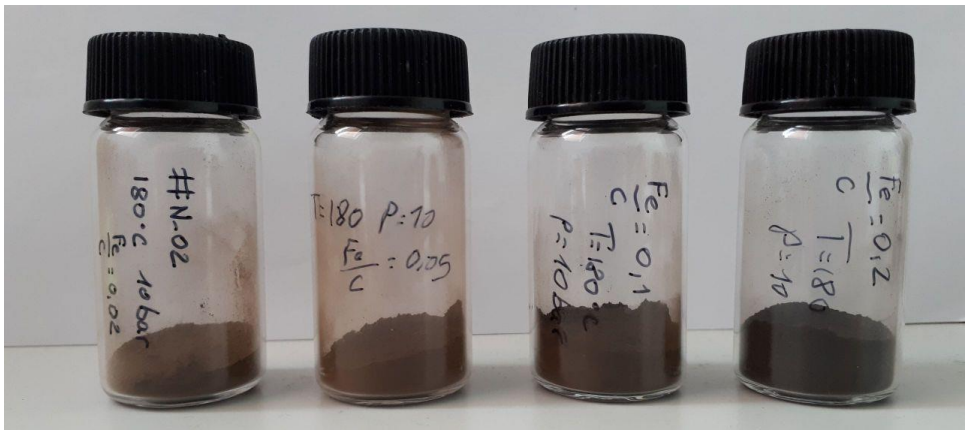

This chapter is based on publication currently under review at Journal of Environmental Chemical Engineering

4.1 Introduction

The need for advanced technologies to remove specific pollutants from wastewater is pushing research all over the world. The problem is very complex due to the extremely wide variety of compounds of concern, to their interactions and, especially, to their very low concentrations. Oxidative processes are most commonly applied, and they involve the use of various chemicals as oxidants (ozone, hydrogen peroxide, etc.) or as catalysts (iron) and/or of physical reactions based on UV irradiation or ultrasounds. Advanced oxidation processes (AOP) typically exploit ozone and/or hydroxyl radicals which must be generated in *situ* (Deng and Zhao, 2015). In some cases, chemical oxidation does not completely mineralize organic pollutants, but transforms them in more biodegradable compounds (as alcohols and carboxylic acids) which can be subsequently removed by biological processes (Esplugas et al., 2007). Another possibility is the removal of micropollutants by adsorption, which partly occurs also in conventional activated sludge process, using activated carbon or other kinds of adsorbents as, for instance, coconut-shell activated carbon (CCAC), porous β-cyclodextrin polymer (CDP), and CDP coated on cellulose microcrystal (CDP@CMC) adsorbents (Ling et al., 2020), or insoluble polymers of β-cyclodextrin (Alsbaiee et al., 2016).

Heavy metals are effectively removed by conventional activated sludge processes, but their residual concentrations in the effluents are often too high with respect to the acceptable levels in the receiving waterbodies (Magni et al., 2015). As it is the case for most pollutants, the removal is particularly hard when the initial concentrations are low (Saeed et al., 2005; Lim and Aris, 2014). Tertiary coagulation-flocculation has variable results according to the specific metal and to the selected coagulant (Hargreaves et al., 2018), while adsorption seems to be effective and is the main pathway for metal removal also in biological activated sludge processes, in constructed wetlands and in microalgae based processes (Fu and Wang, 2011). The variability of removal performances related, among other things, also to the single metal properties and to the initial concentration, is anyway a common feature. Good results can be obtained by membrane filtration, but the cost of such processes is still too high for a large-scale application in municipal contexts.

All the above-mentioned processes present strong limitations due to high capital and operational costs and performances that are often not so reliable. Thus, further research on this topic is needed.

A series of evidences exists about the possibility of exploiting zero-valent iron in advanced oxidation processes (AOP), due to its great efficiency as an electron donor to activate free radicals (Li et al., 2020, Ambika et al., 2020) or as a reductive agent to remove pollutants (Arvaniti et al.

2015). Zero-valent iron (ZVI) is non-toxic, abundant, cheap and easy to produce. It is a reactive metal and an effective reducing agent and can be used for removing both organic and inorganic pollutants (e.g. chlorinated organics, pharmaceuticals, metals, textile dyestuffs) (Crane and Scott, 2014; Hoch et al., 2008, Sunkara et al., 2010; Qiu et al., 2018). This is an important point related to the above mentioned problem of the broad variety of emerging compounds and metal pollution, whose main common aspects are the low concentrations, the long persistence, the high environmental hazard but whose chemical and physico-chemical properties are extremely different.

The application of Zero Valent Iron nanoparticles (nZVI) in wastewater treatment is very interesting due to the high reactivity, reducing properties and high specific surface area. However, a full-scale approach is limited due to its lack of stability, easy aggregation, and difficulty in separating nZVI from the treated solution. Also, the interaction between nZVI and oxygen causes a too fast aging of the nanoparticles, limiting the long-term effectiveness (Calderon et al., 2015). So, research has also considered coated or encapsulated ZVI nanoparticles. Just to cite some cases, a significant removal (38-96%) of perfluorinated compounds (PFC) was obtained by Arvaniti et al (2015) using Mg-aminoclay coated nanoscale zero valent iron (starting pH = 3.0). The maximum efficiency was observed for PFOA (perfluorooctanoic acid), followed, in the order, by PFNA (perfluorononanoic acid), PFOS (perfluorooctane sulfonate), and PFDA (perfluorodecanoic acid) and was attributed both to sorption and to degradation.

nZVI encapsulated in microscale carbon spheres (6−8 μm) via an in situ formation through hydrothermal carbonization (HTC) from an organic compound, followed by self-reduction, have the excellent chemical reducing capability of nZVI, and high sorption capacity, facilitated by the carbon substrate. HTC is a thermal treatment of an aqueous solution or dispersion of a carbon-containing organic material at moderate temperatures and under pressure, which produces a carbon-rich black solid as an insoluble product (Sevilla and Fuertes, 2009). The incorporation of nZVI into solid particles results in its easy separation from aqueous system avoiding aggregation of nZVI (Crane and Scott, 2014). Encouraging results for metal removal (Zn, Cu, Ni, Cd, Cr) have been obtained at lab-scale by Bonaiti et al. (2017) using clarified olive mill waste (OMW) as a source of carbon to produce carbon-encapsulated zerovalent iron nanoparticles (CE-nZVI) by HTC.

Here, the results obtained in the production of microalgal-based carbon-encapsulated iron nanoparticles (ME-nFe) by HTC and in their lab-scale application for metal removal are described. The microalgal biomass produced by a pilot side-stream process for the treatment of

centrate from municipal sewage sludge was used as the carbon source. The hydrothermal treatment of microalgae is really nothing new, as it was mostly proposed to obtain hydrochar for different applications such as energy production and agriculture (Heilmann et al., 2010, Liu et al., 2019) but also in wastewater treatment field (Peng et al., 2014). However, HTC was never used to obtain carbon-encapsulated iron nanoparticles. The novelty of this research consists also in using the microalgae grown on wastewater, directly harvested in a functional microalgal pilot plant in use in the wastewater treatment plant (WWTP) of Bresso-Niguarda (Milan, Italy). The goal is to assess the possibility to integrate the low-cost and low-impact algal-based process, used in the WWTP to reduce the nitrogen load inflow coming from municipal centrate (deriving from the centrifugation of digestate) to the water line, with the recovery and valorisation of the biomass. Through HTC, the microalgae would be exploited to produce a sorbent material to be used in the final treatment of the WWTP effluent as an alternative to conventional tertiary treatments. A successful integration of the two processes would improve the energy balance and the efficiency of the WWTP, as the microalgae are able to make up the oxygen needed for the removal of nitrogen and organic matter (Mantovani et al. 2020) while the microalgal-based iron nanoparticles could be an effective technology to remove heavy metals from the effluents, allowing a substantial improvement in its final quality.

4.2 Materials and methods

4.2.1 Chemicals

During the study the following chemical reagents, of analytical grade, were used: iron (III) nitrate nonahydrate (Fe $(NO_3)_3 \cdot 9H_2O$) and ammonium iron (III) sulfate dodecahydrate (NH_4 Fe $(SO_4)_2 \cdot 12\ H_2O$) (Sigma-Aldrich) as iron source for the production of the ME-nFe; ethanol and methanol (Sigma-Aldrich) for the polyphenols extraction and the nanoparticles washing immediately after the synthesis; Folin-Ciocalteu's phenol reagent 2 M (Sigma-Aldrich) to detect polyphenols in the extracts and $(HO)_3C_6H_2CO_2H \cdot H_2O$ (Fischer Scientific) to prepare the standards for the calibration curve of gallic acid; $ZnCl_2$, $CuCl_2$, $K_2Cr_2O_7$, $CdCl_2 \cdot H_2O$, Ni $(NO_3)_2 \cdot 6H_2O$ (Fischer Scientific) were dissolved in Milli-Q® water to prepare all the metal solutions for the adsorption tests (except for the ones made with the secondary effluent from the Bresso-Niguarda wastewater treatment plant (WWTP) instead of Milli-Q® water); zinc powder and 37% HCl (Fischer Scientific) for the determination of zero valent iron and the calibration of

the method, 2% HNO_3 (Sigma-Aldrich) for the acidification of the samples collected during the Jar tests.

4.2.2 Biomass cultivation, harvesting and characterization

The microalgae used as feedstock for the HTC process were collected from a pilot-scale high rate algal pond (HRAP) (also known as raceway) located at the Bresso-Niguarda WWTP in the suburban area of Milan (Italy) (more details in Mantovani et al, 2020). The centrate from sludge dewatering was used to grow a mixed culture mainly made of *Chlorella* spp. and *Scenedesmus* spp. in a continuous mode from May 2018 to November 2019. The HRAP was covered by a polycarbonate greenhouse to allow the algal growth even during the cold winter months. In Summer, the lateral walls of the structure were removed to favour light penetration, leaving only the polycarbonate roof in place to protect the microalgae from heavy rain events. The microalgae were harvested directly at Bresso using an ELECREM 1 110 / 230 V centrifugal clarifier. The microalgal pellet was then concentrated and dried at 50°C, ground to a fine powder and stored in glass bottles for the characterization and the subsequent syntheses. The elemental analysis of the microalgae was performed on 7 samples collected from March 2019 to November 2019 using a Perkin Elmer CHNS/O analyzer 2400 153 series II. Clearly, the focus was set on the carbon percentage as the aim of the overall study was to produce iron nanoparticles encapsulated in a carbonaceous support and the optimal Fe/C ratio had to be defined. However, also the hydrogen, nitrogen and phosphorus contents were assessed to obtain more data concerning the possible time variability of the biomass properties. Phosphorus was determined after acid digestion (using 7 mL of H_2NO_3 and 3mL of H_2O_2) following the Green algae procedure (DG-EN-25) in a microwave digester (ETHOS1600, Milestone). Due to the important role of polyphenols as reducing agents during the iron nanoparticles production (Calderon et al., 2018), the total phenolic content (TCP) was also determined, according to the Folin-Ciocalteu method (Choochote et al. (2014), Doria et al. (2012)). Briefly, 50 mg of biomass were used for the extraction in 5 mL of methanol in a sonicating bath with 45 minutes contact time. The suspension was filtered on 0.45 µm Millipore filter and the pellet was used for a subsequent extraction following the same steps. 0.1 mL of the obtained filtered solution was then put in a 15 mL falcon test tube adding 0.6 mL of distilled water, 0.5 mL of Folin-Ciocalteu reagent and 1.5 of sodium carbonate (20%). The volume was made up to 10 mL with distilled water. The solution was put in the dark for 30 minutes at room

temperature and then analysed spectrophotometrically at 750 nm wavelength. The quantification was based on a calibration curve of gallic acid (0-0.7 mg mL^{-1}) (Doria et al. (2012).

4.2.3 ME-nFe production

The ME-nFe were produced with a single-step synthesis through the Hydrothermal Carbonization according to Sun et. al (2012) and Calderon et al. (2018). In the present work, the carbonaceous feedstock used consisted of microalgal biomass, replacing glucose and olive mill wastewater, respectively. Microalgae were dried and resuspended in 100 mL Milli-Q® water and mixed with an iron salt, testing four different Fe/C molar ratios (0.02, 0.05, 0.1, 0.2), three process temperatures (180, 200, 225 °C) and two salts as iron sources ($Fe(NO_3)_3 \cdot 9H_2O$ and $NH_4 Fe(SO_4)_2 \cdot 12 H_2O$). 3 g of biomass were used for each run. Basing on the microalgal carbon content on dry weight basis ($\%C_b$), the g of C (m_c) and then the mole of C in the processed microalgae were determined, considering its C atomic weight (12 u), as follows:

$$m_C = \frac{3 * \%C_b}{100}$$

$$mol_C = \frac{m_C}{12}$$

The amount of iron needed was then determined according to the desired Fe/C molar ratio (r) and the molar mass of the chosen iron salts (M):

$$mol_{iron} = r * mol_C$$
$$m_{iron\ salt} = mol_{iron} * M_{iron\ salt}$$

The microalgal and iron salt mixture was then moved to a High-Pressure Laboratory Reactor (BR-300, BERGHOF) and heated, setting the desired temperature ramp for a 3 h residence time. The reactor was then left cooling overnight and the solid product of the HTC process was recovered by vacuum filtration using a 0.2 μm cellulose acetate filter. The solid fraction was subsequently washed with a 50:50 (v:v) water-ethanol solution to remove the tar and other HTC residues and dried at 80°C for 12 h. Finally, it was ground and stored in a glass vial.

4.2.4 ME-nFe characterization

The total iron content of the ME-nFe was determined gravimetrically after muffle combustion at 900-1000 °C for one hour. The presence of oxygen during the thermal treatment led to carbon loss and CO_2 volatilisation:

$$C_{(s)} + O_{2\,(g)} \rightarrow CO_{2\,(g)}$$

At the end of the process, after cooling, the sample was weighted, assuming it was mainly composed of iron oxide. The same treatment was performed on a sample of microalgal-based hydrochar, produced without iron, to assess the ash content deriving from the combustion of the biomass. The zero valent iron determination was performed measuring the hydrogen gas formed through the reaction of metallic iron with an excess of hydrochloric acid, according to Calderon et al. (2018). A graduated buret was connected by a polyvinyl chloride pipe to a separating funnel and a glass vial containing a known quantity of nanoparticles. The system was filled with water. The change in the water height in the buret was due to the hydrogen formed when 1 mL of HCl was added with a syringe to the nanoparticles. The gas formation was proportional to the zero valent iron content of the samples which can be obtained through stoichiometric computation according to the following reaction:

$$2Fe + 6HCl \rightarrow 2FeCl + 3H_2$$

The BET surface area and the pore size distribution of the samples were obtained by physical adsorption on the solid surface of nitrogen gas molecules at 77 K, using a Coulter SA 3100 analyzer at Università degli Studi di Milano. The method for measuring the specific surface area ($m^2\ g^{-1}$) of the material is based on the theory developed by Brunauer, Emmet and Teller (BET). A LEO 1430 Scanning Electron Microscope (SEM) was used to evaluate the size and morphology of the ME-nFe. A Jeol JEM 1220 Transmission Electron Microscope (TEM) (120 KV) was used to verify the iron distribution within the carbonaceous matrix. 0.1 mg of samples was dissolved in 1 mL of Milli-Q® water for the observation. The microscope was connected to a CCD camera Gatan multiscan.

4.2.5 Application of ME-nFe nanoparticles for the removal of heavy metals

The two most promising samples (D1 and N1 which are described in Table 5) were used to test their ability to remove heavy metals (Cu, Zn, Cr, Ni, and Cd) from aqueous solutions by Jat tests. The metals were selected as they are commonly present in wastewater and in effluents from conventional wastewater treatment plants.

The first tests were run using a solution containing all the metals (10 mg L^{-1} each) in Milli-Q® water, comparing two samples (D1 and N1) at two different doses: 2 g L^{-1} and 3 g L^{-1}. A VELP FC 6S Jar tester and 500 mL beakers were used, setting a continuous stirring at 90rpm. A blank beaker was used to quantify water evaporation which could slightly affect the concentrations. 5 mL samples were taken from the beakers at various reaction times and analysed by Inductively Coupled Plasma - Optical Emission Spectroscopy (Optima 7000 DV PerkinElmer) after filtration on 0.2 μm cellulose acetate filters and acidification with nitric acid (2% in volume).

A second series of tests was performed with the same nanoparticle samples and procedures but with a starting metal concentration of 1 mg L^{-1}, more realistic for a treated effluent, to verify if the effectiveness of the treatment was related to the pollutant concentration.

Then, the same procedures were repeated using as solvent the secondary effluent from Bresso WWTP (instead of Milli-Q water) enriched with 10 mg L^{-1} of the selected metals in the first experiments, and with 1 mg L^{-1} in the following ones. The aim was to investigate the performances of ME-nFe in a real matrix where the competition between dissolved solids and the heavy metals for the active sites of the nanoparticles might occur.

All the above described Jar tests were done in triplicate and lasted 54 hours: such a long time was adopted to follow the fate of metals, verifying if the nanoparticles would release the adsorbed metals with time. All the tests were coupled with pH and ORP measures. The Milli-Q test solutions had a starting pH around 5.4 which was not adjusted, while the effluent solutions had a starting pH of 7.

The presence of zero valent iron and iron oxide in the nanoparticles were important not only for their reactivity but provided also interesting magnetic properties allowing an easy recovery of the ME-nFe after use. Most of the nanoparticles could be separated from the liquid solution with a neodymium magnet, holding them at the bottom of the beaker while siphoning the solution

elsewhere. A centrifugation step (5 min at 5000 rpm) was then performed to recover the small residues of ME-nFe.

To understand the potential of reusing the same nanoparticles Jar tests were repeated in the same way using the recovered nanoparticles till the metal removal decreased to 60%.

4.3 Results and discussion

4.3.1 Feedstock characteristics

The chemical characteristics of the biomass are crucial during the synthesis of the iron nanoparticles by HTC. According to the results shown in Table 1, the overall composition did not show relevant seasonal variations with an average carbon percentage of 41 ± 4 %. This was an important information as the chemical composition of the microalgal biomass may change in time following some shifting in the microalgal community in terms of species, which can easily occur, especially in an outdoor cultivation. Similar considerations apply to the total phenolic content. The results reported in Table 2 show an average of 1.3 ± 0.1 mg g^{-1} gallic acid equivalents. Table 2 also provides the composition of the microalgal community tested for this project. *Chlorella* spp. and *Scenedesmus* spp. were the main taxa observed in the microalgal suspension and the first one was always dominant. That stability is reflected also in the TCP content. The measured concentrations are certainly not high with respect to data reported by other Authors: Safafar et al. (2015*)*, for instance, reports values up to 6 mg g^{-1} for *Chlorella sorokiniana* even if there are great differences with other species. However, the values in Bresso's biomass are higher than the one reported by Hemalatha et al., (2013) who measured a TCP content of 0.78 ± 0.03 mg g^{-1} in *Chlorella marina* confirming the wide variation range among different taxa.

Table 1. Elemental analysis data on dried samples of microalgal biomass.

Samples	C tot. (%)	H tot. (%)	N tot. (%)	P tot. (g kg^{-1})
HRAP 21-03	37.3	7.7	8.3	8.2
HRAP 13-05	40.2	8.1	8.9	7.5
HRAP 14-06	46.9	2.3	9.7	3.2
HRAP 24-06	39.8	5.3	8.2	5.1
HRAP 02-07	38.5	7.9	8.8	9.2
HRAP 26-09	38.0	7.9	10.2	9.7
HRAP 08-11	42.3	8.2	9.6	8.9
Average	40.6	7.0	9.3	7.8
Dev. st.	3.6	2.3	0.7	2.3

Table 2. Total phenolic content of microalgal biomass. The results are expressed as mg g^{-1} d.w. as gallic acid equivalent. (n=3)

Sample	Main Taxa	TCP (mg g^{-1})	St. dev.
HRAP 21-03	*Chlorella* spp.	1.23	0.10
HRAP 13-05	*Chlorella* spp. *Scenedesmus* spp.	1.37	0.24
HRAP 28-05	*Chlorella* spp. *Scenedesmus* spp.	1.20	0.15
HRAP 14-06	*Chlorella* spp. *Scenedesmus* spp.	1.41	0.19
HRAP 2-07	*Chlorella* spp. *Scenedesmus* spp.	1.11	0.06
HRAP 25-07	*Chlorella* spp.	1.22	0.07
Average		1.26	0.13

The advantage of the HTC is the possibility to exploit the water content of the biomass. However, the low solid concentration of microalgae entails the need to concentrate the microalgal suspension, obtaining a dense sludge-alike solution. Even if the carbon content and the TCP of Bresso microalgae were quite stable, the standardization of the HTC process was performed using the same stock of dried microalgae (HRAP 24-06) to avoid unexpected effect on the synthesis due to differences in the biomass characteristics.

4.3.2 ME-nFe characteristics

The characterization of all the samples was essential to define a final protocol to produce the ME-nFe. Depending on the salt used for the synthesis, different results were obtained. The nanoparticles produced with iron (III) nitrate nonahydrate had BET area up to 120 m^2g^{-1} that is comparable with literature results on a similar application (Peng et al., 2014), while with ammonium iron (III) sulfate dodecahydrate, the BET area was much lower. Table 3 summarizes the BET surface area of all the produced nanoparticles. As also shown in Figure 1, at 180°C the BET surface area increased with increasing Fe/C molar ratio, with both iron salts. For ammonium iron (III) sulfate dodecahydrate the trend of BET area as a function of Fe/C ratio was opposite at 200°C and no trend was observed at 225°C. The absolute highest value of BET area was obtained with iron (III) nitrate nonahydrate at the lowest temperature (180°C) with the highest Fe/C ratio.

The outcome of the BET analysis clearly suggested to rule out the iron sulfate. The role of the iron salt was not unexpected as a similar trend was described in the work of Peng et al. (2014) where iron doped biochar was produced using a blue-green microalgae. The reasons for such different results from the types of iron salt are still not clear. It is true that the specific thermal decomposition of iron nitrate and iron sulphate occurring during the HTC process is different, and this might have important effects on the final texture of the solid product. However, Peng et al. (2014) achieved satisfying BET area precisely with ammonium iron (III) sulfate dodecahydrate. It is known that the chemical composition of microalgae can sensibly change from species to species but also due to different environmental conditions (Orazova et al., 2014; Batista et al., 2013; Ötleş et al., 2001), so it is possible to assume that the different results could have depended on the different chemical composition of the microalgae and on the interaction between the chemical components of the biomass and the two iron salts during the complex chain-like reactions of HTC.

Total pore volume, measured for one of the samples with the largest BET area (N1), was 0.65 mL g^{-1}. The pore size distribution showed a prevalence of mesopores (48% of the total pores had a diameter between 5-80 nm) and micropores (42% with a diameter <80 nm) and a smaller component of micropore (9% of the pores had a diameter < 6 nm).

Table 3. List of the samples with the synthesis condition and their BET surface area

Salt	Sample	[Fe/C]	T (°C)	BET (m^2g^{-1})	Salt	Sample	[Fe/C]	T (°C)	BET (m^2g^{-1})
$NH_4Fe(SO_4)_2 \cdot 12\ H_2O$	A	0.02	180	8	$Fe(NO_3)_3.9H_2O$	A1	0.02	180	25
	B	0.05	180	9		B1	0.05	180	51
	C	0.1	180	16		C1	0.1	180	73
	D	0.2	180	30		D1	0.2	180	120
	E	0.02	200	54		E1	0.02	200	28
	F	0.05	200	31		F1	0.05	200	50
	G	0.1	200	17		G1	0.1	200	71
	H	0.2	200	20		H1	0.2	200	101
	I	0.02	225	12		I1	0.02	225	27
	L	0.05	225	11		L1	0.05	225	68
	M	0.1	225	12		M1	0.1	225	98
	N	0.2	225	12		N1	0.2	225	110

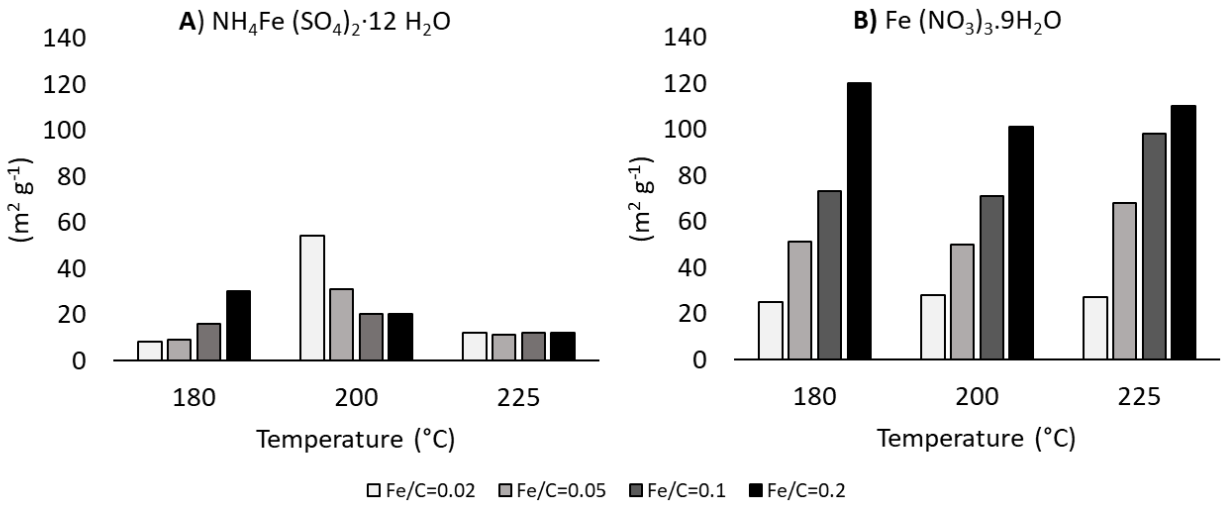

Figure 1. – BET surface area vs Fe/C molar ratio for all the produced ME-nFe.

The differences detected in the BET surface area were confirmed by SEM analysis showing the morphology of the ME-nFe. The samples made with NH_4 Fe $(SO_4)_2 \cdot 12$ H_2O (Samples A-N) clearly showed a sheet morphology that is consistent with their low BET surface area, while the nanoparticles produced at the same condition but using $Fe(NO_3)_3.9H_20$ had a more complex, globular structure (Samples A1-N1). An example of that is given in Figure 2. where the morphology of sample N and N1 are compared. In sample N, the texture is more coarse and almost polygonal, while sample N1 is made of smaller globular aggregates, consistent with higher BET surface area.

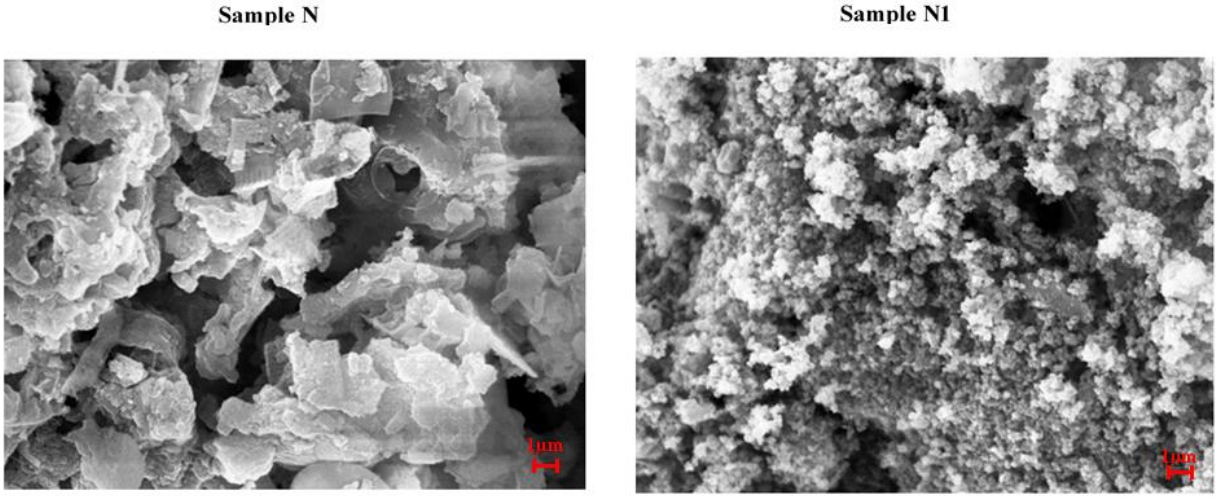

Figure 2. SEM analysis: comparison between the texture of samples N and N1 produced changing only the iron salt, using NH_4 Fe $(SO_4)_2 \cdot 12$ H_2O and Fe $(NO_3)_3.9H_20$ respectively. The iron source was responsible for a different texture.

Increasing the starting Fe/C molar ratio during the synthesis clearly led to a higher total iron incorporation in the final solid products, as suggested in Table 4 which shows the iron concentration in the different samples. The zero valent iron content (%Fe^0) ranges between 7 to 14 % of the final solid product, comparable to the data obtained by Calderon et al. (2018). Such values were always achieved except for samples A and D. No positive correlation was observed between the starting Fe/C molar ratio and the zero valent iron content in the nanoparticles. This is not strange as the reduction of the iron salt depends on the reducing properties of the biomass and, as above explained, the phenolic content of the microalgal biomass was stable in time, providing a similar reducing environment in the reactor for all the synthesis. Accordingly, the iron reducing efficiency data (% Fe^0 /Fe_{tot}) were higher for lower Fe/C ratios. In fact, a higher iron precipitation in the form of iron oxide was achieved by increasing the starting iron dose, while the zero valent iron concentration remained more stable due to the limiting reducing power of the microalgae.

Sample I1-N1 were carefully observed through SEM microscope to obtain high resolution images to detect differences in the texture that could be consistent with their BET surface areas. Figure .3 refers to sample I1 the one produced with a Fe/C of 0.02 at 225°C. B and C are just magnification of different portions of picture A, as suggested by the red and blue frames. It is interesting to note that most of the microalgal cells can still be distinguished in the sample as *Chlorella* sp. (having globular shapes) were only partially eroded. Looking through the samples, there are still some cases in which the surfaces of microalgae are particularly creased, however the iron is not very evident. Therefore, the low BET surface area is consistent with the high heterogeneity of the sample and the integrity of the microalgae that were not fully disrupted by the HTC process. Figure 4. refers to sample L1, produced with Fe/C of 0.05 at 225°C. Again, the picture on the right (B) was obtained by the magnification of the red frame indicated in picture A. The complexity of this sample is certainly evident, resulting in a slightly higher BET surface area than the one of I1. This can probably be attributed to the increased iron load. In fact, the deposition of iron can be noted over the cellular shapes that can still be distinguished in the overall matrix, (i.e. blue frames). This is more evident by observing samples M1 (Figure 5) and especially N1 (Figure 6). Sample N1 appear homogeneous as the interaction between the carbonaceous matrix and the iron was able to produce a more complex, globular structure.

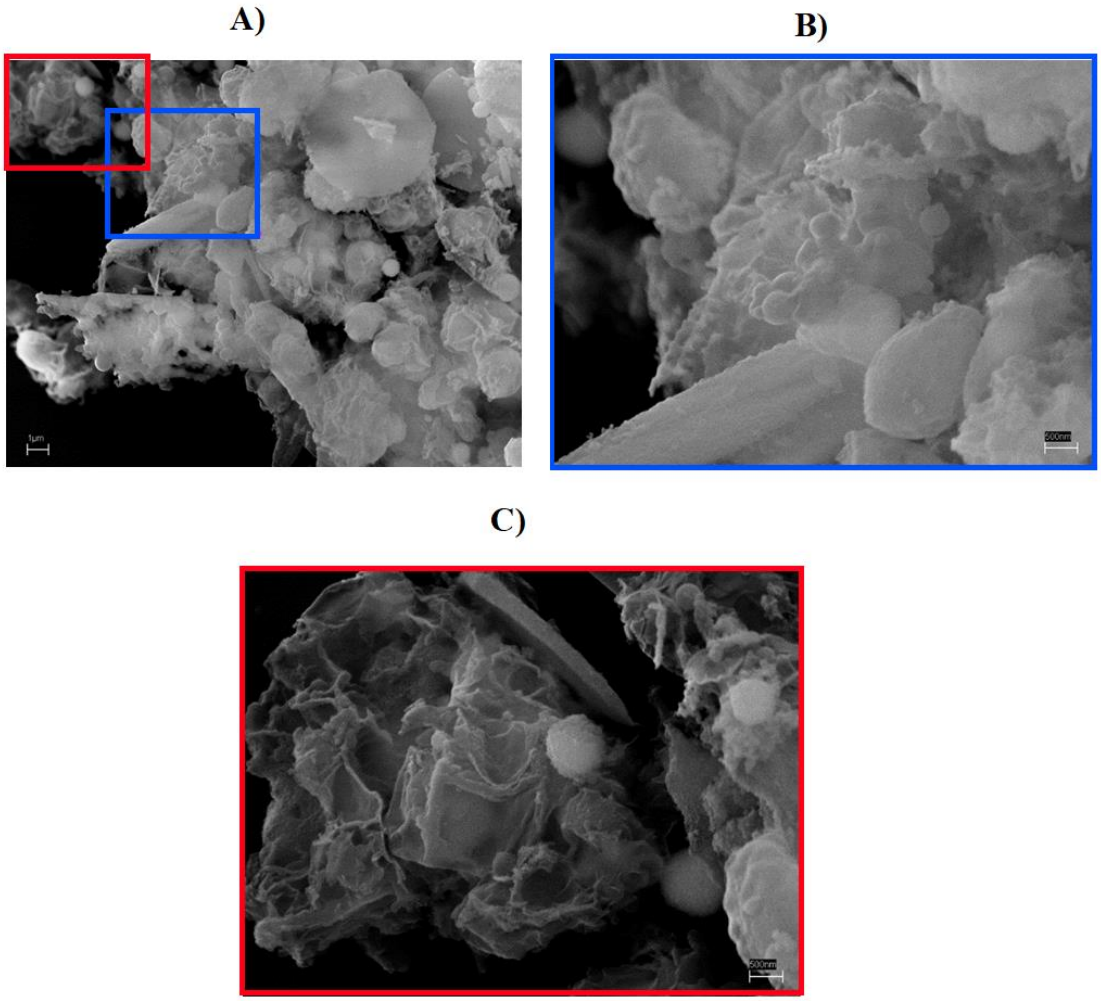

*Figure 3. SEM analysis on sample I1(*Fe/C=0.02 at 225°C*). B and C are details of picture A.*

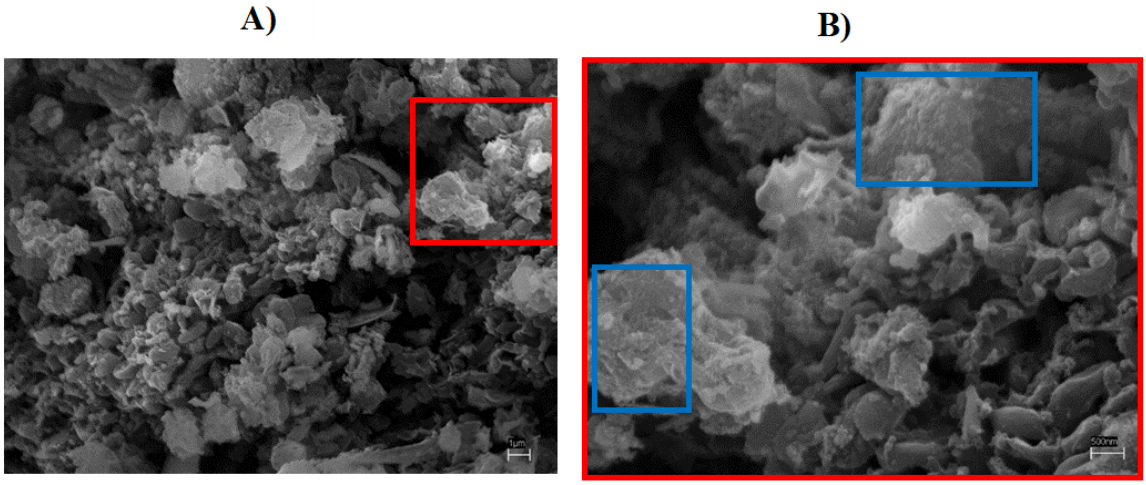

*Figure 4. SEM analysis on sample L1(*Fe/C= 0.05 at 225°C*). B is a details of picture A. Blu frames highlights areas of the samples where iron can be noted.*

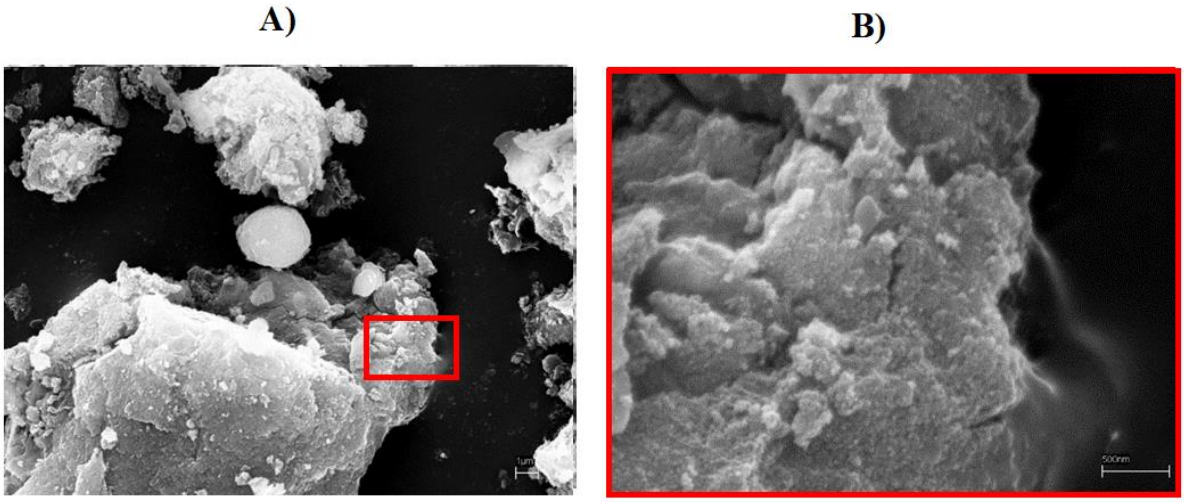

*Figure 5. SEM analysis on sample M1(*Fe/C= 0.1 at 225°C*). B is a details of picture A.*

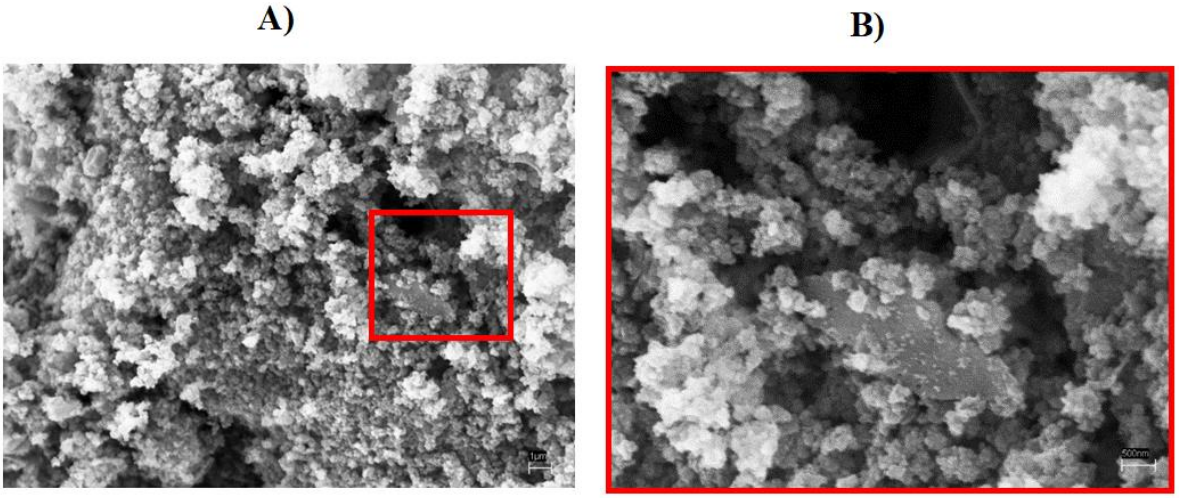

*Figure 6. SEM analysis on sample N1(*Fe/C= 0.2 at 225°C*). B is a details of picture A.*

The samples were also observed at the TEM microscope to detect differences in the structure of the nanoparticles and in the iron distribution within the mass of the ME-nFe. The comparison between sample D1 and N1 is shown in Figure 7, where the more electron dense areas of the photos (representing the iron) seem well distributed into the overall masses. Furthermore, also the iron content seems higher in samples N1, confirming the founding of the gravimetric analysis.

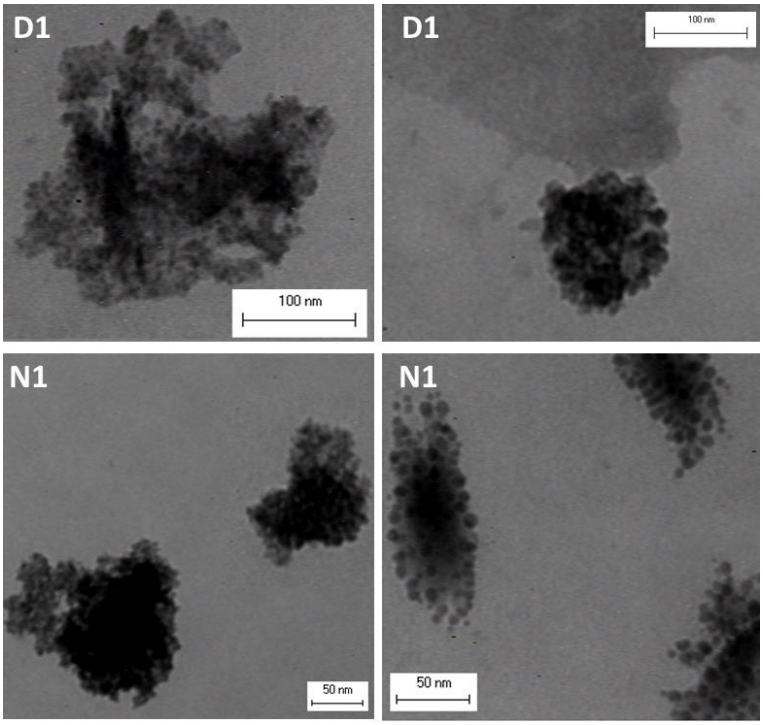

Figure 7. TEM images of samples produced with iron nitrate Fe/C=0.2 at 180°C (D1, upper squares), and at 225°C (N1, lower squares)

Table 4. Zero valent iron content (% Fe0), total iron (% Fe tot) and zero valent iron incorporation efficiency with respect to the total iron (% Fe0/Fe tot) in the produced ME-nFe.

Synthesis		**Sample**		**Fe^0 %**	**Fe_{tot} %**	**Fe^0/Fe_{tot} %**	**Sample**		**Fe^0 %**	**Fe_{tot} %**	**Fe^0/Fe_{tot} %**
T(°C)	Fe/C	ID	Salt				ID	Salt			
180	0.02	A	**$NH_4Fe(SO_4)_2 \cdot 12\,H_2O$**	6.8	28.7	23.7	A1	**$Fe(NO_3)_3 \cdot 9H_2O$**	9.5	17.4	54.4
180	0.05	B		10.6	15.7	67.3	B1		10.2	26.2	38.8
180	0.1	C		8.4	25.9	32.3	C1		10.0	35.5	28.1
180	0.2	D		6.7	40.4	16.5	D1		8.7	42.7	20.4
200	0.02	E		8.8	38.7	22.6	E1		10.1	15.7	64.8
200	0.05	F		14.4	40.2	35.7	F1		8.2	23.9	34.1
200	0.1	G		10.0	58.5	24.4	G1		8.2	34.0	24.1
200	0.2	H		9.5	62.1	15.4	H1		8.0	41.8	19.2
225	0.02	I		9.1	41.5	21.9	I1		10.3	44.4	23.2
225	0.05	L		9.0	42.7	21.1	L1		11.2	45.8	24.5
225	0.1	M		7.4	44.9	16.5	M1		11.3	64.5	17.6
225	0.2	N		8.0	50.4	16.0	N1		8.3	66.6	12.5

4.3.3 Selection of the best ME-nFe

By combining the magnetic properties (tested with a neodymium magnet) with the Fe^0, Fe_{tot}, BET surface area and morphology, the best samples were selected. These were D1 and N1, produced both with iron (III) nitrate nonahydrate with Fe/C molar ratio of 0.2, differing only for the process temperature which was 180°C for D1 and 225 °C for N1. The properties of the two samples are summarized in Table 5.

Table 5. Properties of samples D1 and N1

Sample	[Fe/C]	T (°C)	Salt	BET (m^2g^{-1})	% Fe^0	% Fe_{tot}	% Fe^0/Fe_{tot}
D1	0.2	180	$Fe(NO_3)_3 \cdot 9H_2O$	120	8.7	42.7	20.4
N1	0.2	225	$Fe(NO_3)_3 \cdot 9H_2O$	110	8.3	66.6	12.5

4.3.4 Application of the ME-nFe for heavy metal removal

The selected samples (D1 and N1) were tested to remove cadmium, copper, zinc, chromium and nickel from aqueous solutions and then, from secondary effluents. The test conditions are reported in Table 6 as well as the average results of the three replicates. The trends of metal concentrations in the different tests are represented in Figures 5, 6 and 7.

Table 6. Summary of the adsorption test conditions and results. C_{io} is the starting concentration of the heavy metals in the solution, Cn is the dose of adsorbent used, pH0 is the pH value of the solution at the beginning of the test. All the tests were done in triplicate except for exp 6, where every single phase was done in duplicate

Test	Sample	Conditions	Removal efficiency (%)				
			Zn	**Cu**	**Cd**	**Ni**	**Cr**
Exp. 1	D1	C_{i0} = 10 mg L^{-1}, pH_o = 5.3	6.2 ±3.5	20.8 ±4.6	18.3 ±1.4	3.6 ±1.7	30.3 ±13.2
	N1	C_n= 2 g L^{-1}, 54 h test; Stirring= 90 rpm Water solution	19.2 ±3.2	37.3 ±19.5	38.2 ±2.8	5.9 ±1.7	11.4 ±7.6
Exp. 2	D1	C_{i0} = 10 mg L^{-1}, pH_o = 5.2 C_n= 3 g L^{-1},	13.7 ±2.5	28.2 ±2.0	28.4 ±4.1	8.3 ±1.1	39.9 ±6.6

	N1	54 h test; Stirring= 90 rpm Water solution	83.4 ±1.2	93.7 ±0.4	85.8 ±1.0	24.5 ±5.5	1.4 ±0.4
Exp. 3	N1	C_{i0} = 10 mg L^{-1}, pH_o = 7 C_n= 3 g L^{-1}, 54 h test; Stirring= 90 rpm Bresso effluent	98.5 ±0.1	99.6 ±0.2	97.2 ±0.8	85.2 ±1.2	2.6 ±0.9
Exp. 4	N1	C_{i0} = 10 mg L^{-1} of Cr, pH_o = 5.4 C_n= 3 g L^{-1}, 54 h test; Stirring= 90 rpm Water solution	/	/	/	/	19.4 ±4.23
Exp. 5	N1	C_{i0} = 1 mg L^{-1} , pH_o = 7 C_n= 3 g L^{-1}, 54 h test; Stirring= 90 rpm Bresso effluent	97.8 ± 0.8	96.4 ±0.6	99.6 ±0.1	80.3 ±5.4	12.4 ±11.0
Exp. 6	N1	C_{i0} = 1 mg L^{-1} , pH_o = 5.4 C_n= 3 g L^{-1}, 4 h test; Stirring= 90 rpm Water solution	99.4 98.7 96.2	97.8 97.7 97.4	99.8 99.3 98.4	89.4 79.2 61.3	/ / /

Experiments 1 and 2 were made to compare the overall performance of the two samples, having as sole difference the production process temperature. The ME-nFe produced at 180°C (sample D1) resulted to be inadequate for the use it was designed for, as it released a relevant amount of iron: at the end of the experiments an iron concentration of 1.5 mg L^{-1} was reached, suggesting that the iron was not fully encapsulated in the carbon matrix. The ME-nFe produced at 225°C (sample N1) did not present the same problem. This confirms that temperature is a crucial factor to produce iron nanoparticles through the HTC process (Nizamuddin et al., 2017, Lu et al., 2013). The best achievement with the lowest ME-nFe dose (2 g L^{-1}) was a 40% removal for copper and cadmium. However, no release of metals to the solution occurred, even after a very long time. Better results were obtained with sample N1 at 3 g L^{-1}, as shown in Figure 4 (Exp. 2), while no improvement was observed for D1, still releasing iron. The use of 3 g L^{-1} of N1 allowed the removal of 93 %, 86 % and 83 % for copper, cadmium and zinc, but the effect was negligible for nickel and chromium. The increase of ME-nFE dose was proved to be an effective strategy to improve the overall removal of heavy metals. Exp. 2 was also useful to clarify that the effectiveness of the nanoparticles does not depend only on the surface area, which was higher in

sample D1, but on the combination of different characteristics such as the total iron incorporation and its distribution within the solid product. The differences between the two nanoparticles highlighted by TEM analysis and iron determination might explain the better removal performances of sample N1 that was thus chosen for the subsequent experiments.

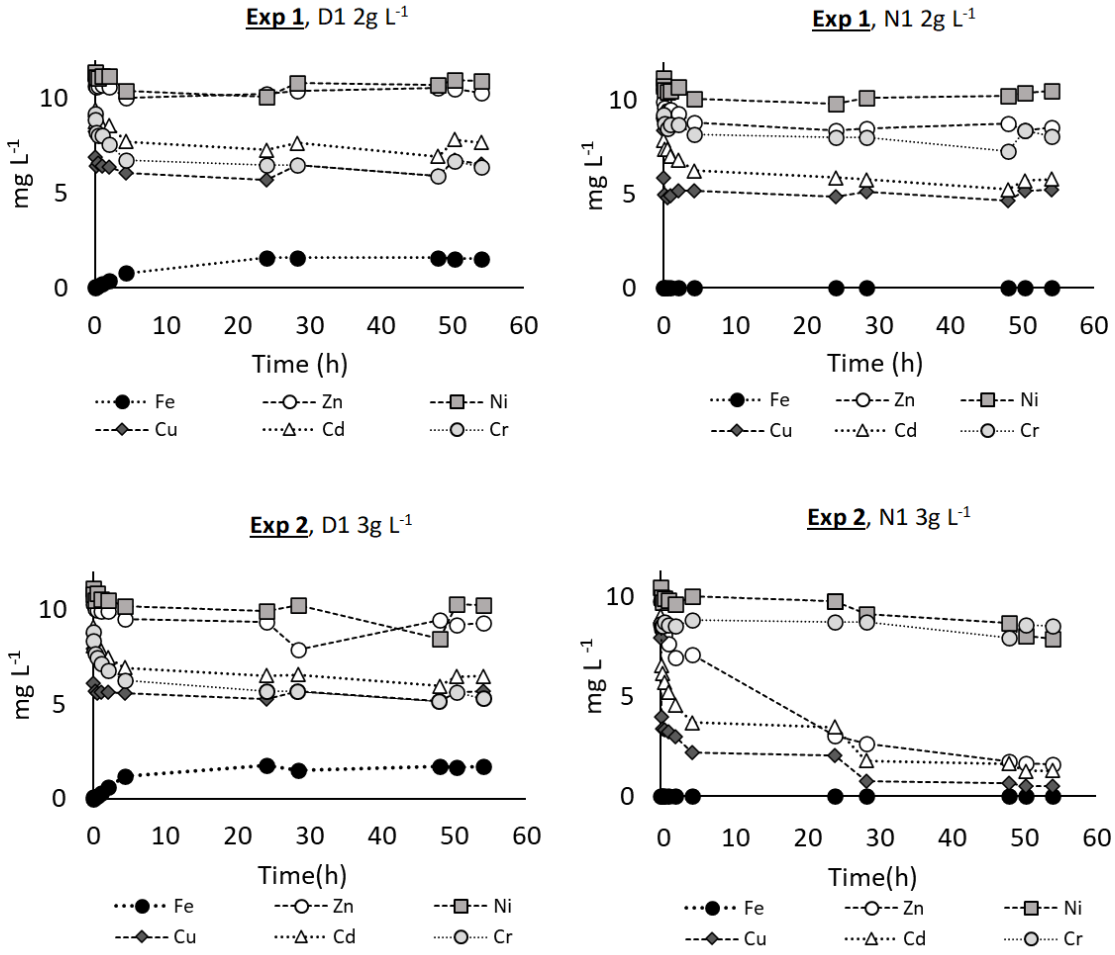

Figure 8. Trend of the residual metal concentrations during the adsorption tests. In the first raw, Exp. 1 compares sample D1 and N1 at the sorbent dose (Cn) of 2g L^{-1}. In Exp. 2, in the second raw of graph, the sorbent dose (Cn) was increased up to 3g L^{-1}.

Exp. 3 (Figure 9) was carried out in the same conditions as Exp.2, but using the secondary effluent from Bresso WWTP instead of Milli-Q® water to prepare the starting metal solutions in order to test the behavior of the nanoparticles in a realistic situation and to observe if and how the nanoparticles interact with the other dissolved and suspended components of the effluents. In that case the results were the best for all the added metals, except for chromium, with removal efficiencies of 99.6%, 98.5%, 97.2% and 85.2% for copper, zinc, cadmium and nickel,

respectively. Such better performance could be due to interaction between the heavy metals, the dissolved solids and the inorganic anions of the wastewater, leading to a better availability for the adsorption on the nanoparticles surface. Also, a natural increase of pH was observed during the trial (as for the other experiments where starting pH was around 5), from the starting value of 7 to the final value of 8.4 which might have favored hydroxide precipitation and adsorption in the core of the nanoparticles. The increase of pH can be explained by the redox reactions involving zero valent iron in a water system. Fe^0 is oxidized to Fe^{2+}, H^+ is consumed while OH^- is released. On the other hand, chromium removal was still minor. According to Zhuang et al. (2014), the surface charge of the nanoparticles changes according to the pH of the solution to be treated. Calderon and Fullana (2015) reported that in alkaline solution an overall negative charge on the nanoparticles surface can determine a low removal and reactivity for dichromate and this could have happened in our experiments due to the raise of pH. So, a Jar test (Exp.4) was conducted at a lower pH (5.4) on a water solution containing only chromium, to avoid possible interferences among heavy metals, but the final result (19.4% average removal efficiency), even if better than the previously obtained one (1.4%) was still not satisfying. It should also be underlined that $K_2Cr_2O_7$ dissolves in water forming dichromate anions which have different chemisorption compared with the other cation metals that were so easily adsorbed.

Exp. 5 (Figure 9) was characterized by a lower contaminant concentration (1 mg L^{-1} for each heavy metal cations) to represent a more realistic scenario. Even with this configuration, the results are comparable with the one of Exp. 3 with an overall removal of 99.6%, 97.8%, 96.4%, 80.3% and 12.4% for cadmium, zinc, copper, nickel and chromium respectively. The outcome suggests that the ME-nFe were not affected by the starting concentration of contaminants, at least in the tested range. The difference in the starting pH in experiments 3 and 5 with respect to the others is due to the use of Bresso effluents as matrix to prepare the starting solution to be tested. No pH adjustment were performed.

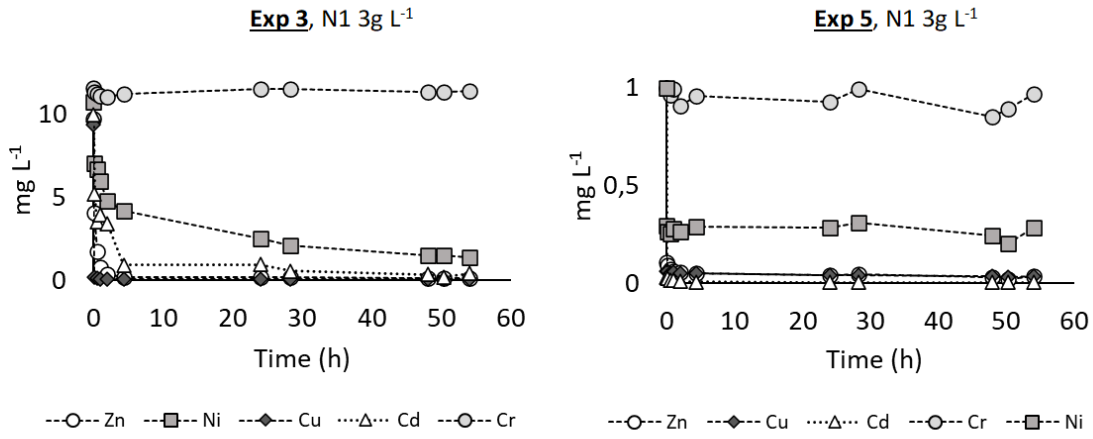

Figure 5. Trend of the residual metal concentrations during the adsorption tests. Exp. 3 and Exp. 5 were done only with sample N1 at different starting metal concentration with Cn=3g L^{-1}. Iron trend was not reported as it was negligible.

The last Jar test (Exp. 6), whose results are shown in Figure 10, had the goal to understand if the same nanoparticles could be re-used for subsequent treatments without losing their effectiveness due to the saturation effect. Considering the negligible removal in the previous experiment, chromium was excluded from the starting solution. The same nanoparticles were indeed used (after recovery and dewatering) for three consecutive Jar tests. Every single phase lasted only 4 h (that was the time when the equilibrium adsorption was reached in the previous experiments) since the release of the cations back to the treated solution was excluded. Even if the performance slightly decreased after every usage, the removal efficiencies were still over 96% for zinc, copper and cadmium, while nickel removal decreased from 89% to 79% in the second test and to 61 % in the third one. The lower removal of nickel was not unexpected as nickel had always shown a smaller affinity for the nanoparticles, so it is likely that it was less competitive than the other tested metals when the availability of active sites decreased.

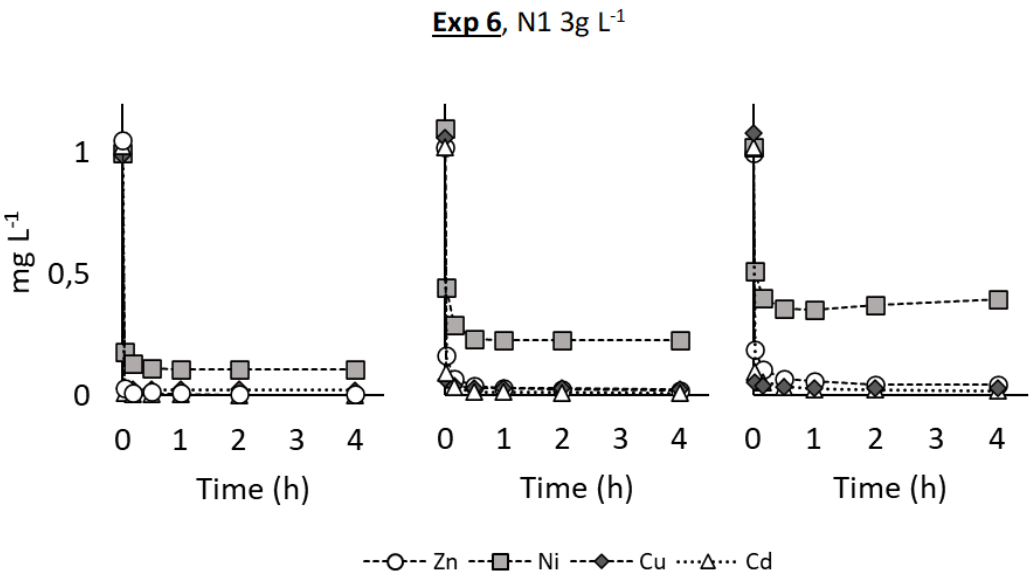

Figure 10. Trend of the residual metal concentrations during the consecutive adsorption tests using the same sample N1, recovered after every single jar test, with a Cn=3g L^{-1}. Iron trend was not reported as it was negligible.

The result obtained in the jar tests were promising even if the ME-nFE should also be tested on smaller range of contaminants (μg L^{-1}) in the future. Comparing the obtained performance with literature is not easy as microalgae were never used to produce iron nanoparticles to remove heavy metal before. The protocol to produce the ME-nFE was indeed similar to the one described in Calderon et al., 2018. Of course, their starting feedstock was different, consisting in olive mill wastewater. Is important to highlight that the final properties of the nanoparticles are strongly influenced by the used biomass. The mentioned authors used their nanoparticles, produced at 200°C, for the removal of Zinc, Nickel, Copper, Cadmium and Chromium, testing their effectiveness with and without post-treatment (consisting in the activation of the nanoparticles under N_2 to increase the zero valent iron content). The first type of nanoparticles were used, testing a load of 1 g L^{-1} to treat a solution containing 10 mg L^{-1} of each heavy metal. Removal efficiency were 34.1, 39.9, 30.4, 87.7, 88.5% for Zn, Ni, Cd, Cu and Cr, respectively. Those results are better than the one obtained in our experiment with the lower dose (Exp. 1) but worse than the one of experiment 2 apart from Cr and Cu. The authors also used the nanoparticles after the pretreatment, testing a sorbent concentration of 2.1 g L^{-1} which gave far better results (removal efficiency >98% for all the heavy metal cations). However, the second test should have been performed with the same sorbent concentration of the previous one, allowing to understand if the improvements were due to increased load of sorbent or to the increased zero valent iron.

4.4 Conclusions

The possibility to valorize the microalgal biomass grown on the centrate from municipal sewage sludge as a starting material to produce iron nanoparticles useful for polishing the final effluent was confirmed at laboratory scale. The microalgae were adequate for the hydrothermal carbonization process, which is considered an environmentally friendly way to produce iron nanoparticles. A protocol for a single-step production was applied to combine the carbonaceous structure of the biomass to an iron salt so that the forming iron nanoparticle could be incorporated into the carbon matrix and be protected from a too fast oxidation. The goal was to produce a nano-porous material with a high sorption capacity (due to the carbon shell) and reducing properties (due to the iron oxide and zero valent iron nanoparticles). Different samples were prepared changing the process conditions, using two iron salts, three different temperatures and four ratios between iron and biomass. Considering the characterization in terms of magnetism, BET surface area, total iron and zero valent iron content the two best prototypes were selected which mainly differed for the temperature of synthesis. After full characterization of the nanoparticles properties, two samples were tested as adsorbents for metal removal and only one of them showed adequate performances: this demonstrated the great importance of the operation parameters of HTC process. Using 3 g L^{-1} dose, the removal of copper, zinc, cadmium and nickel in Jar tests was fully satisfying at high (10 mg L^{-1}) and low (1 mg L^{-1}) starting concentrations, both in water and in the treated effluent from Bresso WWTP, and no iron release was observed during the trials. The removal was always a little less efficient for nickel than for the other metals but, unexpectedly, chromium was removed to a negligible extent. The reason for such different performance of the selected nanoparticles on chromium will need further studies to be understood. In view of scaling up, an important preliminary achievement was the effectiveness of recovered and recycled nanoparticles for 2-3 adsorption trials. The only metal whose removal decreased significantly with time was nickel and the reasons for that will also need further investigation. The possibility of an easy magnetic separation and re-use of the nanoparticles is very important in terms of energy and money saving and in terms of environmental impact of the production and of the final disposal. The study led to interesting new scenarios concerning the use of microalgae for wastewater treatment strategies. In fact, microalgae-bacteria consortia could be integrated in real WWTP as an alternative biological treatment to remove contaminants from wastewater, and the obtained biomass could be exploited to synthetize ME-nFe to be used directly in the plant for a tertiary polishing treatment of the effluent.

4.5 References

Alsbaiee, A., Smith, B.J., Xiao, L., Ling, Y., Helbling, D.E., Dichtel, W.R., 2016. Rapid removal of organic micropollutants from water by a porous β-cyclodextrin polymer. Nature. https://doi.org/10.1038/nature16185

Ambika, S., Devasena, M., Nambi, I.M., 2020. Single-step removal of Hexavalent chromium and phenol using meso zerovalent iron. Chemosphere. https://doi.org/10.1016/j.chemosphere.2020.125912

Arvaniti, O.S., Hwang, Y., Andersen, H.R., Stasinakis, A.S., Thomaidis, N.S., Aloupi, M., 2015. Reductive degradation of perfluorinated compounds in water using Mg-aminoclay coated nanoscale zero valent iron. Chem. Eng. J. https://doi.org/10.1016/j.cej.2014.09.079

Batista, A.P., Gouveia, L., Bandarra, N.M., Franco, J.M., Raymundo, A., 2013. Comparison of microalgal biomass profiles as novel functional ingredient for food products. Algal Res. 2, 164–173. https://doi.org/10.1016/j.algal.2013.01.004

Bonaiti, S., Calderon, B., Collina, E., Lasagni, M., Mezzanotte, V., Saez, N.A., Fullana, A., 2017. Nitrogen activation of carbon-encapsulated zero-valent iron nanoparticles and influence of the activation temperature on heavy metals removal. IOP Conf. Ser. Earth Environ. Sci. 64, 012070. https://doi.org/10.1088/1755-1315/64/1/012070

Calderon, B., Fullana, A., 2015. Heavy metal release due to aging effect during zero valent iron nanoparticles remediation. Water Res. 83, 1–9. https://doi.org/10.1016/j.watres.2015.06.004

Calderon, B., Smith, F., Aracil, I., Fullana, A., 2018. Green Synthesis of Thin Shell Carbon-Encapsulated Iron Nanoparticles via Hydrothermal Carbonization. ACS Sustain. Chem. Eng. 13, 24. https://doi.org/10.1021/acssuschemeng.8b01416

Choochote, W., Suklampoo, L., Ochaikul, D., 2014. Evaluation of antioxidant capacities of green microalgae. J. Appl. Phycol. https://doi.org/10.1007/s10811-013-0084-6

Crane, R.A., Scott, T., 2014. The removal of uranium onto carbon-supported nanoscale zero-valent iron particles. J. Nanoparticle Res. https://doi.org/10.1007/s11051-014-2813-4

Deng, Y., Zhao, R., 2015. Advanced Oxidation Processes (AOPs) in Wastewater Treatment. Curr. Pollut. Reports. https://doi.org/10.1007/s40726-015-0015-z

Doria, E., Campion, B., Sparvoli, F., Tava, A., Nielsen, E., 2012. Anti-nutrient components and metabolites with health implications in seeds of 10 common bean (Phaseolus vulgaris L. and Phaseolus lunatus L.) landraces cultivated in southern Italy. J. Food Compos. Anal. https://doi.org/10.1016/j.jfca.2012.03.005

Esplugas, S., Bila, D.M., Krause, L.G.T., Dezotti, M., 2007. Ozonation and advanced oxidation technologies to remove endocrine disrupting chemicals (EDCs) and pharmaceuticals and personal care products (PPCPs) in water effluents. J. Hazard. Mater. https://doi.org/10.1016/j.jhazmat.2007.07.073

Fu, F., Wang, Q., 2011. Removal of heavy metal ions from wastewaters: A review. J. Environ. Manage. https://doi.org/10.1016/j.jenvman.2010.11.011

Hargreaves, A.J., Constantino, C., Dotro, G., Cartmell, E., Campo, P., 2018. Fate and removal of metals in municipal wastewater treatment: a review. Environ. Technol. Rev. https://doi.org/10.1080/21622515.2017.1423398

Heilmann, S.M., Davis, H.T., Jader, L.R., Lefebvre, P.A., Sadowsky, M.J., Schendel, F.J., von Keitz, M.G., Valentas, K.J., 2010. Hydrothermal carbonization of microalgae. Biomass and Bioenergy 34, 875–882. https://doi.org/10.1016/j.biombioe.2010.01.032

Hemalatha, A., Girija, K., Parthiban, C., Saranya, C., Anantharaman, P., 2013. Antioxidant properties and total phenolic content of a marine diatom , Navicula clavata and green microalgae , Chlorella marina and Dunaliella salina. Pelagia Res. Libr.

Hoch, L.B., Mack, E.J., Hydutsky, B.W., Hershman, J.M., Skluzacek, J.M., Mallouk, T.E., 2008. Carbothermal synthesis of carbon-supported nanoscale zero-valent iron particles for the remediation of hexavalent chromium. Environ. Sci. Technol. 42, 2600–5.

Kadirvelu, K., Thamaraiselvi, K., Namasivayam, C., 2001. Removal of heavy metals from industrial wastewaters by adsorption onto activated carbon prepared from an agricultural solid waste. Bioresour. Technol. https://doi.org/10.1016/S0960-8524(00)00072-9

Li, Y., Zhao, X., Yan, Y., Yan, J., Pan, Y., Zhang, Y., Lai, B., 2019. Enhanced sulfamethoxazole degradation by peroxymonosulfate activation with sulfide-modified microscale zero-valent iron (S-mFe 0): Performance, mechanisms, and the role of sulfur species. Chem. Eng. J. https://doi.org/10.1016/j.cej.2019.03.178

Lim, A.P., Aris, A.Z., 2014. A review on economically adsorbents on heavy metals removal in water and wastewater. Rev. Environ. Sci. Biotechnol. https://doi.org/10.1007/s11157-013-9330-2

Ling, Y., Alzate-Sánchez, D.M., Klemes, M.J., Dichtel, W.R., Helbling, D.E., 2020. Evaluating the effects of water matrix constituents on micropollutant removal by activated carbon and β-cyclodextrin polymer adsorbents. Water Res. https://doi.org/10.1016/j.watres.2020.115551

Liu, H., Chen, Y., Yang, H., Gentili, F.G., Söderlind, U., Wang, X., Zhang, W., Chen, H., 2019. Hydrothermal carbonization of natural microalgae containing a high ash content. Fuel. https://doi.org/10.1016/j.fuel.2019.03.004

Lu, X., Pellechia, P.J., Flora, J.R.V., Berge, N.D., 2013. Influence of reaction time and temperature on product formation and characteristics associated with the hydrothermal carbonization of cellulose. Bioresour. Technol. https://doi.org/10.1016/j.biortech.2013.03.163

Magni, S., Parolini, M., Soave, C., Marazzi, F., Mezzanotte, V., Binelli, A., 2015. Removal of metallic elements from real wastewater using zebra mussel bio-filtration process. J. Environ. Chem. Eng. https://doi.org/10.1016/j.jece.2015.01.017

Mantovani, M., Marazzi, F., Fornaroli, R., Bellucci, M., Ficara, E., Mezzanotte, V., 2019. Outdoor pilot-scale raceway as a microalgae-bacteria sidestream treatment in a WWTP. Sci. Total Environ. https://doi.org/10.1016/j.scitotenv.2019.135583

Nizamuddin, S., Baloch, H.A., Griffin, G.J., Mubarak, N.M., Bhutto, A.W., Abro, R., Mazari, S.A., Ali, B.S., 2017. An overview of effect of process parameters on hydrothermal carbonization of biomass. Renew. Sustain. Energy Rev. https://doi.org/10.1016/j.rser.2016.12.122

Orazova, S., Karpenyuk, T., Goncharova, A., Tzurkan, Y., Kairat, B., 2014. The effect of light intensity to the lipids productivity and fatty acid composition of green microalgae. J. Biotechnol. https://doi.org/10.1016/j.jbiotec.2014.07.413

Ötleş, S., Pire, R., 2001. Fatty acid composition of Chlorella and Spirulina microalgae species. J. AOAC Int. https://doi.org/10.1093/jaoac/84.6.1708

Peng, L., Ren, Y., Gu, J., Qin, P., Zeng, Q., Shao, J., Lei, M., Chai, L., 2014. Iron improving bio-char derived from microalgae on removal of tetracycline from aqueous system. Environ. Sci. Pollut. Res. 21, 7631–7640. https://doi.org/10.1007/s11356-014-2677-2

Qiu, G., Wu, Y., Qi, L., Chen, C., Bao, L., Qiu, M., 2018. Study on the degradation of azo dye wastewater by zero-valent iron. Nat. Environ. Pollut. Technol. 17, 479–483.

Saeed, A., Akhter, M.W., Iqbal, M., 2005. Removal and recovery of heavy metals from aqueous solution using papaya wood as a new biosorbent. Sep. Purif. Technol. https://doi.org/10.1016/j.seppur.2005.02.004

Safafar, H., Wagenen, J. Van, Møller, P., Jacobsen, C., 2015. Carotenoids, phenolic compounds and tocopherols contribute to the antioxidative properties of some microalgae species grown on industrial wastewater. Mar. Drugs. https://doi.org/10.3390/md13127069

Sevilla, M., Fuertes, A.B., 2009. Chemical and structural properties of carbonaceous products obtained by hydrothermal carbonization of saccharides. Chem. - A Eur. J. 15, 4195–4203. https://doi.org/10.1002/chem.200802097

Sun, H., Zhou, G., Liu, S., Ang, H.M., Tadé, M.O., Wang, S., 2012. Nano-Fe 0 Encapsulated in Microcarbon Spheres: Synthesis, Characterization, and Environmental Applications. ACS Appl. Mater. Interfaces 4, 6235–6241. https://doi.org/10.1021/am301829u

Sunkara, B., Zhan, J., He, J., McPherson, G.L., Piringer, G., John, V.T., 2010. Nanoscale zerovalent iron supported on uniform carbon microspheres for the in situ remediation of chlorinated hydrocarbons. ACS Appl. Mater. Interfaces. https://doi.org/10.1021/am1005282

Williams, C.J., Aderhold, D., Edyvean, R.G.J., 1998. Comparison between biosorbents for the removal of metal ions from aqueous solutions. Water Res. 32, 216–224. https://doi.org/10.1016/S0043-1354(97)00179-6

Zhu, X., Liu, Y., Qian, F., Zhou, C., Zhang, S., Chen, J., 2014. Preparation of magnetic porous carbon from waste hydrochar by simultaneous activation and magnetization for tetracycline removal. Bioresour. Technol. 154, 209–214. https://doi.org/10.1016/j.biortech.2013.12.019

Zhuang, L., Li, Q., Chen, J., Ma, B., Chen, S., 2014. Carbothermal preparation of porous carbon-encapsulated iron composite for the removal of trace hexavalent chromium. Chem. Eng. J. https://doi.org/10.1016/j.cej.2014.05.038

Chapter 5

5. Management of the hydrothermal carbonization liquid fraction (HTC-LF)

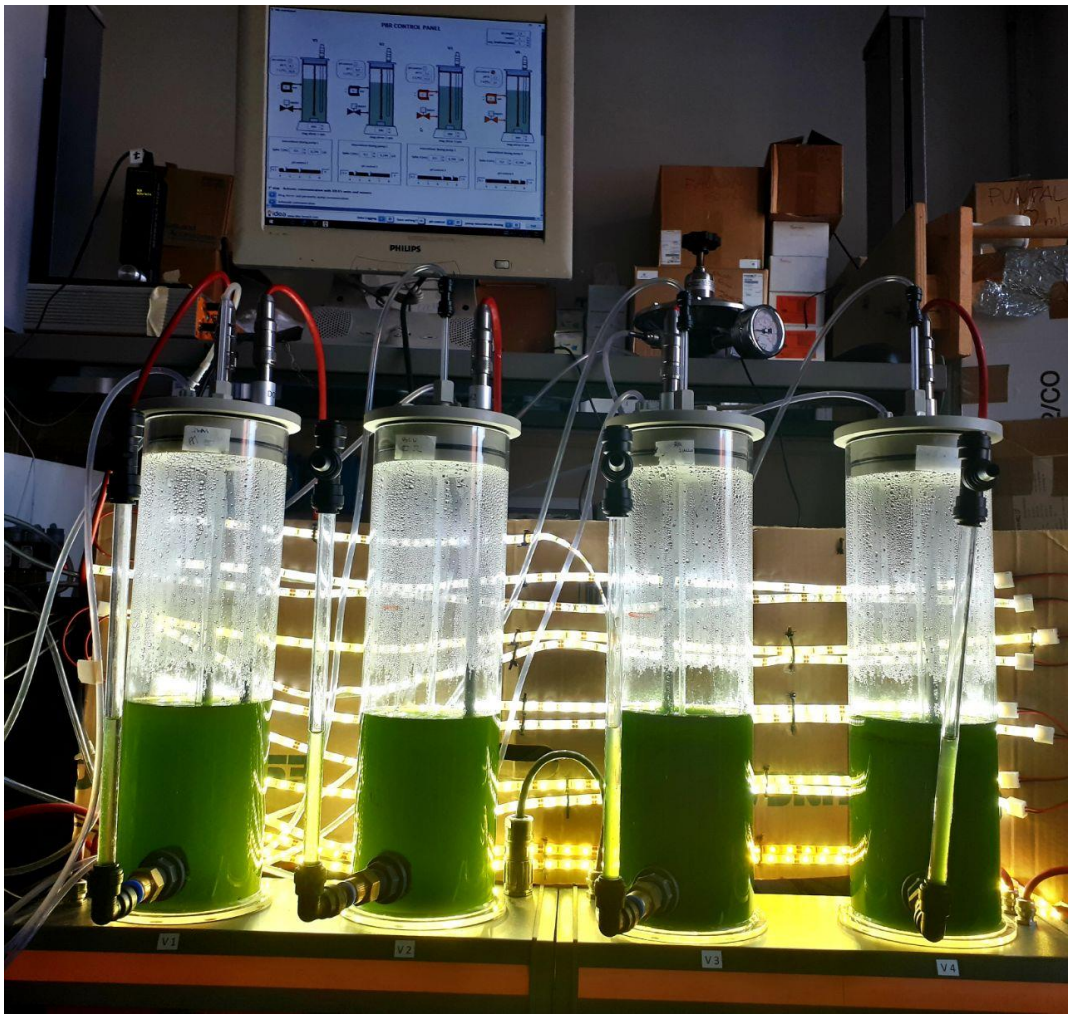

5.1 Introduction

The HTC process generates three different products. While the solid material was the focus of the previous two sections of the thesis, the gaseous (HTC-GF) (which is forming in low quantities), and the liquid fraction (HTC-LF) are byproducts that need a precise characterization and a proper management plan.

Depending on the feedstock and operative settings (T and P) the chemical composition of the HTC-LF does change (Wang et al., 2018). Little information can be found in literature about the quantitative composition of the LF deriving from the hydrothermal liquefaction of microalgae at high temperature, and even less data are reported for LF from hydrothermal carbonization. The presence of phenols, alkales, volatile fatty acids (VFAs), cyclic amines and benzenes are mentioned as well as inorganic nutrients like nitrogen (in the forms of NH_4-N) and phosphorus (Chen et al., 2014; Roberts et al., 2013). It is also important to highlight that the high concentration of organic compounds, which are forming during the chain-like HTC chemical reactions, might determine a severe toxicity not only for water compartment but also for plants and algae (Usman et al., 2019). Pretreatments must be performed prior to disposal. Anaerobic digestion, for example, could be a suitable option as it was demonstrated that it could reduce the COD content of HTC wastewaters up to 44-60%. (Chen et. al., 2016). Weide et al. 2019 tested a continuous treatment of LF from HTC of wood and sewage sludges by two subsequent anaerobic steps and a final aerobic one at pilot scale. Two volumetric loads (0.44 and 0.88 g COD L^{-1} d^{-1}) were used for 367 and 135 days, respectively. COD removal efficiency was 58% and 55%, showing a negligible effect of the volumetric loading, within the tested range.

So, a straight management plan of the HTC-LF is required to obtain a sustainable process to produce ME-nFe using the microalgae from Bresso. Based on these considerations, Microtox test and PAM analysis were performed on the produced HTC-LF to study its toxicity for water compartment. Furthermore, since the HTC-LF was characterized for high nutrient concentrations in terms of ammonium and phosphorus, but not so different if compared to the ones of Bresso centrate, the feasibility of using it as a growth media for microalgae was evaluated, designing the entire production of the ME-nFE as indicated in Figure 1.

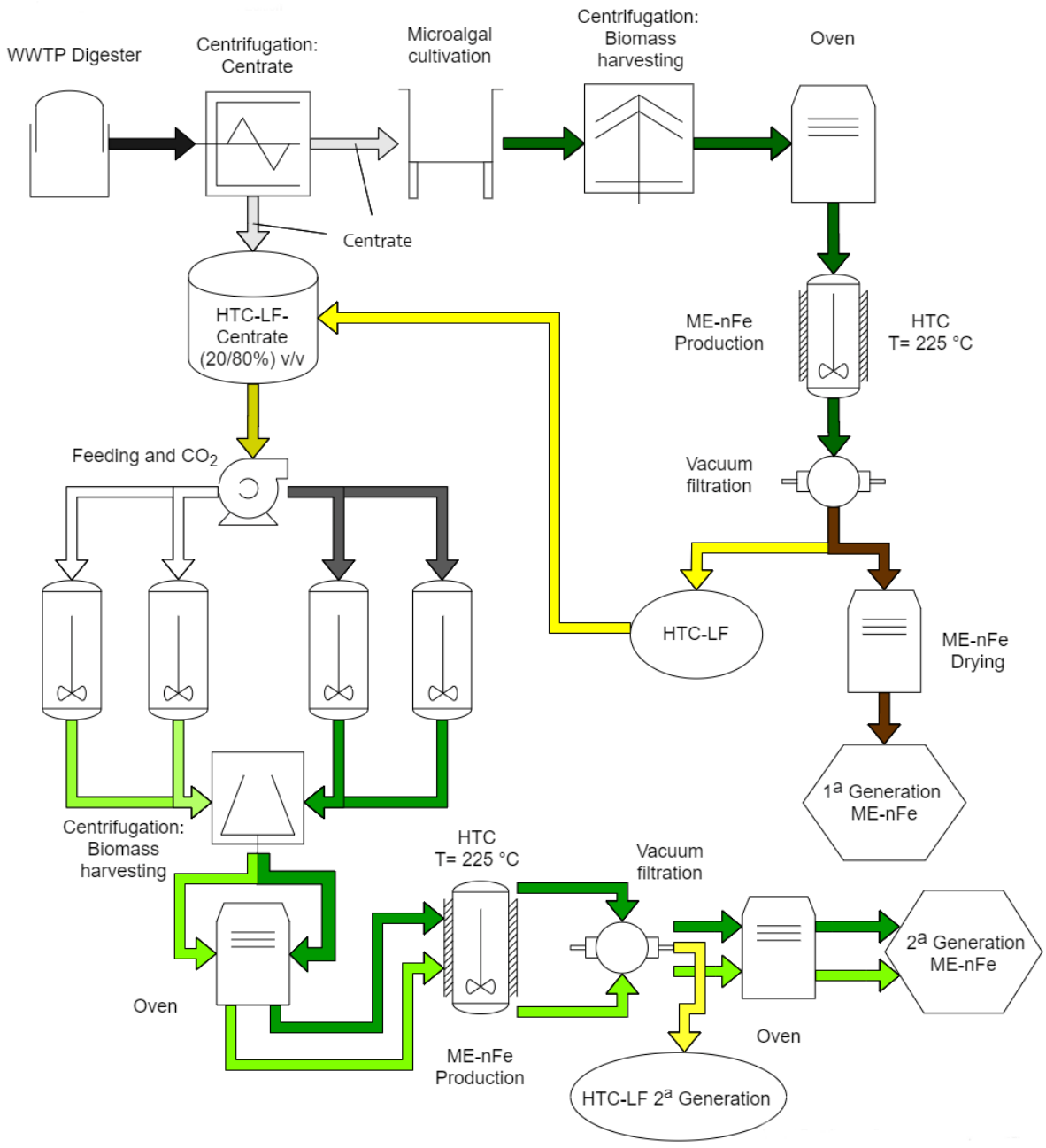

Figure 1. ME-nFe production cycle. The centrate from municipal digestate is treated by microalgae which are harvested to produce microalgal-based carbon-encapsulated iron nanoparticles. The liquid bioproduct produced during the HTC process (HTC-LF) is used in a new microalgal cultivation unit, alongside municipal centrate, to grow new biomass for subsequent synthesis of nanoparticles.

5.2 Materials and methods

5.2.1 Biomass cultivation, harvesting and HTC synthesis

The microalgae used as feedstock for the HTC process were collected from the pilot-scale high rate algal pond (HRAP) located at the Bresso-Niguarda WWTP as was described in Chapter 2. The biomass was treated via HTC, maintaining the operative parameters that were already described in Chapter 4. 3 g of dried microalgae were resuspended in 100 mL of distilled water and mixed with 8 g of iron (III) nitrate nonahydrate ($Fe(NO_3)_3 \cdot 9H_2O$). The reactor temperature was set to 225°C for a 3 h residence time. The HTC-LF was recovered after vacuum filtration, following the washing process of the nanoparticles with 100 mL of distilled water. At the end of the process 200 mL of HTC-LF were recovered and stored in glass bottles for the subsequent steps of the work.

5.2.2 HTC-LF characterization

The HTC-LF produced with the ME-nFe is an ochre or transparent straw-yellow liquor having a pungent smell, suggesting the presence of dissolved volatile substances in it. Table 1. reports the average characterization in terms of nutrient concentrations, pH and solid content (TSS and OD680) of the HTC-LF. The analyzed samples were characterized for relatively high level of NH_4-N and high concentration of COD, deriving from the liquid phase reactions occurring during the HTC process of the microalgal biomass. The presence of nitrogen and phosphorus and the general aspect of the HTC-LF are quite interesting, making that specific wastewater look like Bresso centrate, which was already proved to be suitable for microalgal growth (Marazzi et a. 2017, Marazzi et. al 2019, Mantovani et al. 2020, Rossi et al. 2020). Also, the low solid content and optical density are features that make the HTC-LF interesting for microalgal cultivation. On the other hand, the high COD concentration stands out as the main criticism as it is too high to allow microalgal growth. The observed variability in the nutrient concentration could depend on differences in the composition of the microalgae that were used (this must always be considered as the HRAP in Bresso is an outdoor cultivation system, where changes in the community composition can be common and fast). However, differences among the HTC reactions yield cannot be ruled out leading to the formation of different class of substances.

Table 1. Chemico-physical characteristics of the HTC-LF. All data are expressed as mean ± standard deviation (n=6)

NH_4-N (mg L^{-1})	NO_3-N (mg L^{-1})	NO_2-N (mg L^{-1})	PO_4-P (mg L^{-1})	COD (mg L^{-1})	TSS (mg L^{-1})	Optical density 680nm	pH
490 ± 118	1.1 ± 0.8	14.4± 2.3	6.8± 0.8	2410± 184	23±20	0.1± 0.1	6.8±0.5

5.2.3 Microtox assay

Microtox is an in vitro testing system which uses bioluminescent bacteria (*Allivibrio fischeri*) to investigate the acute toxicity of water and solid samples. Toxicity is detected as a decrease of the bioluminescence after 5 and 15 minutes of exposure. Acute toxicity was performed using a Microtox M500 analyzer (MODERN WATER INC, Delaware, USA) for the detection of the luminescence inhibition on *Vibrio fischeri* according to BS EN ISO 11348-1:2007. Tests were performed following the 81.9% Basic test protocol which consists of a control and serial dilutions of the sample. The inhibitory effect was determined first on the raw sample of HTC-LF as median effect concentration (EC50) and then on pretreated samples. In fact, chemical precipitation following pH adjustment (pH was first increased with NaOH 1M, the supernatant was then recovered and finally pH was restored adding HCl 1M) was tested as a way to reduce toxicity as well as centrifugation and adsorption on activated carbons.

Adsorption through Jar tests, having a 4h contact time, were carried out using a commercial wood-derived activated carbon (Norit® CA1, Sigma Aldrich, Saint Louis, USA). Two adsorbent loading were used (2 and 3gL^{-1}). After adsorption, the activated carbons were separated from the supernatant through centrifugation (10 minute at 5000 rpm).

5.2.4 Microalgal growth and toxicity evaluation

A lab-scale test was carried out to investigate the feasibility of using different HTC-LF dilutions (60%, 40%, 20% and 5%) as a growth medium for *Chlorella vulgaris*. The pure microalgal culture was provided by Istituto Spallanzani (Rivolta d'Adda, CR, Italy). Basal bold medium (BBM) was used as control and diluent. 250 mL Erlenmeyer flasks were put on an orbital shaker at 120 rpm and were artificially illuminated at 100 µmol m^{-2} s^{-1} with a 12 h/12 h light/dark cycle for 72 h. Every HTC-LF dilution was prepared in duplicate. *Chlorella* spp. was inoculated in the flasks to reach a starting optical density (OD680) of 0.1. The growth test was coupled with acute toxicity evaluation at different exposure times (0, 1, 24, 48 and 72h) through Phyto-PAM tests, which were performed using a Phyto-PAM II (HeinzWalz GmbH, Eeltrich, Germany). Samples of the algal suspensions were diluted to reach a OD (680nm) of 0.1 and then were kept in the dark for 20 min. F0, which is the minimal florescence in the dark-adapted condition was assessed after 45 second of acclimation using a low intensity light condition (PAR = 1 µmol m^{-2} s^{-1}). Fm, which is the maximal fluorescence was measured after a saturation light pulse (PAR = 26 µmol m^{-2} s^{-1} width 500 ms). Photosynthetic efficiency is an adimensional value, determined according to Kitajima and Butler (1975) and Marazzi et al. (2019) as follows:

$$Fv/Fm = (Fm - F0)/Fm$$

OD680, total suspended solids (TSS) and algal counts through hemocytometer were detected at the same time to quantify the algal biomass. SYTOX Green assay was performed to measure the viability of the microalgal communities using the SYTOX Green nucleic acid stain. Following the staining process between the nucleic acids of the microalgae and SYTOX Green dye, cells are characterized for a bright green fluorescence when excited by light at the wavelength of 450–490 nm. However, this can occur only in dead cells as the dye cannot penetrate the cell walls of living microalgae, which can be easily distinguished for their red color induced by the autofluorescence of chlorophyll (Zetsche and Meysman, 2012). For the staining step, the microalgal suspension (1 mL) of each samples was centrifuged for 10 minutes at 10000 rpm. The pellet was then resuspended in 1 mL of distilled water and SYTOX-Green was added (0,5 µL). The dye-labeled samples were then kept in the dark for ten minutes and they were observed using a Zeiss fluorescence microscope Axio Scope HBO 50. An average of 300 cells were counted randomly

through the slide, noting the proportion between dead and living cells (green and red, respectively). The viability of every sample was obtained as follows:

$$V\% = \frac{G}{R+G} * 100$$

Where V% is the cell viability percentage, G is the number of observed green cells (dead) and R is the number of red cells (alive).

5.2.5 Preliminary batch cultivation

A 40-days batch cultivation was performed at lab scale on the 20% HTC-LF dilution, reproducing the same conditions of the previous experiment in terms of type of reactor (Erlenmeyer flasks), illumination and mixing. However, the HTC-LF was mixed with Bresso centrate (20/80% v/v) instead of the BBM as the goal was to test the possibility to recirculate the HTC-LF in a microalgal cultivation unit to grow fresh microalgal biomass for new HTC processes. *Chlorella vulgaris* was inoculated in duplicate to reach a starting OD680 value of 0.3. A control was also prepared using only centrate as grow medium.

5.2.6 Continuous cultivation

A continuous cultivation of 40-days was performed using a specific designed reactor for microalgae culturing (IDEA Bioprocess Technology Srls, Dalmine, BG, Italy). It consists of four columns photobioreactors (PBRs) (operative volume of 1.5L) equipped with probes for the monitoring of temperature, pH and dissolved oxygen. Each column is connected to a stirring bloc which contains a magnetic rotor, providing mechanical mixing through a powerful stirring bar (ASTEROID 40, 2mag AG, Muenchen - Germany). Every column is also supplied with independent feeding units consisting of four peristaltic pumps. An insufflation line drive CO_2 bubbling to reactor 3 and 4, controlling pH under a chosen value (set point pH=7.5). This system was not connected to reactor 1 and 2, having free pH. The culturing system was also equipped with artificial illumination (100 µmol m^{-2} s^{-1}) working on a 12/12 h cycle. Every column was filled with the HTC-LF/centrate solution (20/80% v/v) and inoculated with a mixed microalgal community (made of *Chlorella* spp. and *Euglena gracilis*) from Bresso HRAP to reach a starting OD680 value of 0.1. All the PBRs were first maintained in batch for 10 days to allow better

adaptation to the new conditions; after that they were fed continuously, setting a hydraulic retention time (HRT) of 10 days chosen as it is the usual HRT of Bresso HRAP. The discharged microalgal suspension of each PBR was collected and centrifuged on daily basis. The biomass was dried at 50°C using an electric oven and stored for future analysis.

5.2.7 Analytical Determinations

Nitrogen containing nutrients (NH_4-N, NO_3-N, and NO_2-N), phosphate (PO_4-P), and soluble Chemical oxygen demand (COD) were detected through spectrophotometric test kits (Hach-Lange, Düsseldorf, Germany, LCK303, LCK 340, LCK 342, LCK 348, and LCK1414, respectively), on filtered samples (0.45 µm). pH and temperature were measured using a laboratory probe (XS PC 510 Eutech Instruments) during the preliminary growth test and the batch cultivation. However, pH and temperature were measured online by the culturing system and recorded during the continuous test. Microalgal concentration was assessed in different ways: measuring the total suspended solids (TSS) and volatile suspended solids (VSS) according to standard methods (APHA/AWWA/WEF, 2012); through optical density (OD680) using a DR 3900 Hach Lange (Germany) spectrophotometer and by algal cell counts. Microalgae were counted using an optical microscope 40X (B 350, Optika, Italy) and a hemocytometer (Marienfeld, Germany). Morphology and size were used as indicator to distinguish different strains. The cell concentration was obtained as the mean of 72 square observation (0.04 mm^2) and expressed as cell mL^{-1}.

5.2.8 Statistical analyses

Statistical analyses were carried out using R project software (R Core Team, 2018). T-test for unpaired data was performed to highlight differences between PBRs grown with and without CO_2 for the nutrient percentage removal efficiency (η PO_4-P, η COD and η NH_4-N), microalgal growth rate (rTSS) and Ammonia Oxidizing Bacteria growth rate (rAOB). p-values <0.05 were deemed to be significant.

5.3 Results and discussion

5.3.1 Microtox

Figure 2. shows the results of the Microtox assay. 81.9% Basic tests were performed on the raw HTC-LF first, showing a very strong effect even on very diluted samples (Exp.1, EC50= 1.8% after 15 min). This was not an unexpected result as the toxicity of wastewater derived from the HTC of different biomass is known by literature. Mihajlović et al. 2018 tested the liquor obtained during the HTC of *Miscanthus giganteus* performed at the temperature of 180, 200 and 220°C, highlighting comparable EC50 to the one of the present work (1.29%, 1.05% and 0.69%, respectively). Unfortunately, no reports on Microtox test using HTC wastewater from microalgae were found for a direct comparison.

The test was than repeated after a pre-treatment step, consisting in causing the precipitation of dissolved iron after pH adjustment. However the final toxicity was still very high, proving that the problem was not the dissolved iron but probably the presence of some toxic organic compounds or maybe the combination of both (Exp.2, EC50= 6.8% after 15 min). However, a centrifugation step (10 minute at 5000 rpm) was also tested showing no better results (Exp. 3, EC50= 6.5% after 15 min). The most effective pre-treatment was certainly the adsorption through activated carbons. Both the tested concentrations ($2gL^{-1}$ and $3\ gL^{-1}$) were able to sensibly reduce the wastewater toxicity, with the best result achieved using the $3g\ L^{-1}$ dose (Exp. 4, EC50= 60% after 15 min). The last graph shows the comparison in terms of toxicity of the raw HTC-LF and the different pre-treated samples, proving that the adsorption with activated carbons could be an interesting strategy to reduce the toxicity of the HTC-LF in view of a more sustainable management.

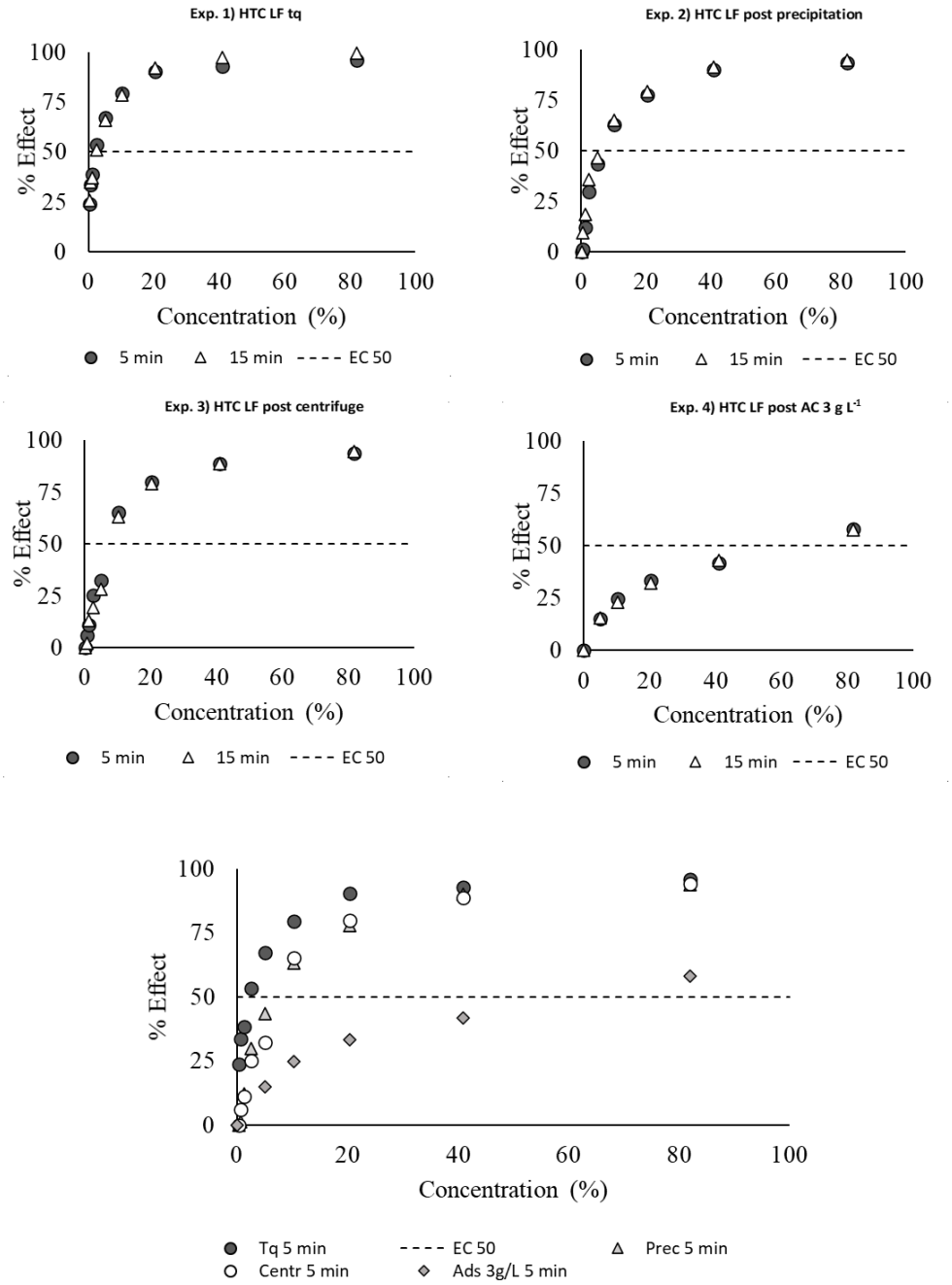

Figure 2. Microtox toxicity evaluation: Exp.1 was performed on the raw HTC-LF as obtained after the ME-nFe synthesis; Exp.2 was repeated on the supernatant of HTC-LF after pH adjustment to let dissolved iron precipitate; Exp.3 was performed on the supernatant of HTC-LF after centrifugation; Exp.4 was carried out on a pre-treated sample of HTC-LF with activated carbon.

5.3.2 Microalgal growth and toxicity evaluation

During the preliminary test all the microalgae were able to grow and the only sensible inhibition was observed in the sample with the highest HTC-LF concentration (60%). Figure 3. highlights the maximal photochemical efficiency trend over time (Fv/Fm). All the samples were characterized by values higher than 0.5 suggesting good photosynthetic efficiencies (Ranglová et al., 2019). However, samples grown on the highest HTC-LF concentration showed an evident decrease of Fv/Fm. On the other hand, the viability assay with Sytox Green did not show differences between the samples and the control even after 72 h (Table 2). Table 2 also reports the microalgal concentration at the end of the test. As for the cell counts, comparable data were obtained among the samples and the control (with the only exception represented by the microalgae grown on the 5% HTC-LF that reached the highest concentration). However, TSS value were very different among the samples and the control. In particular, the higher the HTC-LF percentage to form the growth media, the higher was the TSS concentration. Those differences were explained by the developing of bacteria, which could be observed at the optical microscope especially in samples D and E. Those samples were the ones in which nutrients and COD were higher due to the high percentage of HTC-LF. The availability of organic matter and O_2 produced by microalgae might have promoted heterotrophic bacteria, leading to higher total biomass. The phenomenon observed in those samples was indeed curios but still very interesting, proving that some bacteria could be more resistant than *Allivibrio fischeri*. By considering those results, the 20% dilution was chosen as the best compromise for further analyses.

Table 2. TSS concentration obtained at the end of the test, expressed as mean ± st.dev (n=4); Cell counts (Cell mL^{-1}) and percentage of living cell (%)

Samples	TSS (gL^{-1})	Cell counts (Cell mL^{-1})	Viability (%)
A Control	0.21 ± 0.1	$5.49x10^6$	81
B HTC-LF 5%	0.22 ± 0.1	$1.18x10^7$	81
C HTC-LF 20%	0.28 ± 0.3	$3.83x10^6$	86
D HTC-LF 40%	0.4 ± 0.3	$2.53x10^6$	80
E HTC-LF 60%	0.5 ± 0.4	$2.15x10^6$	80

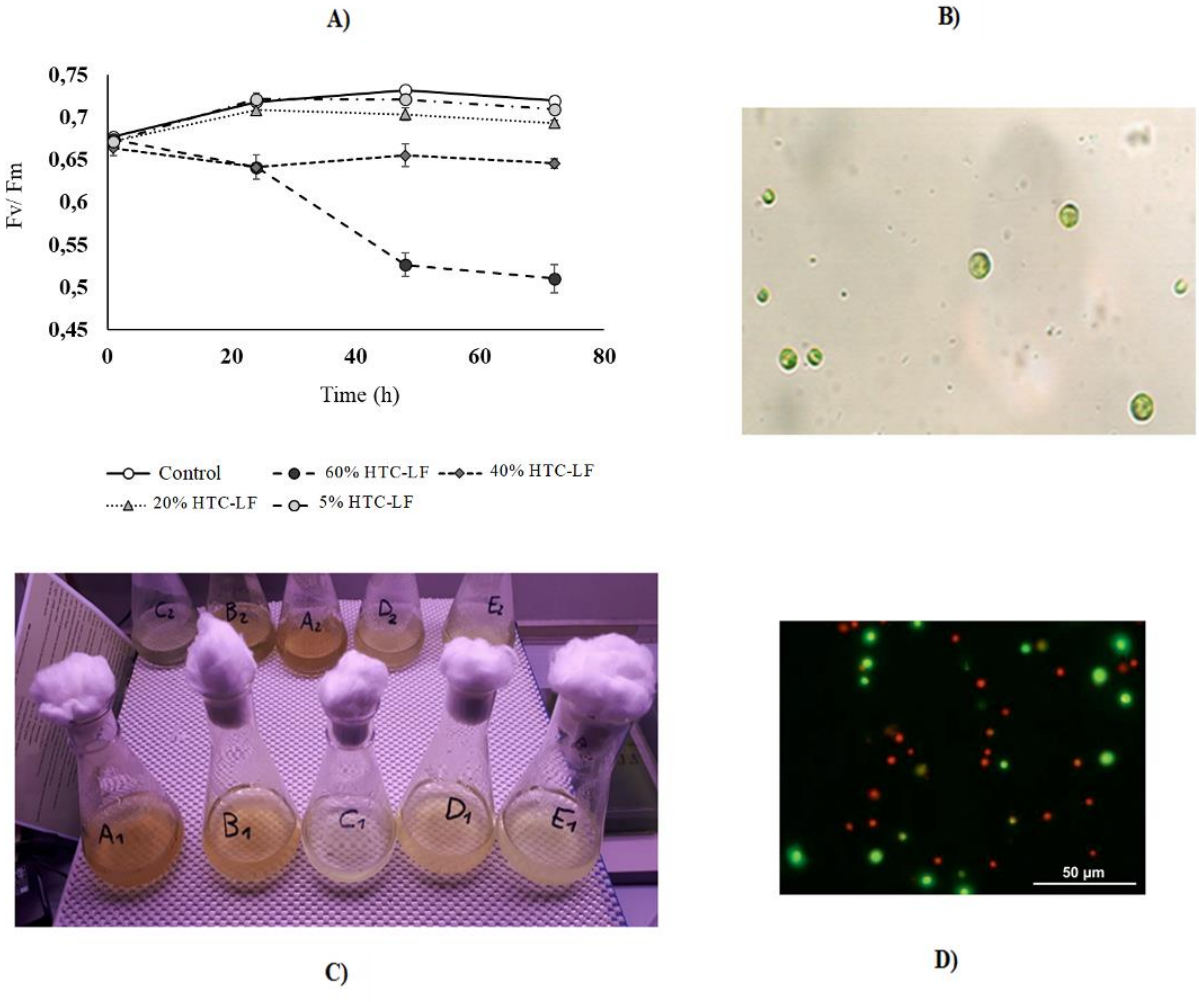

Figure 3. Maximal photochemical efficiency trend over time (Fv/Fm) data are shown as mean ± standard deviation (n=4) (A); Chlorella spp. at the optical microscope (B); Samples in duplicates grown on the different dilutions of HTC-LF at t0 (C); Sytox-Green assay showing red cells (alive) and green cells (dead) (D)

5.3.3 Preliminary batch cultivation

The test lasted almost 40 days, showing interesting results which are reported in Figure 4. The first graph on the left is the trend of TSS in time, which is a good proxy for the microalgal concentration in a medium. A long lag phase was observed in both samples as high flocculation (even after sonication) occurred. The microalgal concentration at day 7 and 14 seems lower than time zero, but it was mainly due to flocculation making difficult to collect a representative sample. However, *Chlorella* was able to adapt to the new environment and did grow after two weeks, reaching high TSS concentration over $1 gL^{-1}$ at the end of the test. NH_4-N and PO_4-P were rapidly

consumed in the control, but the trend was much slower in the samples as the algae were not fully adapted. However, after 20 days, during the exponential growth phase, consumption of nutrients became very fast even in A1 and A2. As expected from past studies (Marazzi et. al 2019, Mantovani et al. 2020) the COD of the Bresso centrate is not very degradable, so it was constant in time in the control. However, the starting COD was higher in samples A1 and A2 due to the HTC-LF contribution. On the contrary, COD was rapidly consumed after two weeks in both A1 and A2 as the algae started to adapt till COD values reached the one in the control. This was very interesting as it shows that the COD fraction of the HTC-LF could be consumed by microalgae.

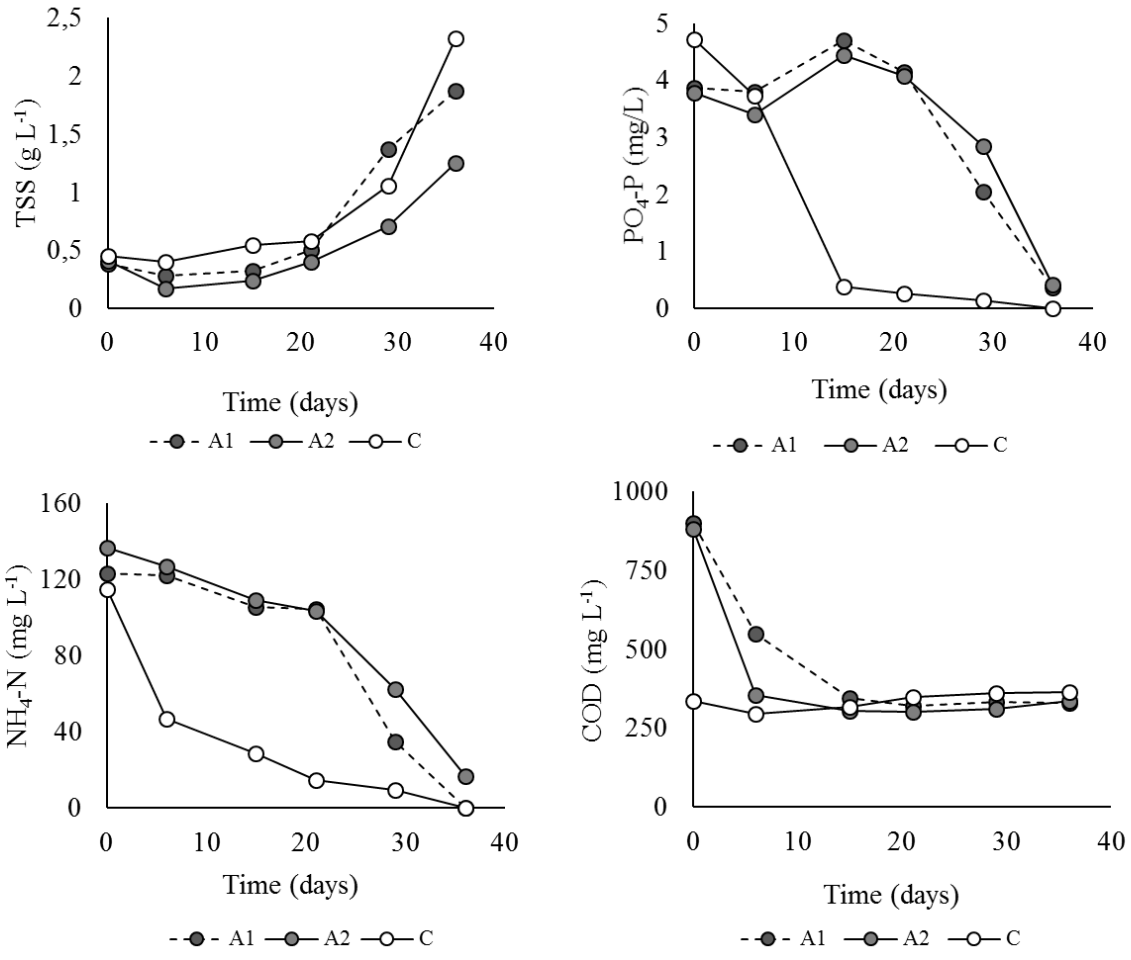

Figure 4. Total suspended solids (TSS) and nutrients consumption (NH_4-N, COD, PO_4-P) over time.

5.3.4 Continuous cultivation

Both microalgae with and without CO_2 were able to grow during the 35-day continuous cultivation, having an average microalgal growth rate (rTSS) of 43 ± 8 and 62 ± 5 $mgL^{-1}d^{-1}$, respectively. Figure 5. compares the trend of TSS concentration (including both microalgae and bacteria biomass) and OD680 of the samples. By looking at the graphs, it is evident that the two proxies for microalgal concentration seems in discordance. On the left, the TSS trend would suggest that the microalgae could grow better in the PBRs with CO_2. However, the OD680 had similar evolution only at the beginning of the test. In fact, microalgae were able to double their OD level after 10 days when CO_2 was bubbled, while microalgae without CO_2 needed more time. After day 17, a strong drop in terms of optical density occurred only for samples grown under CO_2, while the other ones could still increase their concentration, reaching a final OD value of 1.7. The presence of bacteria biomass alone is less convincing this time to explain the difference between the trend of TSS and the other variables. However, a shift in microalgal community composition was observed during the trial: in the PBRs without CO_2 *Chlorella* spp. became dominant and *Euglena gracilis* disappeared. *Euglena gracilis* is known to prefer pH between 4 and 8 (Danilov and Ekelund, 2001) and this condition was not respected in PBRs without CO_2, which had higher pH at least in the first part of the test. On the contrary, PBRs with CO_2 maintained the original microalgal composition as pH was stable around 7.5. Since *Euglena* is characterized for way bigger cells than *Chlorella*, the overall TSS in PBR with CO_2 was probably higher even when the OD680 was not as high as in PBR without CO_2.

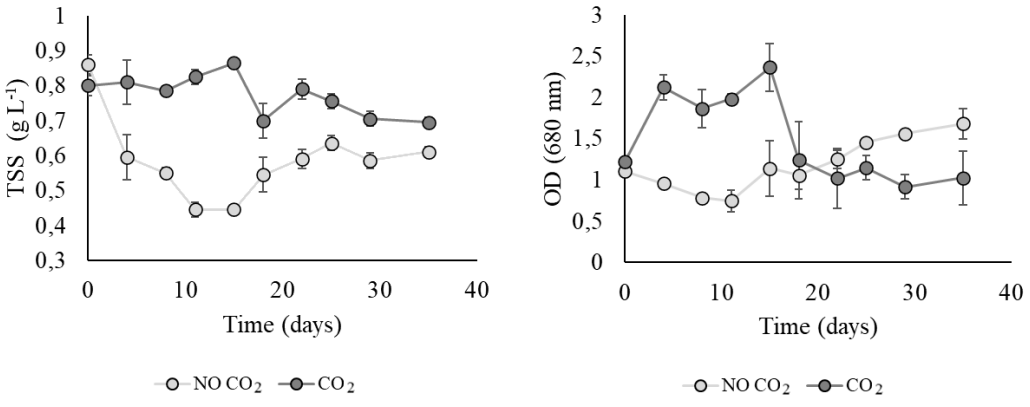

Figure 5. TSS concentration (on the left) and OD680 (on the right) trend over time. Data are shown as mean ± standard error (n=2).

The microscope cell counts ranged between 10^6 and 10^7 cells mL^{-1} throughout the test. The trends over time, which are reported in Figure 6. are very similar to the ones of OD680. At first, the microalgal concentration was higher in the PBR with CO_2 intake but the situation was reversed during the second part of the trial. A strong correlation between total cell counts and optical density was indeed highlighted both in PBRs with and without CO_2 (R^2=0.85 and R^2=0.83, respectively). However, no correlation was observed between TSS and total algal counts (Figure 7.).

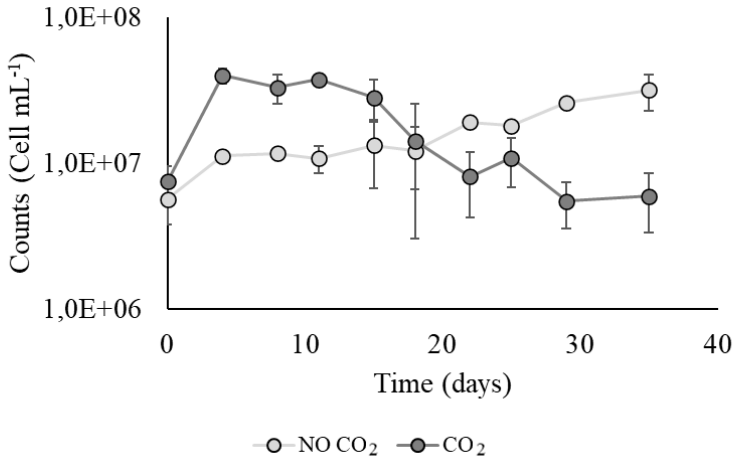

Figure 6. Microalgal cell counts trend over time. Data are shown as mean ± standard error (n=2)

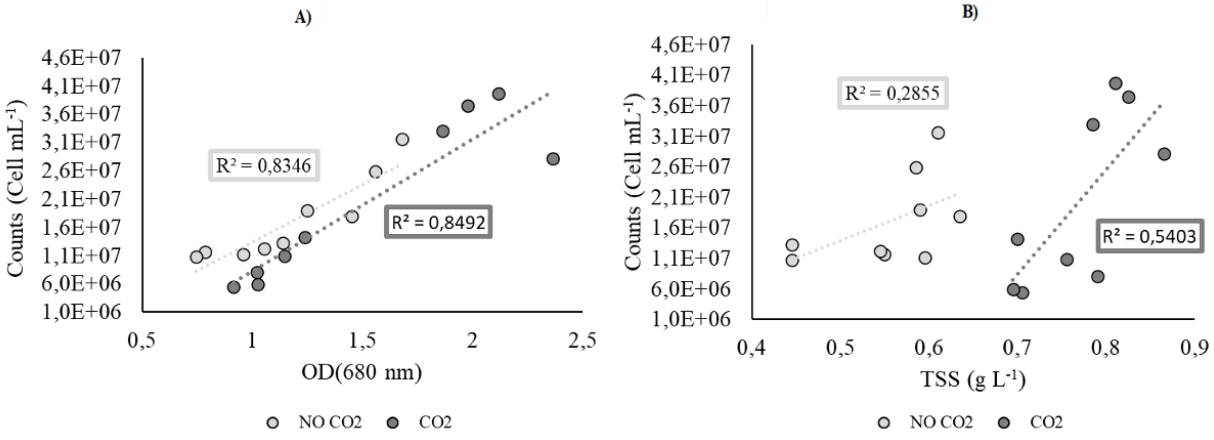

Figure 7. A) Linear regression between total counts and OD (680) showing strong correlation; B) Linear regression between total counts and TSS showing no correlation.

Temperature and pH evolution in time are plotted in Figure 8. As can be seen, temperature in the reactors did strongly change during the test, following the environmental temperature in the laboratory. The probes registered a maximum of 27.7 °C at the beginning of the cultivation and a minimum of 18 °C of day 31. pH control did work quite fine in the samples grown under CO_2 and was very stable around the set point of 7.5. Of course, pH value vas higher in the samples grown without CO_2 and it was very stable during the first two weeks. After day 15, a partial nitrification started with the accumulation of $N\text{-}NO_2$ which was responsible for the decrease of pH from 8.8 to 7.8.

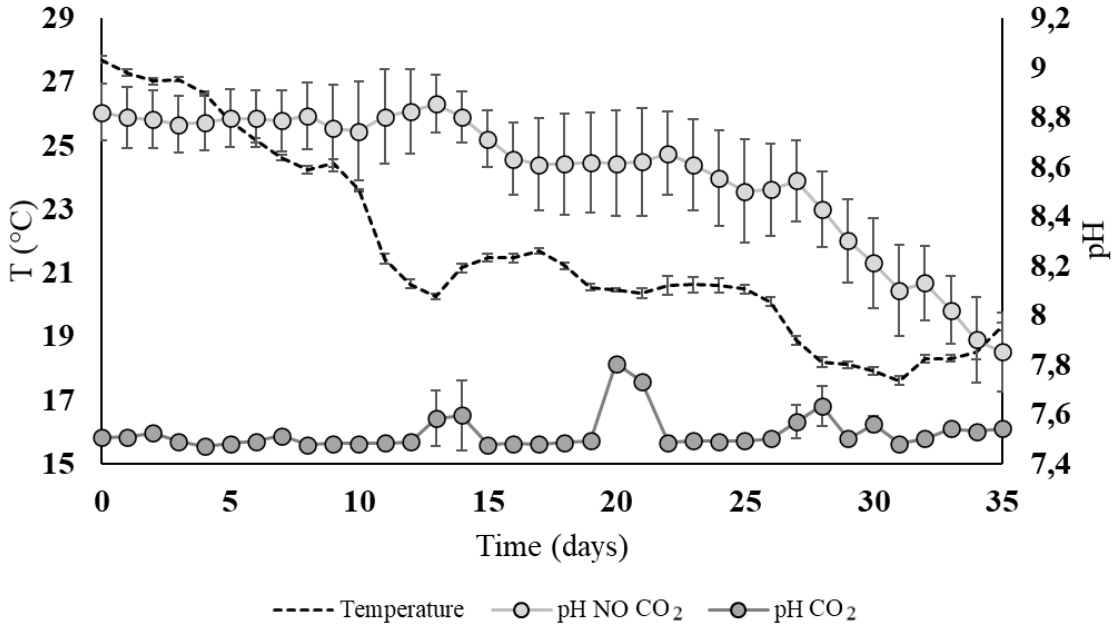

Figure 8. Temperature and pH trend in time registered by the online probes. Data are shown as mean ± standard error (n=2)

Phyto-PAM analyses suggested that the microalgae were able to adapt to the 20% HTC-LF as the photosynthetic efficiency was high and stable during all the cultivation. At first, Fv/Fm was only 0.5 suggesting that the microalgae still needed to adapt properly to their new media. However, as reported in Figure 9., just after few days of continuous feeding the Fv/Fm increased, remaining between 0.6 and 0.7 afterwards.

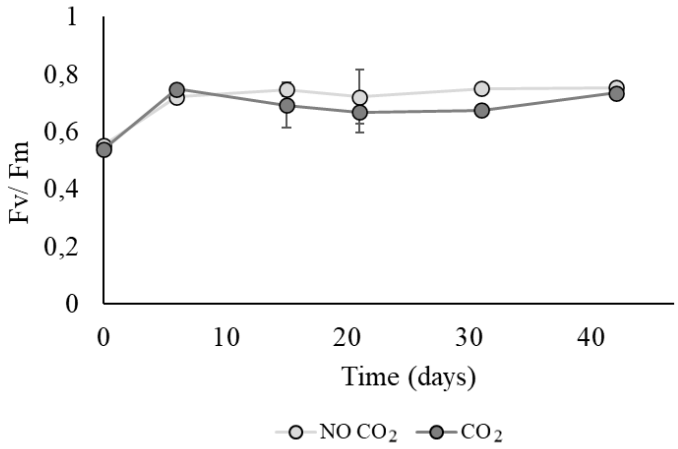

Figure 9. Photosynthetic efficiency, expressed as Fv/Fm. Data are shown as mean ± standard error (n=2)

As visible in Figure 10, an effective removal of phosphorus (A) was achieved rapidly and maintained during the whole test, with average values of 91% and 94% for the microalgae grown without and with CO_2, respectively. COD removal (B) was interesting too, with average percentage of 62% and 65% for the microalgae grown without and with CO_2, respectively. Those data confirmed the ones found during the batch-cultivation step. On the other hand, the NH_4-N removal (C) was low in all the reactors at least till day 20 when partial nitrification started, especially in the community grown without CO_2 (Figure 11). The t-test for unpaired data showed that the microalgal growth rate (rTSS) and the ammonia oxidizing bacteria growth rate (rAOB) were significantly different between samples (Figure 12). Of course, a higher microalgal productivity was expected where CO_2 was bubbled with the double aim of sustaining the photosynthesis and maintaining the pH under a certain level to limit nitrogen stripping. However, the community grown without CO_2 was still able to grow without limitation, probably exploiting the CO_2 produced during the oxidation of COD. Nevertheless, what is less clear is why the partial nitrification was promoted faster in the PBRs without CO_2. It is known that nitrifying bacteria are very sensitive to pH. Skadsen et al., (2002) reports an optimum pH range for *Nitrosomonas* between 7 and 8. However, AOB can be deeply influenced also by other parameters such as free ammonia, temperature and light making it difficult to predict the nitrification process (Van Hulle et al., 2010). T-test for unpaired data were performed also on $P\text{-}PO_4$, COD and NH_4-N percentage removal (η PO_4-P, η COD and η NH_4-N). However, the differences were not statistically relevant as suggested by the boxplots reported in Figure 13.

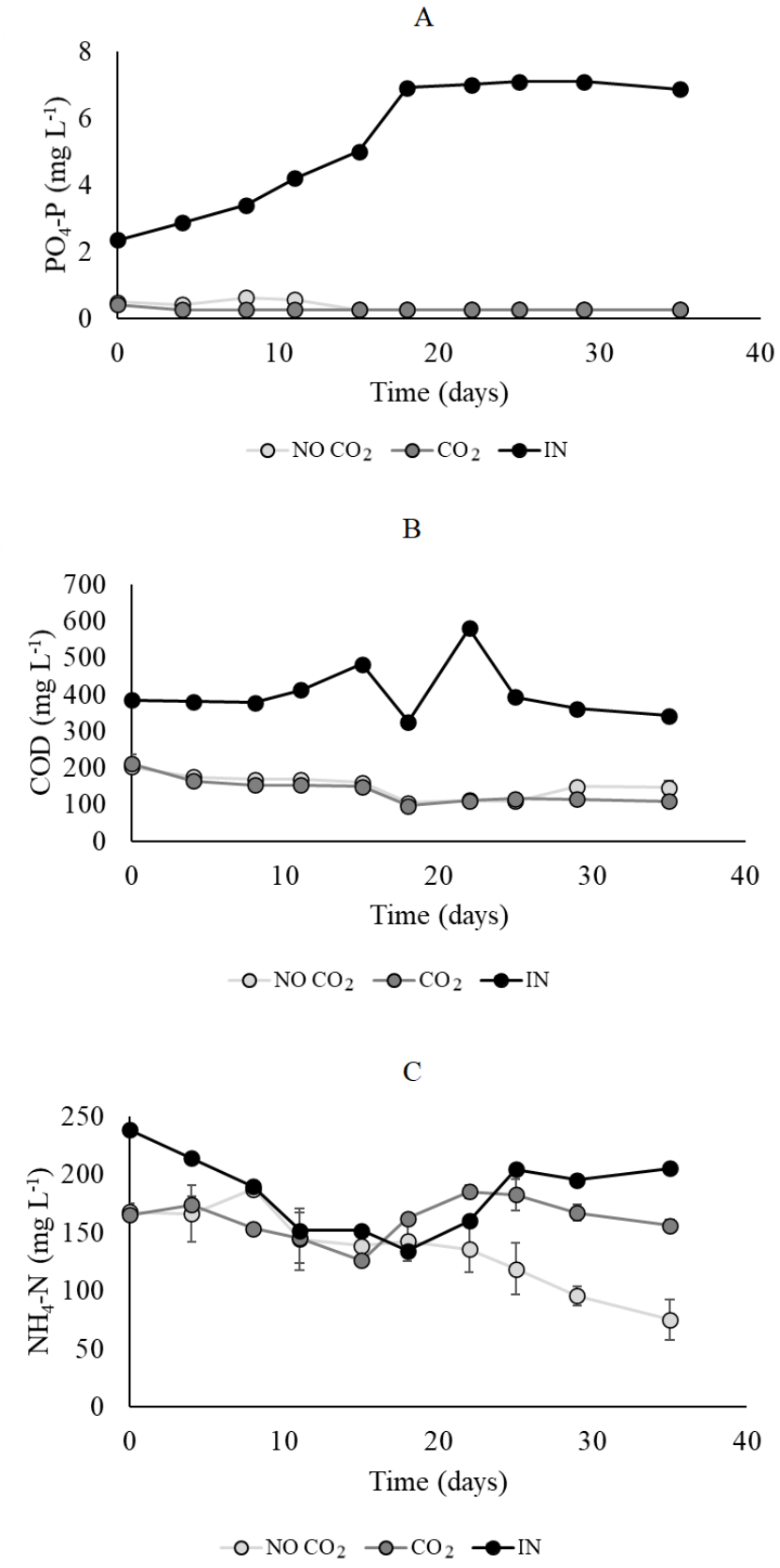

Figure 10. PO_4-P (A), COD (B), and total NH_4-N (C) concentrations in the PBRs during the continuous test. Data are shown as mean ± standard error (n=2).

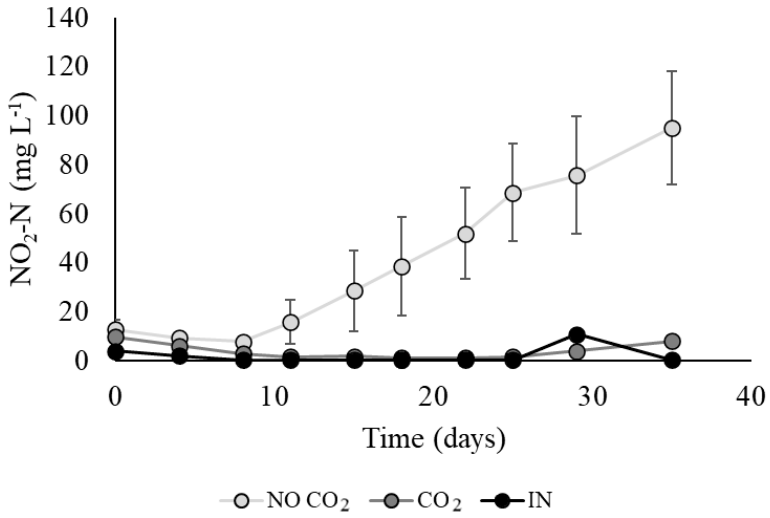

Figure 11. NO_2-N concentrations in the PBRs during the continuous test. Data are shown as mean ± standard error (n=2)

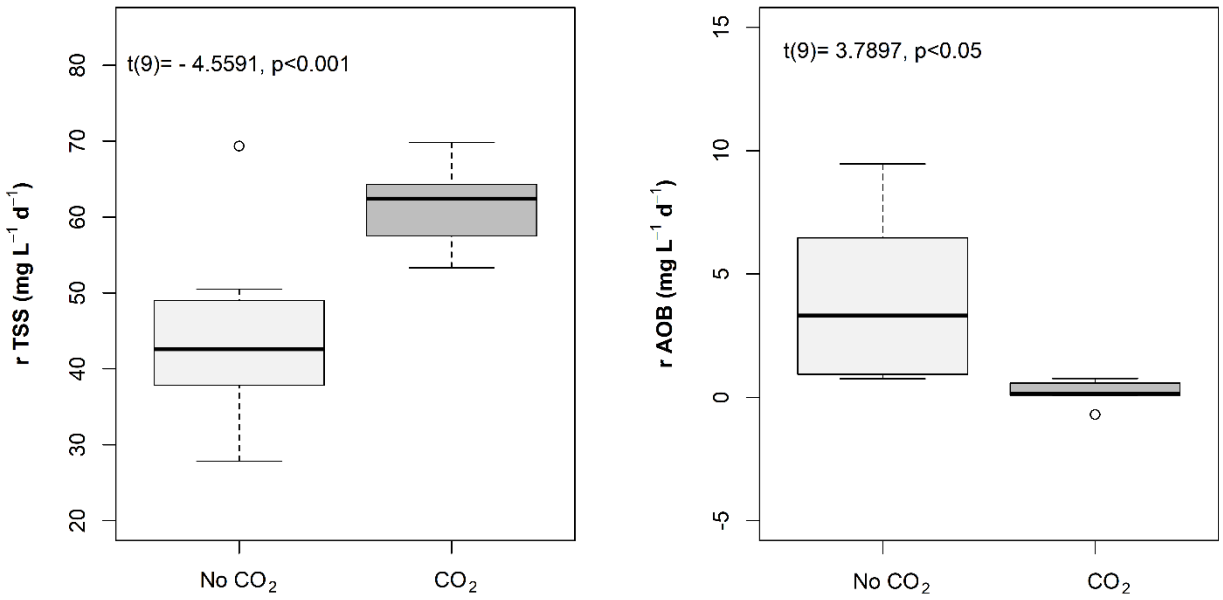

Figure 12. Boxplots representation showing the means of rTSS and rAOB. Boxes show the range between the 25th and 75th percentiles. The whiskers go from the edge of the box to the minimum and maximum data values. The horizontal line indicates the median value.

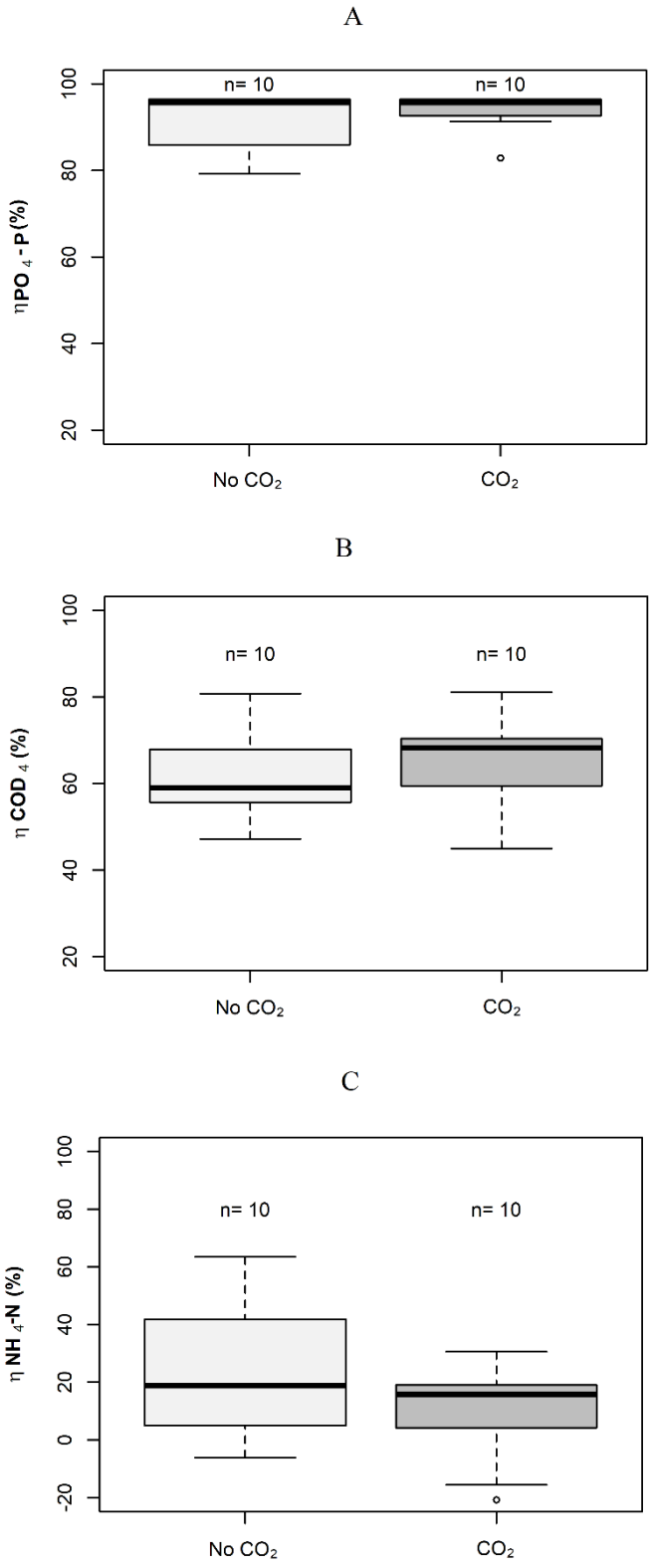

Figure 13. Boxplots representation showing the means of η PO_4-P (A), η COD (B) and η NH_4-N (C). Boxes show the range between the 25th and 75th percentiles. The whiskers go from the edge of the box to the minimum and maximum data values. The horizontal line indicates the median value.

As explained in the previous section of this thesis, the interaction between microalgae and bacteria seems crucial to achieve high performance in nutrients removal from municipal centrate. This consideration seems valuable also in this experiment. The increasing nitrite concentration in the PBRs was very interesting, showing that Ammonia Oxidizing Bacteria (AOB) could grow even in the 20% dilution of the HTC-LF. Of course, rAOB was relevant only in the samples grown without CO_2, however an increase of NO_2-N was starting in the other PBRs as well. (Figure 11 from day 29). Furthermore, the COD removal was also an evidence of intense heterotrophic bacteria activity, still compatible with the HTC-LF, leading to the release of CO_2 which could be used by microalgae themselves. Finally, a sample of each microalgal suspensions have been collected at the end of the batch cultivation (day 40) and the liquid fractions (obtained after centrifugation) were than tested via Microtox, comparing their toxicity with the one of the HTC-LF-centrate solution used as growth medium. As can be observed in the graph reported in Figure 13, a substantial decrease of toxicity was observed after the microalgal cultivation. The EC50 rose from 20% in the HTC-LF-centrate solution (IN) to 30% in the samples (CO_2 and No CO_2). Of course, the supernatants were still toxic after the microalgal treatment, highlighting the need to further pretreatments before a safe disposal. However, other toxicity assay involving different trophic levels could be interesting to have a better knowledge of the situation.

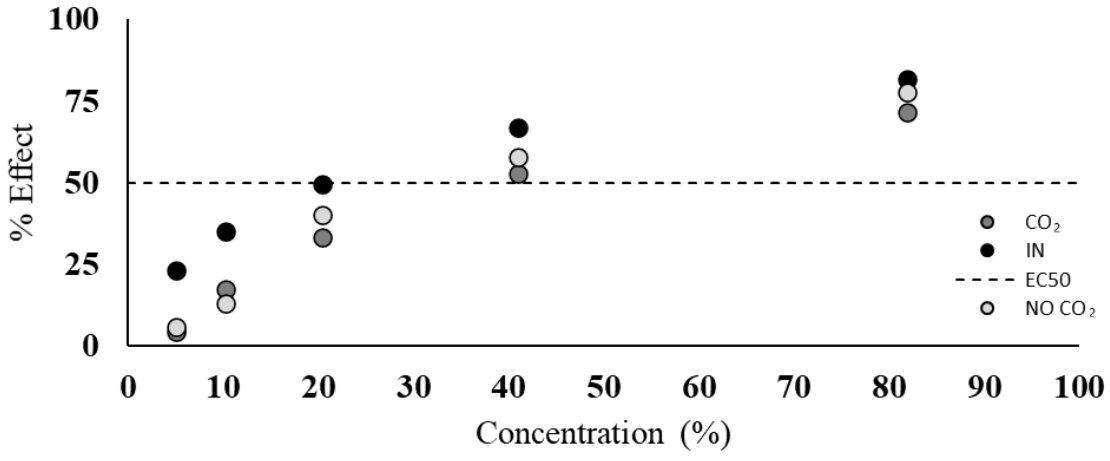

Figure 13. Microtox toxicity evaluation comparing the HTC-LF-centrate solution used during the microalgal cultivation (IN) and the supernatant of the samples of microalgal suspension (CO_2 and NO CO_2) collected at day 40.

The possibility to grow microalgae on HTC wastewater was already proposed by different authors precisely for the presence of high concentration of nutrients, however those tests were mainly performed as short batch experiments on very diluted wastewaters. Comparisons are not that simple as the HTC wastewaters might differ depending on the nature of the starting biomass and the HTC conditions. Du et al. (2012) tested the potential of *Chlorella vulgaris* to grow in different dilutions (from 50 to 200 times) of the HTC-LF. The microalgae were able to grow and to remove 45.5- 59.9% of total nitrogen (TN), 85.8- 94.6% of total phosphorus (TP) and 50.0 - 60.9% of COD. A similar approach was evaluated by Belete et al. (2019), using the liquid fraction of HTC of activated sludge to enrich the brackish water from the Sede Boker saline aquifer (Israel) to cultivate *Coelastrella* spp. and *Chlorella* spp. However, the mixture was also enriched with micronutrient (1 ml L^{-1} of the A5 solution from the Zarrouk medium). The microalgae were able to grow during a short-term batch tests (5 days) having growth rates similar to the one of the control grown on BG11 medium.

5.4 Conclusions

The HTC-LF obtained during the synthesis of ME-nFe was proved to be toxic for *Allivibrio fisheri*, suggesting a harmful potential against water compartment. However, the overall toxicity was reduced through adsorption with wood-derived activated carbons. On the other hand, the possibility to grow microalgae on the HTC-LF was demonstrated as no sensible inhibition in the photochemical activities was detected for *Chlorella vulgaris*. Giving the presence of nitrogen and phosphorus, a 20% dilution of the HTC-LF was tested both in batch and continuous experiments as a growth medium for microalgae (using both pure cultures and mixed microalgal community grown on the supernatant of municipal digestate). The studies demonstrated that the microalgae could grow in the HTC-LF with or without CO_2 addiction to foster the photosynthesis. The microalgal treatment was able to reduce the nutrient concentration and partial nitrification also occurred, proving that AOB bacteria could resist in the HTC-LF. COD removal, which was around 60%, was particularly interesting, demonstrating that some organic components of the HTC-LF could be degraded by the synergy of microalgae and bacteria, leading to a slightly decrease in terms of toxicity. The study could provide an interesting option for the management of the liquid wastewater produced with the ME-nFe. The entire production of iron nanoparticles could be designed as a cycle in which the liquid byproduct is redirected in a new microalgal cultivation unit and used to obtain new biomass for subsequent synthesis of second generation

ME-nFe. After being used as growth medium, the HTC-LF could be treated through adsorption with activated carbons to decrease its toxicity, allowing a final and safer disposal.

5.5 References

APHA/AWWA/WEF, 2012. Standard Methods for the Examination of Water and Wastewater. Stand. Methods 541. https://doi.org/ISBN 9780875532356

Chen, H., Wan, J., Chen, K., Luo, G., Fan, J., Clark, J., Zhang, S., 2016. Biogas production from hydrothermal liquefaction wastewater (HTLWW): Focusing on the microbial communities as revealed by high-throughput sequencing of full-length 16S rRNA genes. Water Res. https://doi.org/10.1016/j.watres.2016.09.052

Chen, W.T., Zhang, Y., Zhang, J., Yu, G., Schideman, L.C., Zhang, P., Minarick, M., 2014. Hydrothermal liquefaction of mixed-culture algal biomass from wastewater treatment system into bio-crude oil. Bioresour. Technol. https://doi.org/10.1016/j.biortech.2013.10.111

Danilov, R.A., Ekelund, N.G.A., 2001. Effects of pH on the Growth Rate, Motility and Photosynthesis in Euglena gracilis. Folia Microbiol. (Praha). https://doi.org/10.1007/BF02818001

ISO, 2007. ISO 11348-3:2007 - Water quality -- Determination of the inhibitory effect of water samples on the light emission of Vibrio fischeri (Luminescent bacteria test). Int. Organ. Stand. (ISO)

Kitajima, M., Butler, W.L., 1975. Quenching of chlorophyll fluorescence and primary photochemistry in chloroplasts by dibromothymoquinone. BBA - Bioenerg. https://doi.org/10.1016/0005-2728(75)90209-1

Mantovani, M., Marazzi, F., Fornaroli, R., Bellucci, M., Ficara, E., Mezzanotte, V., 2020. Outdoor pilot-scale raceway as a microalgae-bacteria sidestream treatment in a WWTP. Sci. Total Environ. 710, 135583. https://doi.org/10.1016/j.scitotenv.2019.135583

Marazzi, F., Bellucci, M., Fantasia, T., Ficara, E., Mezzanotte, V., 2020. Interactions between microalgae and bacteria in the treatment of wastewater from milk whey processing. Water (Switzerland). https://doi.org/10.3390/w12010297

Marazzi, F., Bellucci, M., Rossi, S., Fornaroli, R., Ficara, E., Mezzanotte, V., 2019. Outdoor pilot trial integrating a sidestream microalgae process for the treatment of centrate under non optimal climate conditions. Algal Res. 39, 101430. https://doi.org/10.1016/j.algal.2019.101430

Marazzi, F., Ficara, E., Fornaroli, R., Mezzanotte, V., 2017. Factors Affecting the Growth of Microalgae on Blackwater from Biosolid Dewatering. Water. Air. Soil Pollut. 228. https://doi.org/10.1007/s11270-017-3248-1

Mihajlović, M., Petrović, J., Maletić, S., Isakovski, M.K., Stojanović, M., Lopičić, Z., Trifunović, S., 2018. Hydrothermal carbonization of Miscanthus × giganteus: Structural and fuel properties of hydrochars and organic profile with the ecotoxicological assessment of the liquid phase. Energy Convers. Manag. https://doi.org/10.1016/j.enconman.2018.01.003

Ranglová, K., Lakatos, G.E., Manoel, J.A.C., Grivalský, T., Masojídek, J., 2019. Rapid screening test to estimate temperature optima for microalgae growth using photosynthesis activity measurements. Folia Microbiol. (Praha). https://doi.org/10.1007/s12223-019-00738-8

Roberts, G.W., Fortier, M.O.P., Sturm, B.S.M., Stagg-Williams, S.M., 2013. Promising pathway for algal biofuels through wastewater cultivation and hydrothermal conversion. Energy and Fuels. https://doi.org/10.1021/ef3020603

Rossi, S., Casagli, F., Mantovani, M., Mezzanotte, V., Ficara, E., 2020. Selection of photosynthesis and respiration models to assess the effect of environmental conditions on mixed microalgae consortia grown on wastewater. Bioresour. Technol. https://doi.org/10.1016/j.biortech.2020.122995

Skadsen, J., 2002. Effectiveness of high pH in controlling nitrification. J. / Am. Water Work. Assoc. https://doi.org/10.1002/j.1551-8833.2002.tb09508.x

Usman, M., Chen, H., Chen, K., Ren, S., Clark, J.H., Fan, J., Luo, G., Zhang, S., 2019. Characterization and utilization of aqueous products from hydrothermal conversion of biomass for bio-oil and hydro-char production: A review. Green Chem. 21, 1553–1572. https://doi.org/10.1039/c8gc03957g

Van Hulle, S.W.H., Vandeweyer, H.J.P., Meesschaert, B.D., Vanrolleghem, P.A., Dejans, P., Dumoulin, A., 2010. Engineering aspects and practical application of autotrophic nitrogen removal from nitrogen rich streams. Chem. Eng. J. 162, 1–20. https://doi.org/10.1016/J.CEJ.2010.05.037

Wang, T., Zhai, Y., Zhu, Y., Li, C., Zeng, G., 2018. A review of the hydrothermal carbonization of biomass waste for hydrochar formation: Process conditions, fundamentals, and physicochemical properties. Renew. Sustain. Energy Rev. https://doi.org/10.1016/j.rser.2018.03.071

Weide, T., Brügging, E., Wetter, C., 2019. Anaerobic and aerobic degradation of wastewater from hydrothermal carbonization (HTC) in a continuous, three-stage and semi-industrial system. J. Environ. Chem. Eng. 7, 102912. https://doi.org/10.1016/j.jece.2019.102912

Zetsche, E.M., Meysman, F.J.R., 2012. Dead or alive? Viability assessment of micro- and mesoplankton. J. Plankton Res. https://doi.org/10.1093/plankt/fbs018

6. Conclusions and future perspectives

This thesis focuses on the potential of microalgae in the wastewater treatment field, aiming at integrating those microorganisms directly within functional wastewater treatment plants (WWTPs) to improve their efficiency end their overall sustainability. As microalgae are very versatile, they can adapt to very harsh environments, including wastewaters. Therefore, they can be exploited to remove inorganic nutrients such ammoniacal nitrogen and phosphorus from domestic waste streams like centrate from municipal digestate. The first part of this thesis, which was presented in chapter 1, focused on the management and the monitoring of a pilot plant located in the Bresso-Niguarda WWTP. The pilot plant, consisted in a high rate algal pond (HRAP) which was placed in the sludge line of Bresso WWTP, growing a mixed microalgal community on the centrate. The synergy observed between microalgae and nitrifying bacteria was quite interesting as it was proved that the microalgal photosynthesis was adequate to cover the oxygen demand for the biological nitrification process. The microalgal-bacteria system had a very high overall ammoniacal nitrogen removal, up to 86% on average. This is an important aspect in view of a scale-up as the mechanical insufflation of O_2 is one of the main capital costs in a conventional WWTP. However, a valorisation strategy for the produced microalgal biomass was still needed to make the entire process economically attractive and more sustainable. Literature data testifies that microalgae can be exploited to extract high-valuable compounds. This is surely true for pure and controlled indoor microalgae cultures, where the best strains are selected according to their ability to produce bio-compounds of interest. However, since microalgae are naturally present in wastewaters, trying to maintain a pure community in an outdoor full-scale application within a WWTP is not an easy task and it would involve a significant increase of complexity and costs. Currently, the end-uses of microalgal biomass grown on wastewaters still needs concrete proposal. Therefore, the second part of the thesis focused on a promising pretreatment process used in recent years to improve the characteristics of a wide range of organic feedstocks. As described in chapter 3, the hydrothermal carbonization (HTC) was carried out also on microalgae to form carbon-enriched materials (hydrochar) to be used in different fields of application. Among literature data, the most interesting finding was the production of microalgal-based hydrochar to be used as adsorbent agent in water remediation. Therefore, the microalgae grown in Bresso WWTP were used to produce microalgal-based carbon-encapsulated iron nanoparticles (ME-nFe) through the hydrothermal carbonization process (HTC). The laboratory-scale study, which was described in chapter 4, shows that:

- Microalgae grown on Bresso centrate were adequate to be used as feedstock for the HTC process, having a high carbon content and reducing power.
- Different settings to produce the nanoparticles were tested, changing the HTC temperature, the iron salt and the proportion between iron and microalgae.
- Based on the properties of the samples, the final protocol to produce ME-nFE foresaw a temperature of 225°C and a Fe/C molar ratio of 0.2.
- The best sample, having a specific surface area of 110 m^2g^{-1}, was tested in the removal of heavy metals from water solutions and treated effluents. Jar tests had positive outcomes in the removal of Zinc, Cadmium, Copper and Nickel. However, the removal of Chromium was negligible.
- Recovered and recycled ME-nFE were used for 3 consecutive adsorption tests, without losing their effectiveness.

The promising lab-scale results could pave the way toward a new solution for the valorization of microalgae grown on municipal wastewaters. While the microalgal metabolism could be used in the sludge line of conventional WWTPs (treating centrate), the microalgal-based ion nanoparticles could constitute a valuable alternative to tertiary treatment for the final polishing of effluents.

Among the limitations of the HTC process, the formation of a potentially toxic by-product must be considered. During the thesis, the liquid wastewater produced during the synthesis of the ME-nFE (HTC-LF) was characterized in terms of nutrients content and toxicity toward water compartment. As expected, the HTC-LF proved to be very toxic for *Allivibrio fisheri* but the toxicity could be decreased after adsorption through activated carbons. However, both pure culture of *Chlorella* spp. and a mixed microalgal community were able to grow on a 20% dilution of the HTC-LF. That was a key finding, allowing to design the entire process to produce Me-nFE as a cycle in accordance with circular economy.

Those results could create the conditions to continue the experimental work in the future. The promising removal efficiencies toward heavy metals, both on high and low starting concentrations (10 and 1 mgL^{-1}) should be confirmed also for even smaller ones (μgL^{-1}). Furthermore, since the Me-nFE does combine reducing properties and high adsorption capacity they could be effective also for the removal of organic compounds which still need an effective and scalable treatment solution. Finally, a Life Cycle Assessment (LCA) would be needed to evaluate the environmental and economic sustainability of the project in a real scale scenario.

7. Acknowledgments

Firstly, I would like to express my gratitude to my supervisor Prof. Elena Collina and of course to Prof. Valeria Mezzanotte for their patience, kindness and continuous support. They trusted me since day one, giving me the opportunity to develop a personal and scientific growth path that has enriched me deeply. I could not have wanted better mentors for my training.

Beside them, I want to thank the members of my teamwork: Prof. Elena Ficara, Prof. Marina Lasagni, PhD Simone Rossi and all the students who worked with us. Special thanks goes to PhD Francesca Marazzi; PhD Riccardo Fornaroli and phD Micol Bellucci as we shared not only the lab and the office but also special everyday moments. The last three years would never have been so fun without their presence.

My sincere gratitude goes to Prof. Andres Fullana, who provided me an opportunity to join his teamwork in Alicante. Even if it was a brief experience, it was essential for the development of my work and gave me the opportunity to experience life in a different country. I would also love to thank the external reviewers for their valuable comments and suggestions, which stimulated me to widen my research.

I would like to express my heartfelt gratitude to my family: Sandra, Massimo and Barbara, who love me unconditionally and are my first sponsors. Thanks to my friends. I won't name names, but I am sure that “They” know how much they mean to me.
Finally, a little reminder for myself: “I’ve never been a natural, all i do is try, try, try”.